EVALUATION OF MOISTURE STRESS IN CROPS BY MEANS OF REMOTE CONTROL AERIAL SURVEILLANCE

by

P.S. FOUCHÉ AND N. BOOYSEN

Department of Soil Science
University of the North
Private Bag X1106, Sovenga, 0727

Report to the Water Research Commission on the Project:
"Evaluation of moisture stress in crops by means of remote control aerial surveillance"

Head of Department : Professor P.S. Fouché

Project Leader : Professor P.S. Fouché

WRC Report No 229/1/94
ISBN 1 86845 048 1

ACKNOWLEDGEMENTS

The research described in this report resulted from a project funded by the Water Research Commission and entiteld:

" Evaluation of moisture stress in crops by means of remote control aerial surveillance."

The steering committee responsible for this project, consisted of the following persons:

Dr P C Reid	:	**Water Research Commission**
Mr H C Chapman	:	**Water Research Commission**
Mr F P Marais	:	**Water Research Commission**
Prof. M S Burgers	:	**University of the North**
Prof. P S Fouche'	:	**University of the North**
Mr N Booysen	:	**University of the North**
Mr D F M Korf	:	**Department of Water Affairs & Forestry**
Mr F B Reinders	:	**Department of Agriculture**
Mr J F Erasmus	:	**Agricultural Research Council**

The financing of the project by the Water Research Commission and the contribution of the members of the Steering Committee are acknowledged gratefully.

This project of five years duration was benefited by the contributions of other international researchers. The authors therefore wish to record their sincere thanks to the following:

Prof. C Blazques , Citrus Research and Education Centre, University of Florida, Lake Alfred, Florida, USA, for information on infrared aerial photography.

Mr J Everitt and Mr D Escobar, Remote Sensing Centre, USDA, Weslaco, Texas, USA, for valuable notes on infrared video cameras.

Prof. F E Sistler, Department Agricultural Engineering, Louisiana State University, Baton Rouge, Louisiana, USA, for help in obtaining image processing software.

Prof. P T Tueller, Department of Rangeland, Wildlife & Forestry, University of Nevada Reno, Reno, Nevada, USA, for information on videography and image analysis.

Dr D J King, Department of Geography, Carlton University, Ottawa, Canada, for information on infrared video cameras and narrow band filters.

Mr J Walker, Brigham Young University, Provo, Utah, USA, for information on aerial surveillance systems and aerial photography.

Mr M Scriba, CSIR, for the development of a multispectral video camera.

EXECUTIVE SUMMARY

EVALUATION OF MOISTURE STRESS ON CROPS BY MEANS OF REMOTE CONTROL AERIAL SURVEILLANCE

By

P.S. FOUCHE' and N. BOOYSEN

DEPARTMENT OF SOIL SCIENCE

UNIVERSITY OF THE NORTH

CONTRACT RESEARCH PROJECT

SPONSORED BY THE

WATER RESEARCH COMMISSION

1.1. BACKGROUND AND MOTIVATION

Moisture stress assessment techniques can be generally classified into three categories : soil based, plant based and mathematical model approaches. Since plant based techniques measure crop water status and soil or meteorological methods only estimate crop water status, plant based methods are decidedly best.

Plant stress measurements with an infrared thermometer have become popular in the past 10 years. Digital displays of foliage temperature allow for quick and easy measurements. Using remote control aircraft fitted with an infrared thermometer, a large crop area can be scanned in a short time to assess the crop canopy temperature.

Colour infrared photography and videography have also shown to be sensitive to shifts in the spectral reflectance of a crop under moisture stress conditions. Processing these infrared images by computer software, the moisture stress conditions in the crops can be classified into stressed and non-stressed categories. Comparing this with the canopy temperatures of the crop, a more quantitative estimation of stress conditions in the crop can be achieved.

1.2 Objectives

(a) To develop the use of remotely controlled aircraft to serve as an inexpensive platform for remote sensing of crop water stress and other parameters related to the estimation of crop water stress requirements and attainment of maximum crop water use efficiency (plant density, crop growth, nutrient disorders, irrigation uniformity etc.)

(b) To develop the use of various on-board sensing techniques for obtaining the required measurements and data. These include colour and infrared photography, infrared thermometry and infrared video image acquisition.

(c) To evaluate the accuracy with which moisture stress related parameters can be estimated by means of these remote control surveillance techniques.

(d) To establish the spatial coverage and resolution attainable with the technique

1.3 Research procedures

(a) Different remotely piloted aircraft (RPA's) were developed and modified as inexpensive platforms, carrying on-board sensing instruments for low altitude remote sensing of agricultural crops. These include colour infrared photography, video acquisition and crop canopy temperature by infrared thermometry.

(b) Three crops viz. soybean, wheat and maize received irrigation treatments which resulted in well watered and moderately stress conditions. A remotely piloted aircraft carrying an infrared thermometer and video equipment, was used in sensing the crop canopy temperature of the three crops.

(c) Variables were measured every second day and included canopy temperature by aerial surveillance, ambient air temperature and soil moisture potentials. Infrared aerial photography was also conducted simultaneously over the period when stress conditions developed on the crops.

(d) The obtained colour infrared transparencies were scanned into and processed on a computer using image processing software. The processed images were compared with canopy temperature data of the crops obtained by infrared thermometry.

1.4 Major results

(a) The large aircraft (¼ scale types), having wingspans of up to 4 meter with payload capacities of up to five kilogram, were more suitable for carrying infrared thermometers and video equipment. They needed landing strips of $\pm$ 50 m x 5 m. The smaller aircraft, with maximum wingspans of 2 m, could carry 35 mm cameras of up to one kilogram mass. These aircraft could be used in more confined areas on smaller landing strips of up to 30 m length. Some of these aircraft were also equipped with an autopilot and parachute retrieval system for ease of operation in difficult flying areas.

(b) Canopy temperatures of the crops, as measured by aerial surveillance, gave a much quicker method than the ground method to assess moisture stress development on the crop.

(c) The ΔT-value (canopy temperature minus the air temperature) was shown to be effective in assessing moisture stress in crops such as soybean, maize and to a lesser extent, on wheat.

(d) The CWSI (crop water stress index) also signalled at higher threshold values, the need for irrigation on both crops such as soybean and maize. Successful use of the CWSI depends on the determination of a corrected non-water stress baseline which could change throughout the growing season.

(e) The TSD-value (temperature stress difference) which gave the difference between the canopy temperature of water stressed and well watered plots, also differentiated between different days of irrigation and developing stress conditions on soybean and wheat.

(f) All three moisture stress indices could be used positively to estimate developing moisture stress on the short term crops. A highly significant correlation was also found between Tc; ΔT and TSD for both soybean and wheat over the study periods from 1989 to 1992.

(g) Aerial infrared photographs taken of soybean and wheat at different stages of the irrigation cycle and processed on a computer, showed that the computer images gave a positive differentiation of developing moisture stress areas on the crops. Stressed areas could also be quantitatively expressed as percentage area-values of the total irrigated area.

(h) Areas of moisture stress development were also observed from the air by a multispectral video camera. The best results in differentiating between low moisture and high moisture stress areas, were obtained using a narrowband infrared filter on the video camera. Although resolution proved to be poorer than the colour photographic infrared images, computer imaging still showed differences in the moisture stress conditions on the crops.

(i) The classified moisture stress images also compared well with the canopy related indices such as ΔT, CWSI and TSD.

(j) Using low altitude aerial infrared photography and computer processing, rootrot diseased trees in citrus-, avocado- and cashew nut orchards could be identified and differentiated from healthy trees.

(k) In a wheat field-experiment that was fertilized at different levels of phosphorus, areas with P deficiency and sufficient P could be classified on the processed aerial colour infrared image. Soil -P and wheat yield correlated well with the classified colour infrared image.

1.5 Attainment of Objectives

In general terms the main objective (¶ 1.2(a)) relating to the development of remotely controlled aircraft to serve as an inexpensive platform for remote sensing of crop water stress and other parameters for crop water use efficiency, was attained.

The second objective (¶ 1.2(b)) relating to the development of on-board sensing techniques was also achieved which included infrared photography and -thermometry. The infrared video acquisition by using a multi spectral camera showed poorer image resolution and more development on the camera will be needed.

The third and fourth objectives (¶ 1.2 (c) and (d)) were both met in comparing different moisture stress parameters with infrared processed images of irrigated crops by quantification of the spatial coverage of stressed areas.

All these objectives have mostly been met, principally because of the design and development of the remote controlled aircraft which can be used in local farming areas for assessment of stress conditions on crops. Some of the technology developed has already been applied on large citrus- and avocado estates.

Results of the study indicate that the use of low altitude aerial colour infrared photography obtained from remotely controlled aircraft and image processing computers, can be a relative inexpensive technique to assess crop stress conditions.

* Three papers on the research work were presented during 1989, 1991 and 1993 at the Biennial Colour Aerial Photography Workshops in Plant Sciences, held in America. These papers are available in the proceedings as published by the American Society for Photogrammetry and Remote Sensing.

* Papers were also presented at Conferences of the S.A. Soil Science Society during 1990 and 1992.

* Two papers were also published on the use of low altitude remote control aircraft to assess crop stress in **Applied Plant Science, 1991** and **Geocarto international, 1993.**

1.6 Future recommendations

It is hoped that the applications generated by the project will continue along two distinct paths, viz:

1.6.1 Technology transfer

The use of remote controlled aircraft as a platform for remote sensing should by used in practice because of its inexpensiveness and ability of low altitude aerial surveillance properties. This should fill the gap between large aircraft used for high altitude aerial surveillance and remote satellite imagery. The technology lends itself for practical use in assessment of stress conditions on crops grown on small areas viz 5 to 50 hectare for example on the following:

* Assessment of crop water stress development on centre pivot irrigation systems by using infrared videography combined with infrared thermometry for timely irrigation scheduling or testing existing irrigation scheduling models.

* Checking tree crops such as citrus or avocado by infrared aerial photography for root related diseases resulting from over irrigation and poor soil drainage.

* Monitoring the effectiveness of distributing water soluble fertilizers such as Nitrogen through irrigation systems on short term crops viz maize, soybean and wheat by colour aerial videography.

* Using computer processed aerial infrared images of long term tree-crops such as citrus as a useable tool for recording orchard condition over different seasons.

* Infrared aerial videography can be used to monitor pollution of dams over time.

* Water leakage from underground pipes could be observed at low altitudes using infrared photography and computer processing.

* Soil erosion and donga formation could be studied and monitored effectively at low altitudes and recorded by video for soil conservation.

* Areas of soil salinization especially on crops such as irrigated sugar can be aerial photographed by infrared cameras and mapped out using computer processing.

1.6.2 Recommended future research.

* To developed a cost effective irrigation scheduling system using aerial surveillance by near-, mid- and thermal infrared video cameras.

* To compare results of crop water stress as observed by infrared video cameras and Landsat TM satellite data.

* To evaluate new aerial photographic platforms such as remote controlled balloons.

TABLE OF CONTENTS

CHAPTER 1

INTRODUCTION

Crop production in semi-arid climates is dependant on supplement water addition. Where the need for crop irrigation exits, so does the necessity for scheduling water applications. Moisture stress assessment techniques can be generally classified into three categories : soil based, plant based and mathematical model approaches. Since plant based techniques measure crop water status and soil or meteorological methods only estimate crop water status, plant based methods are decidedly best.

This chapter provides an overview of the objectives of the project in addition to a literature review of the assessment of crop moisture stress conditions and the use of airborne techniques for crop survey.

1.1 Objectives

(a) To develop the use of remotely controlled aircraft to serve as an inexpensive platform for remote sensing of crop water stress and other parameters related to the estimation of crop water stress requirements and attainment of maximum crop water use efficiency (plant density, crop growth, nutrient disorders, irrigation uniformity etc).

(b) To develop the use of various on-board sensing techniques for obtaining the required measurements and data. These include colour and infrared photography, infrared thermometry and infrared video image acquisition.

(c) To evaluate the accuracy with which moisture stress related parameters can be estimated by means of these remote control surveillance techniques.

(d) To establish the spatial coverage and resolution attainable with the technique.

1.2 Literature review

A major factor limiting plant growth, productivity and even survival, is the lack of water. When there is insufficient soil water available to meet the transpirational and physiological demands of the plant, a water stress may develop. External and internal symptoms vary among species, but one effect that appears common to all species, is that leaf reflection changes as water deficit stress develops (Knipling, 1970; Jackson, 1986). It has been found that different spectral regions are useful for the detection of plant water stress. One is the near infrared (NIR) 0.7-1.3 μm region characterized by high reflection caused by multiple reflectance and scattering of light in the spongy mesophyll structure of plants (Horler and Barber, 1981 ; Ripple, 1986 ; Jackson, 1986). Second is the middle infrared (MIR) 1.3-3.0 μm region dominated by strong water absorption bands (Everitt et al, 1987a; Grant, 1987; Escobar et al., 1988) and directly affected by leaf water content (Tucker, 1980; Grant, 1987). A third method is by sensing the thermal infrared radiation, 8 to 14 μm, of the plant canopy as a whole (Jackson et al., 1977; Jackson, 1982; Fouche', 1993). As water becomes limited, transpiration is reduced and leaf temperature increases above the air temperature because of the absorption radiation.

In the NIR range, changes in reflection due to water stress have been observed by colour infrared photography. Plants under stress conditions, whether affected by disease, low moisture or nutrient deficiency, produce changes in the internal leaf structure which cause predictable shifts in the spectral reflectance of the canopy (Hoffer and Johannsen, 1969; Ripple 1986;Ripple & Schrumpf, 1987; Boyer et al., 1988). Hoffer (1989) evaluated the versatility of aerial CIR photography for resource managers to assess various stress conditions in crops. MIR reflectance is more directly controlled by leaf water content

(Gates et al., 1965; Knipling, 1970). Escobar et al., (1988), used a mid-infrared video camera to identify crop irrigation management potential. Everitt et al. (1988) used the same camera to differentiate between succulent and non-succulent plant species. Applications using MIR video have been somewhat limited by its low resolution and low atmospheric penetration capabilities (Mausel et al., 1992).

In 1977, Idso et al. and Jackson et al., used thermal infrared thermometers to measure canopy temperatures. By subtracting the air temperature from the canopy temperature, the Stress Degree Day (SDD) equation was developed (Jackson et al., 1981). This equation was developed as a possible irrigation scheduling tool using the thermal infrared thermometer as the main sensor. Geiser et al. (1982) aligned the canopy minus air temperature with net radiation and vapour pressure data to use as an irrigation scheduling tool. Gardner et al. (1981) suggested that canopy minus air temperature difference may be climate, crop and soil specific. Their conclusion was that canopy temperature and plant water potential are correlated but not linearly.

The advancement in the state of the art in infrared technology the past years, has brought about the production of lightweight, hand held infrared thermometers. These operate in the 8-13 μm thermal spectrum and can measure plant canopy temperatures accurate and rapidly. Some of the shortcomings of the IR-thermometer are that its field of view is restricted to its distance from the subject of measurement. On ground level at a height of 1 m from the crop canopy, only areas of roughly 25mm x 25mm are measured (Fuchs, 1990). To cover a large area of 50 ha, many measurements have to be made and can take a long time. A further difficulty is measuring the canopy temperature of row crops in early stages (Howell et al., 1984) and the fact that canopy temperature based irrigation-scheduling, allows determination of irrigation timing but not amounts (Nielson, 1990). Therefore, standardi zation of and consistency in the procedure, is important.

Idso et al. (1981a) developed the C W S I (Crop water stress index) that normalizes the stress degree index for environmental variability, specifically vapour pressure deficit. The C W S I (based on IR-measurements) is determined by plotting the canopy temperature minus the air temperature vs air pressure deficit to give a non-water stressed baseline. As the crop goes from maximum transpiration to zero transpiration, the C W S I will range from 0 to one (Idso et al., 1981b).

Estimating environmental stress conditions of agricultural crops, can sometimes be difficult on large areas under cropping. Aerial imaging systems for monitoring crop conditions have been effectively utilized in the past (Myers et al., 1983). Fouché and Booysen (1989) used remotely piloted aircraft at low altitude to survey and photograph crops to obtain good quality colour infrared aerial photographs for crop stress evaluation. The sport of radio controlled model aircraft has developed rapidly over the past years with the development of improved radio control systems (Sales 1986). Because piloted aircraft surveillance is very expensive, Gottwald and Teddes (1986) used a radio controlled model aircraft as a research platform to study biological control of agricultural pests. Stum (1988) also used a lightweight radio controlled aircraft fitted with a 35 mm auto camera to study prehistoric Indian sites in Northwestern Mexico. Benzon (1983) concluded that radio controlled aircraft could be economically used for ultra low volume application of pesticides although he was not optimistic about the wide application in agriculture and public health control applications. Fouché (1986) used radio controlled aircraft for aerial photography to test irrigation efficiency on centre pivot systems used for different crops. He found it to be more suitable and inexpensive for low altitude large scale reconnaissance than full scale aircraft. Dommert et al., (1988) proved radio controlled aircraft to be quite versatile as a platform for aerial surveillance of polluted dams.

Airborne videography as a remote sensing tool has greatly expanded during the past five years, although a sustained interest in using video cameras has existed for a decade (Everitt et al., 1991a). Analyzing photographic and video data, particularly multispectral, varies from simple to complex. Blazquez (1989) made use of computer processing of colour infrared transparencies of citrus orchards to distinguish between stress conditions of the trees. Image processing software has been developed to photo interpret aerial colour infrared photographs and video data (Everitt et al., 1988b; Yaun et al., 1991; Fouché and Booysen, 1991; Mausel et al., 1992).

In the light of the reviewed literature, the main objectives were to assess moisture stress by infrared photography and thermal infrared surveillance, because of the availability of these techniques. A platform for low altitude surveillance would be constructed to carry suitable remote sensing instruments. Although infrared videography was still new in South Africa, this technique would also be investigated for assessment of moisture stress conditions on crops.

CHAPTER 2

MATERIAL AND METHODS

2.1 Development of remote control aerial surveillance platforms

The aim of this study was to develop and modify different remotely piloted aircraft (RPA) to carry sensing instruments to be used in this project. These aircraft had to be inexpensive and easy to operate in difficult conditions such as windy weather; poor take off/landings strips ; high and low flying altitudes ; easy to transport ; easy to repair when damaged etc.

2.1.1 RPA - 1

This aircraft was the main platform to be used for sensing moisture stress on different crops such as wheat and soybean. The airframe design was a biplane (Fig. 1 & 17) with a wingspan of 2440 mm ; a chord of 406 mm for the upper wing ; 2290 mm and 406 mm for the lower wing ; and a fuselage length of 2040 mm. The top wing was flat and the lower wing had a 2.5° dihedral angle. The front portion of the fuselage was 250 mm wide to enable the fitting of a variety of instrumentation. The engine cowling and front fuselage were modified for easy access of instrumentation by adding a removable hatch. The RPA which was constructed mainly from balsa and spruce was strengthened around the engine bay and payload area with fibre glass. The airframe was covered with an iron- on fabric and the wings painted red on the top surface and yellow on the bottom surface. The fuselage was black with yellow top decking. This colour scheme was chosen for visibility when flying at higher altitudes. Initially a 30 cm^3, 3.5 hp single cylinder two stroke glow engine was used as a powerplant. This was later substituted (to overcome excess vibration) with a twin cylinder four stroke 50 cm^3, 5 hp engine.

A 55 cm x 25 mm propeller was used on the 50cm^3 motor. A 675 ml fuel tank located at the back of the engine firewall gave ample flying time of ± 20 minutes. A pair of 150 mm air wheels were fitted for ease of landing on rough areas. The undercarriage was also strengthened with 5 mm spring steel wire to carry the extra payload. The radio control system consisted of an 8- channel PCM transmitter/receiver with built-in fail-safe system and plug-in radio frequency modules on 60.375 MHz. The receivers and servos were powered by a 1000mAh 9.6 V rechargeable nickel cadmium battery. Standard servos (3 kg/cm) were used, one on each aileron, one on each elevator half and one heavy duty (13 kg/cm) on the rudder. Nett mass, with radio control system was 12.8 kg, giving a wing loading of 70g/dm^2. A 100 g/dm^2 wing loading is quite acceptable for this quarter scale type aircraft giving a stalling speed of well below 45 km/h.

An Everest infrared thermometer (see details in ¶ 2.2.1) for measuring crop canopy temperature was fitted in the nose section just behind the firewall (see Fig. 1). This instrument pointed ± 90° downwards with the aircraft in level flight. A small wrist type altitude meter was mounted next to the instrument panel of the infrared thermometer. [1]Data displayed by these two instruments were viewed by a colour video camera mounted at a slight angle towards the right, on the centre of the top wing (Fig. 1). The reason for this mounting was to view a part of the area which was surveyed by the RPA as well as the instrument display. Video images were transmitted from the video camera to the ground by means of a 12 volt 390 mw video transmitter and receiver operating at 390 Mhz. The transmitter used an omnidirectional skirted dipole antenna fitted at the bottom of the RPA, while the receiver used a ringbeam antenna with a mast amplifier giving a total of 20 db gain. From the receiver, video data was fed into a monitor powered by a 12 v DC battery pack. A 12 v DC video recorder stored all video images on VHS tape.
Nett mass of the RPA -1 with instruments was 16.25 kg giving a final wing loading of 100 g/dm^2. Total payload was 3500 g. The RPA was used to fly in straight strips over experimental blocks of crop measuring 100 x 350 m each.

---

[1] Data from the infrared thermometer could have been directly transmitted to a ground station and overlaid onto the video image from the camera (Berry, 1991) but at this stage was to costly to develop. The above setup was much cheaper and simpler to operate.

2.1.2 RPA - 2

A shoulder wing aircraft with wingspan 2500 mm, fuselage 1750 mm, was used as the second surveillance platform (Fig. 2). This quarter scale aircraft was powered by a 30 cm^3 two stroke engine and 45 cm x 15 mm propeller. It also had functional flaps for short take off and landing capability.

[1] A colour video camera, having a resolution of 280 lines and wide angle F 1.4 ALC lens, was mounted at the centre of gravity of the aircraft. The camera pointed directly downwards, just behind the landing gear and used 24 v DC NiCd battery pack as power source. The same TV link system as described for the RPA-1 was used to transmit video images to a ground station. A 35 mm reflex camera was also added next to the video camera (Fig. 2). Relayed colour images were recorded for later evaluation in the laboratory. Colour or infrared photographs of problem areas, as viewed by the video camera, at the video monitor on the ground station, were photographed using a supplementary channel on the R/C transmitter which triggered the 35 mm camera from a servo in the aircraft. Either UV (colour) or Wratten 12 (CIR) filters were used on the 28 mm wide angle lens of the camera. Total mass of the RPA-2 including cameras, TV link system and batteries, amounted to 11.8 kg, giving a wingloading of 106 g/dm^2. The payload of this aircraft was 2500 g. With this wingloading and functional flaps, the aircraft could take off and land on a 50 m x 5 m strip.

---

[1] This camera was later on substituted by a Sanyo Hi-band 8mm CCD camcorder fitted with its own battery pack and having a resolution of 400 lines. This camera weighed only 750g.

2.1.3 RPA - 3

This was a smaller shoulder wing aircraft with a 2000 mm wing span tricycle landing gear and 15 cm^3, two stroke engine driving a 35 cm x 15 mm propeller (Fig. 3 & 18). The tricycle landing gear was later on replaced with a conventional tailwheel landing gear which coped better with dirt roads from which the aircraft was flown. A Pentax 35 mm reflex camera fitted with an autowinder and automatic exposure system was used for aerial photography. The camera which had a 28 mm F 1.4 wide angle lens was fitted at the centre of gravity directly beneath the receiver/servo installation. The camera was triggered by an electronic device connection between the receiver and the camera. The RPA and camera were controlled using a 7 channel radio. Flaps were fitted for short take-off and landing capability. The aircraft weighed about 6 kg (fully loaded). By using a Wratten 12 filter, CIR photographs were taken of moisture stress conditions on the different crops. Because of its good handling capabilities, the RPA-3 was also used in restricted areas such as avocado- and citrus orchards where narrow dirt roads were used as airstrips. The aircraft was later on fitted with an automatic pilot system which controlled the ailerons and elevator. This was used when flying at high altitudes of ± 700 m when the aircraft became a mere speck in the sky. The aircraft was kept level and in a straight line by the auto-pilot system.

2.1.4 RPA - 4

This was a simple design hand launch unit for use in confined areas where no runways were available. The RPA-4 is based on a hang-glider design and consisted of a plastic rogallo type wing, foam polystyrene pylon and narrow 75 x 75 mm square fuselage (1500 mm long) tapering to 50 x 50 mm at the back. Arrow flight type of tail surfaces were used for control (see Fig. 3(right)). A small camera box, which contained a servo for triggering a small 35 mm auto camera, was attached at the centre of gravity, beneath the fuselage. Wire landing skids were fitted under the fuselage for protection of the camera when landing in grass patches. A 10 cm^3 two stroke glow engine with a tune pipe exhaust was used as power source and fitted with a 30 cm x 15 mm propeller (The aircraft weighed 5000 g with the camera and had a payload of 500 g). The RPA-4 was normally used to photograph centre pivot systems where annual crops such as maize, wheat and soybean were grown. A 4 channel radio was used to control rudder, elevator, engine throttle and camera. The small autofocus selfwind camera was quite suitable for aerial photographic work although at high engine speeds, vibration posed a problem. The cost of this RPA was much cheaper compared to the other and was most suitable on windy days.

2.1.5 RPA - 5

For multispectral video acquisition, a special camera was built by the CSIR. This camera was quite bulky and heavy and a suitable aircraft had to be developed to carry this camera and its video transmission equipment. A mono wing aircraft with a wingspan of 3800 mm, wing chord 504 mm and fuselage length 2250 mm, was constructed from mainly ply, balsa and spruce (Fig. 4 & 19). This aircraft had a large surface area which resulted in a low wing loading. Its total mass with equipment was ± 15 kg. Compared to the previous RPA's this aircraft was much larger and had a large cockpit area of 200 x 600 x 400 mm in which the multispectral video camera and other equipment could be fitted. The powerplant was a 62 cm^3 5 hp two stroke engine turning a 55 cm x 25 mm propeller. Some vibration was experienced which effected the image of the video camera. The engine was therefore equipped with a selfstarter unit so that it could be started or stopped in the air. After reaching the correct flying altitude the engine was killed, the aircraft set in a straight glide path and surveillance done by the multispectral video camera without vibration interference. A power control panel working from a 12 v Nicd battery was fitted to the aircraft to operate the multispectrum camera, selfstarter and video transmission equipment. The same TV transmission system as described for the RPA-1, was used in this aircraft. The main purpose of this aircraft was to scan moisture stress conditions on different crops using the multispectral video camera.

2.1.6 Parachute retrieving system

A parachute was also constructed to retrieve the RPA's in case of landing problems. This item was not intended to replace the landing skills of the pilot flying the R/C aircraft, but was designed as a backup system in case of emergency landings. The parachute used had a 2 m diameter and handled an aircraft with a mass of ± 6 kg. It was mainly used on the RPA-3. The parachute was stored in a container mounted on top of the centre part of the wing on the centre of gravity of the aircraft. Deployment of the parachute was done by activating a servo to release the flush mounting hatch on the container. As the hatch cover opens, the parachute is caught by passing air and a drogue chute on the main parachute pulls the main chute from the container. The parachute deploys in less than 2 seconds, halting the forward progress of the aircraft. The aircraft is then lowered to the ground in a wheel first attitude which allows any impact to be absorbed by the landing gear (Fig.5).

2.2 On-board instrumentation for assessment of crop water stress

Areas of moisture stress on crops can be assessed by either infrared aerial photography or measuring the canopy temperature of the crop by infrared thermometry. Crops under moisture stress have also shown a shift in their spectral reflectance to the near infrared which can be detected by colour infrared photography or multispectral videography (Mausel et al., 1992). The following on-board instruments were used to conduct the research project.

2.2.1 Infrared Thermometer

The infrared thermometer measures radiant energy beyond the sensitive range of human eyes. All objects radiate this energy with an intensity relative to the temperature of the object. Measurement of infrared radiation is possible due to the flow of net infrared radiation from a hotter to a cooler object. Infrared radiation also exhibits the same optical behaviour associated with light that is visible to the eye such as shadowing, reflection and refraction. Assuming that the instrument is the cooler of the two, the front-end optical telescope collects a sample of infrared radiation from the hotter object. The sample of infrared radiation collected by the optics is then focused on the infrared detector. The infrared detector converts the radiation to an electrical signal which again is converted to an equivalent digital signal reading the temperature as display numbers in degree Celsius.

The Everest infrared thermometer has a tenth degree resolution and responds in a fraction of a second over the temperature range of -25°C to 75°C. The emissivity is set at 0,98 which reduces the possibility of taking readings at an incorrect setting. The spectral passband is 8 to 14 μm and operating distance 2 cm to infinity. The instrument which weighs 1.0 kg is mounted in the front of the aircraft (RPA-1) and points directly downwards when the aircraft flies level. The instrument has a rechargeable 12 v NiCd battery which provides 30 hour continuous operation from a full charge. A toggle switch on the front panel allows you to choose between data averaging and fast readings. The data averaging mode requires five seconds to come up to an accurate reading. It smooths the data with respect to time. This mode operated the best when taking measurements on the ground by hand. In the aircraft the "fast" mode gave the best results while flying over the crop. The instrument is automatically turned on by a touch sensitive switch which is built into the handle. In the aircraft a metal clip on the handle is used to trigger the IR-thermometer continuously. The instrument has a field of view of 3° and the scanning area varies according to D/20 where D is equal to the height flown by the aircraft. An altitude of 100 m will thus give a scanning strip of 5 m wide. The temperature displayed by the liquid crystal on the front panel was captured using a video camera and transmitted and recorded at a ground station as described in ¶ 2.1.1. The infrared thermometer was calibrated using a hand-held, self-contained portable calibration source. The operation of the infrared thermometer was checked with 0.25°C accuracy.

2.2.2 Infrared Photography

Vegetation like grass, trees or other plants, look green in the visible spectrum. This is because the blue and red component of light are absorbed by the plant leaves and used for photosynthesis. The green component, in turn, is reflected back causing the visible green colour of leaves. If the vegetation is healthy, there is also a strong reflection of the near infrared light, just beyond the humanly visible light range. If the vegetation is not healthy, such as under moisture stress, the invisible near infrared component is reflected weaker and this results into a predictable shift in the spectral reflectance of the canopy. When using infrared film, the emulsion reflects the near infrared component whether strong or weak.

Kodak Aerochrome 35 mm infrared film 2443 was used in the reflex camera fitted with a 28 mm wide angle lens and a Wratten 12 filter. Exposures were made using ASA film speed at f8 and 1/250 second setting on the camera. It was of importance that exposures were done in broad sunlight without shadow interference of clouds. (Photography was done mainly at 200 m altitude to cover the 15 ha experimental area). Films were developed by the E 4 process. The CIR slides were kept for image processing on the computer.

2.2.3 Video Image Acquisition

Improvement and advancements in video and computer image processing technology during the 1980's helped to greatly stimulate the interest in video remote sensing (Everitt et al., 1991a). Video has many attributes that are attractive for remote sensing. Amongst the most prominent are : (a) the near real-time availability of imagery, (b) video cameras have higher light sensitivity than film cameras, that permits imaging in narrow spectral bands and give sensitivity further into the infrared spectrum, and (c) the immediate potential for digital processing of the electronic signal for subsequent computer analysis. Video images have the shortcoming that their resolution is much lower than photographic film. The last two years of the research period were spent on investigating the use of video cameras. A colour and B/W multispectrum video camera were used in this investigation.

2.2.3.1 Colour Video Camera

A Sanyo Hi-8, 8 mm camcorder was used in the RPA-1 which was modified to carry the camera. The camera had an integrated 8 mm video cassette recorder. Onboard images could be recorded while flying over the crop. The CCD sensor on the camera had a resolution of about 450 TV lines. By using Hi-8 tape (similar to S-VHS) an image resolution of 420 TV lines could be recorded. This was much better than standard VHS. The camera also had a TV outlet so that the image could be simultaneously transmitted to the ground station while onboard recording proceeded. The camera used its own DC NiCd 7.5 v battery pack for up to 2 hour recordings. The total mass of the camera was 850 g.

2.2.3.2 Multispectral Video camera

The multispectral video camera was constructed around a high resolution CCD Pulnix TM-6 black and white video camera. The total spectral bandwidth of the camera was from 0.4 to 1.1 μm

which essentially matches some of Landsat's MSS satellite spectral coverage. At a wavelength of 1μm which is the near infrared spectrum, the camera had a relative spectral response of 70%, without the multispectral filters.

A filter turret having eight holes and containing seven filters covering the whole spectrum, was constructed to run in front of the CCD sensor. The camera had a control circuit in order to select and change the filters remotely. When the filters were selected from the ground by radio control, a video text generator displayed the wavelength of the filter which were transmitted to a monitor on the ground.

Seven Sindler and Hoyer interference filters were used :

Wavelength	Transmittance
514 nm	40%
546 nm	40%
589 nm	40%
650 nm	35%
707 nm	35%
853 nm	35%
cut infrared filter RG 850nm	90%

The cut infrared filter transmits infrared at wavelenghts larger than 850nm . Taking into account that the spectal sensitivity of the camera in the near infrared range is near 70% and has a low - light sensitivity of 1 lux, a filter transmitting light between 35- and 40% still gives a sharp image on a cloud-free day. The TM-6 video camera had a TV resolution of 590 (H) x 575 (V). This resolution was however limited by the VHS-video tape on which the transmitted image was recorded. VHS video tape provides a maximum horizontal TV resolution of 240 lines. The camera was mounted in the RPA-5 pointing directly downwards when the aircraft was in level flight. A wide angle 8 mm F 1.3 TV lens was used on the camera to scan the crop. Images were transmitted to a ground station and stored on VHS tape as described in ¶ 2.1.1. A 12 V 1800 mah NiCd battery was used to power the video camera. Total mass of the multispectrum camera was 2.3 kg.

2.3 Experimental planning of the surveillance sites and procedures

The RPA-1 as previously described was the main platform for sensing moisture stress in three different crops namely maize, soybean and wheat. The IR-thermometer was the main instrument used for measuring moisture stress. The experimental site was situated at Syferkuil, University Experimental farm. The experimental area for the crops under linear irrigation consisted of the following :

(i) **Marginal stressed block -**
replicated twice and receiving water only after ±9 days or when the canopy temperature has increased well above the air temperature.

(ii) **Well watered control block -**
replicated twice and receiving normal irrigation as for the whole crop ± every 6 days. The amount of water applied, varied from 30 to 70 mm depending on the evaporation pan scheduling method.

The experimental block measured 100 x 350 m (3.5 ha) and received water from the linear sprinkler system. Measurements were normally made for maize and soybean during January to middle March and wheat during August to September. The layout of the experiment is presented in Figure 13.1 . White cloth sheets (10 m length) were used as markers and positioned as reference points on the border of adjacent blocks. The RPA-1 was flown in straight strips at a altitude of 50 m over the blocks to measure the canopy temperature. The markers on the border of the block were also pinpointed by the video camera and a running comment on the flight path of the RPA-1 was recorded simultaneously. The crop canopy temperature as measured in flight by the IR-thermometer was recorded by the video camera, transmitted to the ground and videotaped. These measurements were also made on the ground with a handheld IR thermometer. Crop canopy temperatures were measured every second to third day, (in the active growing season) and depended on weather conditions. It was of importance that the measurements started after maximum ground coverage by the crop. This was necessary because of soil temperature interference on the IR-thermometer. Air temperature, relative humidity and soil moisture (by Neutron densitometer) were also monitored simultaneously.

All the data viz. Tc (crop canopy temperature), Ta (air temperature), RH (relative humidity) and days of irrigation were plotted onto graphs for further evaluation. Infrared photographs were taken at an altitude of 200 m when stress conditions started to occur in the stress blocks. These 35 mm transparencies were digitized on the computer using MIPS software. The same procedure was also followed in testing the multispectral video camera.

2.4 Parameters for estimation of crop water stress

Several crop water stress indices based on crop canopy temperature are proposed by researchers for estimating crop water stress.

2.4.1 S D D - Stress degree day

The SDD, defined as the accumulation of positive canopy temperature (Tc) minus air temperature (Ta) measured near solar noon, was proposed by Idso et al. (1977). Jackson et al. (1981) defined the SSD as follows :

$$\text{SDD pos} = \sum_{n=i}^{N} (Tc - Ta)_n$$

The SSD pos. is plant canopy temperature (Tc) minus air temperature (Ta) with values of (Tc - Ta) < 0 being set equal to 0, i is the first day after irrigation, and N is the number of days required for SDD pos to reach a predetermined value.

For the purpose of this investigation, the SDD was modified and Tc - Ta, expressed as (ΔT), was plotted against the day of measurement during the crop growing season under irrigation. Instead of SDD pos., accumulated between irrigation events, ΔT was taken as an indicator of water stress development for the crops over the days of measurement (Throssel et al. 1981).

2.4.2 C W S I - Crop water stress index

Idso et al. (1981) developed the CWSI that normalizes the SDD for environmental variability, specifically, vapour pressure deficit. The CWSI is developed by plotting ΔT, measured when the crop is transpiring at the maximum potential rate, vs air vapour pressure deficit (VPD) to give a non water stressed baseline. The non-water stress baseline is the minimum potential ΔT a crop can reach at a specific VPD. The approximate upper limit that ΔT may reach in the absence of transpiration was determined using the non-water stressed baseline and procedures described by Idso et al. (1981) and Nielson & Gardner (1990).

The CWSI was calculated by :

$$CWSI = \frac{Tc - Ta - D2}{D1 - D2}$$

where
- Tc = canopy temperature
- Ta = air temperature
- D2 = Tc - Ta predicted from the baseline equation
- D1 = approximate maximum difference between Tc and Ta

2.4.3 T S D - Temperature stress difference

TSD is defined as the difference in Tc between well watered and water stressed plots (Gardner et al, 1981). With the TSD, the reference plot that is not stressed must be in very close proximity to a field that is stressed. The TSD compensates for environmental effects such as vapour pressure deficit and air temperature with the use of the well watered plot as reference. In this study, the TSD values were plotted against the period of irrigation in days and evaluated.

2.5 Image processing by computer

2.5.1 Software program

Map Image Processing System (MIPS) marketed by MicroImages, U.S.A., was used to photo interpret aerial colour infrared photographs of crops under different stress conditions. The software program also had a facility to frame grab images of moisture stress on crops from video recordings made by the video cameras. A sub-program called " On Screen, Feature Mapping", was used to process the displayed images on a VGA monitor. The goal of feature mapping is to identify, mark and measure features in a set of processing rasters by combining knowledge of the study site. Prototype cells are selected by the user and similar cells are identified and highlighted on the display raster. In the simplest case, the program does cell matching, i.e. finding all cells that have the same colour value as the selected prototype cells. These cells may be classified categorically, into feature type. Each output raster object which shows a feature marked in colour, selected for a classification group, has an output file which contains the summary of feature, category and overall measurements. It includes feature area, cell counts, centroids, boundary lengths and percentage of total area covered by the feature.

2.5.2 Hardware configuration

The computer used in this study was a desktop AT 386 with a 80386 processor and 80387 math co-processor operating at 20 MHZ. It was equipped with an Everex - 16 color graphics card capable of handling both composite and RGB PAL video signals. A high resolution RGB/composite monitor was used as display device. This was coupled with a 180 dpi colour printer for low cost printing of text and images.

2.5.3 Scanning of Images

Aerial photographs (35 mm CIR transparencies) were scanned at 500 dpi,into the computer using a 35 mm slide scanner. The scanner uses fluorescent RGB light sources to digitize the colour transparencies at 500 to 2000 dpi and transmits the data over a GPIB, 8 bit, parallel interface at a rate of 100 k bytes per second to the host computer. Data transfer is through a GPIB interface card installed in the computer. Using MIPS software with the scanner (configured by MIPS), selected areas were scanned and viewed on the monitor. This resulted in a 512 x 484 pixel (500dpi) three channel image file.

CHAPTER 3

RESULTS AND DISCUSSION

3.1 Evaluation of Remotely piloted aircraft (RPA)

3.1.1 RPA - 1

After flight testing the RPA-1 with the infrared thermometer (IRT) and video camera, it was found that the 30cm^3 two stroke engine was not powerful enough and caused excessive noise and vibrations. This effected the digital display of the IRT and produced unstable readouts. To eliminate the vibration, a new type of engine was installed. This was a 50 cm^3 twin cylinder four stroke engine. The engine performed much better with less vibration and developed enough power to fly the RPA-1 smoothly with a 55 cm x 25 mm propeller. Temperature readings of the crop canopy could be viewed from the monitor via the video camera and an area of 50 ha was completely scanned within 50 minutes. For a handhold IRT to scan the crop a height of 0,5 m above the crop surface, it took more than 2 hours to cover the same area. The most reliable canopy temperature measurements were obtained when flying at about 100 m altitude. Some side radiation was picked up when flying at heights of 300 m over a 200 m x 350 block bordered by vegetation and open soil. At lower altitudes (30 m) the temperatures varied rapidly making the estimation of the average crop canopy temperature more difficult.

The RPA-1 handled it's payload easily and took off on a very short runway of 25 m. Being a taildragger configuration it was always better to take off and land into the wind. Because of the short runway requirement, it was an advantage to have two or more runways in the direction of prevailing winds. Markers on the ground were easily identified on the monitor so that the different experimental irrigation blocks could be pinpointed. A running commentary of the RPA-1 flight pattern was done on video tape using a microphone connected to a video recorder and helped later in evaluating the canopy temperature data stored on video tape. The RPA-1 was flown in different kinds of weather such as hot windy days and remained quite stable as a remote sensing platform under these conditions. The main problems that were experienced were with the TV-link systems. Flat batteries and loose wire connections caused the main malfunctions during flight operations.

3.1.2 R P A - 2

The 30 cm^2 two stroke engine in the RPA-2 provided moderate power to lift the aircraft into the air. However, quite high vibration levels were experienced on the RPA-2 when flying at full power. This effected the video images and the aerial photography causing some blurring. The engine had to be throttled back after reaching the required height to give more stable video images. A self starting system was later added to the engine. After flying to the required altitude the engine was stopped and the aircraft glided over the area to be surveyed. This resulted in very clear video images and photographs of the crop. Real time information was collected on crops such as maize, wheat, soybean, citrus and avocado. The 35 mm camera with a 28mm wide angle lens operated the best at f8 and 1/500 sec using ASA 200-400 colour film speeds. The RPA-2 was also equipped with a strobe light which could be activated by radio. This was necessary when flying against a clear sky at an altitude of 500 m. The best results for aerial surveillance of crops were at an altitude of 100 to 200 m, especially for orchard crops such as citrus and avocado. This RPA proved quite versatile in surveying areas of up to 200 hectares. With functional flaps this RPA handled well on short runways which usually was a farm road of about 30 x 5 m. As in the case of the RPA-1, the aircraft took off and landed much better into prevailing winds.

3.1.3 R P A - 3

The RPA-3 which had a tricycle landing gear, handled crosswinds on take off and landings much better than the RPA-1 and RPA-2.

However, sandy and grassy strips did cause some difficulties on take off. Much less vibration was experienced with the smaller 15 cm^3 engine and blur-free photographs were taken with medium speed colour or colour infrared film. With functional flaps the RPA-3 could take off and land on difficult runways especially where a narrow corridor existed between citrus tree plantings. Because this aircraft could handle payloads of up to ± 1000 g, a good quality reflex camera with interchangeable lenses could be used. This RPA proved to be versatile for routine aerial photography of different agricultural crops. A strobe light was used when flying at higher altitudes. Because of stoney and sandy roads experienced on farms, the tricycle gear was replaced with a conventional landing gear to improve the take off properties of the aircraft. The aircraft was also fitted with an auto pilot system which was very helpful when taking photographs at very high altitudes of ± 800 m. The autopilot system is also advantageous when training pilots in flying R/C aircraft. A parachute as previously describe in chapter 2, was also attached to the RPA-3. The RPA-3 could be brought down safely without any damage. This was very helpful when flying over areas having poor landing strips.

3.1.4 R P A - 4

The RPA-4, mainly used in confined areas, was useful in photographing landmarks during soil surveys. Although the photographs from the small auto-cameras were not of the same quality as those obtained with reflex cameras, they still gave good information on the areas flown. On windy days this RPA was much easier to handle and could be positioned over a predetermined spot for photographing, where it virtually hovered like a kite over the spot. Flying this RPA was much easier than the fixed wing type, although when landing on bare ground surface some skill in controlling the engine speed was needed. Usually the RPA was landed by gliding it onto the crop in the case of wheat or soybean or nearby grass in the veld. Unfortunately the pocket sized auto camera has a limited field of view and at a height of

200 m only 10 hectare was covered with one photograph.

3.1.5 R P A - 5

The RPA-5 which was constructed to carry the multispectrum camera, was mainly used in the irrigation experimental area. Because of the large size of the aircraft, strong winds affected the stable flying of the aircraft. The best results were obtained on calm days. Because of the engine vibration the aircraft had to be glided with the engine switched off to get clear video images. The selfstarting system on the engine functioned without difficulties. The aircraft need a landing strip of 50 m x 5 m for safe take off and landing. The petrol engine of 62 cm^2 was powerful enough to fly the aircraft to altitudes of 200 to 400 m where video surveillance of the crops were made. The on-board 12 V 1800 mAh battery also provided enough power to run the selfstarter, video camera and video transmission system. The glide ratio of the aircraft was also satisfactory and the aircraft could be glided for almost 5 minutes before the engine was restarted.

3.1.6 Cost estimate of RPA's and equipment

Most of the parts of the RPA's have to be imported from Japan, Taiwan or the USA. At current import taxes, costs have risen quite rapidly. All materials are mostly available from hobby shops in South Africa. The prices of engines and radios vary and depend on the manufacturer. Imports from Taiwan are cheaper and just as reliable as the other brands. The estimated prices for 1993 are the following :

RPA - 1

Aircraft frame	R 2 000
7 Channel FM radio	R 2 000
50 cm^3 Four stroke engine	R 3 500
B/W Video camera	R 1 500
TV transmitter	R 1 000
TV receiver (video recorder)	R 2 000

Monitor	R 1 500
Infrared thermometer	R10 000
Accessories - batteries, field box, fuelpump etc.	R 500
Total	**R24 000**

RPA - 2

Aircraft frame	R 2 000
7 Channel FM radio	R 2 000
30 cm^3 Two stroke engine	R 1 500
Selfstarter unit	R 1 500
Video camcorder	R 4 000
TV transmitter	R 1 000
TV receiver (videorecorder)	R 2 000
Monitor	R 1 000
35 mm autowind reflex camera with wide angle lens	R 2 000
Total	**R17 000**

RPA - 3

Aircraft frame	R 1 500
7 Channel FM radio	R 2 000
15 cm^3 Two stroke engine	R 700
35 mm autowind reflex camera with wide angle lens	R 2 000
Total	**R 6 200**

RPA - 4

Aircraft frame	R 500
5 Channel FM radio	R 1 200
10 cm^3 engine	R 600
Automatic camera	R 600
Total	**R 2 900**

RPA - 5

Aircraft airframe	R 2 500
7 Channel FM radio	R 2 000

62 cm^3 two stroke engine	R 1 800
Selfstarter unit	R 1 500
TV transmitter	R 1 000
TV receiver (video recorder)	R 2 000
Monitor	R 1 000
Multispectrum video camera	R25 000
Total	**R36 800**

Extra items which could be added but not a necessity :

Auto pilot system	R 2 500
Parachute	R 1 000

3.1.7 Comparison of model aircraft to large aircraft for aerial photography

The total cost of a 2 m wingspan model aircraft (trainer type) fitted with a wide angle lens automatic camera will be about R6000 (RPA-3). With this system clear colour or infrared photographs can be obtained of agricultural crops. The fuel consumption of such a type of aircraft is ± 1 litre per hour costing R5 per litre. The aircraft can also be transported by trailer or small truck to the site to be photographed. Only short landing strips are needed which could be a dirt road of 50 x 5 m. For detailed aerial photography, the model aircraft can be flown slowly at low altitudes of 25 to 100 m. Should there be an engine cut in the air, the aircraft can be glided to a suitable area for landing. Damage caused by crash landings can be quickly repaired using fast drying glues and balsa wood.
When looking at conventional large aircraft, the cost of aerial photography can be high. First the camera must be mounted on the aircraft facing vertically to the ground. A special bracket is also needed to mount the camera on the aircraft. High wing aircraft such as Cessnas are fitted with wing struts which are suitable for mounting cameras. Some remote control device will also be needed to trigger the camera from the aircraft cockpit. To hire a Cessna-type aircraft with its pilot, will cost R600 - R800 per hour. The pilot must also be skilled to fly the aircraft slow enough at low altitudes eg. 50 - 60 km/hour and 50

to 100 m above the ground. Normally the flying speed of a large aircraft must be kept around 80 km/hour to prevent stalling. This makes aerial photography at low altitudes more difficult. A micro-light type of aircraft can be used for slow speed flying but they are again affected by winds and updrafts. Should the aircraft have an engine failure at low altitude, which the micro-lights are prone to, the pilot and photographer will be endangered. To own a big aircraft is costly and prices can range from R150 000 (Cessna-type) to R30 000 (micro-light type). A flying licence and medical fitness are also required and can cost R10 000 to obtain. The aircraft has to be serviced on an annual basis which is also costly and can range from R1 000 to R5 000. Insurance cost can also be high. Although model aircraft also require some skill to fly, training is inexpensive and can be done at model flying clubs for a mere membership fee of ± R60 per year. Model aircraft can be flown to a maximum height of 600 m when they become difficult to see. Area coverage by one photograph using a wide angle lens will be ± 70 ha. The most suitable height to fly a model aircraft is about 50 to 300 m covering 5 to 25 ha per photograph. The remote control radio has a range of 1 km and about 200 ha can be photographed on a flight survey. If a larger area eg 500 ha is to be photographed, a large aircraft will be needed to fly at higher altitudes.

3.1.8 Requirements and maintenance for aerial surveillance by RPA's

Aerial photography using remote control aircraft requires some experience. Knowledge of model aircraft construction is important in building an aircraft for photographic use. As with large aicraft intensive training is needed in flying the aircraft and the more experienced the pilot, the safer his flying will be. Cameras and other onboard electronic equipment on the aircraft are effected by engine vibration. The onboard equipment should be safely wrapped in spongy material to damp the vibration effect. Rubber mounts on the engine also help to overcome this problem. Some basic knowledge of cameras such as ASA speed of the film and camera F-stop, is needed to take clear pictures. The focal length of the camera is normally set to infinity. See ¶ 3.1.2 for further details.

A good workshop and storage area are also needed to build and maintain aircraft and equipment. When using video equipment on the aircraft a good quality monitor and video recorder are needed for editing. Depending on the size of the aircraft, such as quarter scale types with 2.5 m wingspan, a large trailer is needed for transporting the aerial surveillance equipment to the research site. Usually one or two helpers are also needed on the ground to setup the aircraft and electronic surveillance equipment. While the pilot is preparing to fly the aircraft these helpers are used to setup markers on the ground . When assessing moisture stress on crops, temperature measurements have to be recorded by the research team. The ground operater controlling the video equipment has to keep a lookout and warn the pilot of large aircraft approaching the area which is important for general safety.

Some important notes on operating and maintenance of RPA's and electronic equipment are the following:

(1) The day before operation charge all aircraft- and video equipment batteries overnight.
(2) Check and secure all links on flying surfaces. Tighten engine bolts.
(3) Inspect the propeller for any damage and tighten the propeller nut.
(4) Inspect the fuel system and check the tank and fuel tubing for leakages. Check if the engine-glowplug is in order and that the glowplug driver battery is fully charged.
(5) Inspect the camera and see that the lens is clean and that the film is loaded. Set the camera correct for the prevailing light conditions. Before flying take one picture on the ground to see if the camera is working

properly.

(6) When using video cameras check if it is working before installing in the special spongy material on the aircraft. Camcorder cameras can also be used to record diectly in the aircraft . Check if the video tape is installed. Focus the camera on a nearby object at full enlargement. Then turn the enlargement setting to infinity.

(7) When using video transmittance from the air to ground check all electronic connections. In the most cases, poor video image transmittance is caused by bad wire connections. Vibration on previous flights can loosen these electronic connections. Sometimes oxidization on the connecting male/female plugs can also cause a poor image.

(8) Before flying check the wind direction and take note of obstacles such as trees, fences, telephone wires, animals, people, etc. which may be in the takeoff/landing area . Keep a strip of 5x50 m clear for landing the aircraft.

Radio control aircraft are not toys but miniature flying aircraft just as dangerous as large ones and safety precautions must be taken when flying.

3.2 Evaluation of crop water stress parameters

The RPA-1 as previously described in Chapter 2, was the main platform used for sensing moisture stress in different crops. An infrared thermometer and handheld thermometer were respectively used to measure the canopy- and air temperatures of the crops. Measurements were made on three crops viz. soybean, wheat and maize. Four seasons stretching from 1989 to 1992, were used to measure moisture stress conditions on soybean and wheat. Maize was planted only in 1989 and this season was used for canopy measurements. Infrared photography and videography was done mainly in the 1991 and 1992 season using the RPA-2, RPA-3 and RPA-5 as the main platforms. Graphs describing canopy measurements are presented in the Figures.

3.2.1 Comparison of aerial- and handheld infrared thermometers at different altitudes.

Figure 6.1 presents the ΔT (Canopy-minus Air temperature) measurements made by aerial surveillance at different altitudes on maize. In comparing the ΔT-measurements at 50 m and 200 m altitudes, only a slight difference was found. A t-test of the unpaired data showed the P-value to be 0.51 with mean difference at 0.82 which was not significant at 0.05 level. To be significant a mean difference of 2.46 was required. The 200 m showed a slightly higher value which could be explained by the larger area which the infrared thermometer measured viz. 10 m strips. At 50 m altitude, 2.5 m strips were covered. When flying at higher altitudes, air turbulence caused the aircraft to rock sideways and some radiation was picked up from the area outside the planted crop. This rocking effect could also be seen on the transmitted TV image. The soil of the outside veld area gave much higher Tc-values than the Tc on the crop and probably caused the higher Tc-values when flying at high altitudes. It was decided that an altitude of 50 m gave the most reliable Tc-measurements on the crop.

Aerial infrared thermometry was also compared with the handheld method measuring ± 0.5 m above the crop canopy of wheat. These results are represented in the ΔT-graph in figure 6.2. Only a slight difference was found between the methods, and a t-test of unpaired data showed P = 0.58 which was not signicant at the 0.05 level. Compared to the handheld infrared measurements, a much larger area was covered in a shorter time by the aerial method.

3.2.2 Canopy- and air temperature

The canopy temperature (Tc) was measured every second day during the growing season of the different crops. These measurements depended on the weather conditions such as rainy- and windy days. Because of these conditions, measurements could not always be obtained every second day and was only available for certain periods. On days when flying was not possible, the canopy temperature was measured on the ground.

3.2.2.1 Tc- and Ta- measurements on soybean

Measurements were made over four seasons (1989-1992) and all the information is given in figures 7.1.1 to 7.1.4. During the 1989 season, good rains in February and early March made collecting of data difficult. In the 1990 season, the air temperature was higher than the canopy temperature of the soybean. This was mainly caused by abundant rain which fell during this period. The air temperature fluctuated between 20°C and 30°C and the canopy temperature more or less followed this pattern. (figure 7.1.2). During the 1991 season, the air temperature stayed quite stable and some stress conditions started to develop on the stress blocks because of an increase of canopy temperature (figure 7.1.3). The 1992 season was very hot and dry and stress conditions developed quite rapidly.
Comparing all the seasons in figure 7.1, the 1992 season was the driest and the well watered soybean could be clearly differentiated from the stress blocks.

3.2.2.2 Tc- and Ta- measurements on wheat

The Tc- and Ta- data for wheat are presented in figures 7.2.1 to 7.2.4. Measurements on wheat during the 1990 season could not be followed through because of data lost due to the theft of the video tape which contained some of the data. For this reason the 1989, 1991 and 1992 seasons were compared. In 1989, the Tc- and Ta- values in figure 7.2.1 fluctuated according to the weather pattern. A sharp decrease in Ta during early September was caused by cold spells moving over the area. Ta dropped from 25°C to 19°C and increased again to 27°C. The Tc followed the same trend. During the 1991 season, the air temperature was much warmer although some sharp decrease in Ta was experienced on certain days (figure 7.2.3) The Tc- values of the different treatments also showed this fluctuation. The Tc in the 1992 season (figure 7.2.4), showed a gradual increase from August to

September. The Ta also followed this trend and was much lower than the previous season. The Tc was also effected by the sharp decrease in Ta on certain days.

Comparing all the seasons in figure 7.2, the canopy temperature of the wheat on the stress blocks showed the sharpest increase during 1991 and 1992. Tc of well watered (control) blocks stayed more or less the same for all seasons and depended most of the time on irrigation and air temperature. The canopy temperature alone did not give a clear indication of stress occurrence and some other indices had to be used to differentiate moisture stress conditions.

3.2.2.3 Tc- and Ta- measurements on maize

The temperature measurements were only available for 1989 season when maize was planted as a commercial crop. From figure 7.2.5 it can be seen that some hot days occurred early in February resulting in stress development on the maize crop. Tc of the stress blocks showed an increase compared to well watered control blocks. On the first 40 to 48 Julian days, both the control- and stress blocks showed a rapid increase which was caused by the increase in air temperature. The following week, cloudy and rainy conditions followed. Irrigation and temperature changes were not so drastic although the Tc on the stress blocks still increased.

3.2.3 Canopy temperature - minus Air temperature (ΔT)

The difference between Tc and Ta is a much better indication of developing stress conditions than Tc alone. By calculating the Tc-Ta value as the ΔT over the observed period, the results on the crops were graphically presented.

3.2.3.1 ΔT on Soybean

The ΔT values of soybean are presented in figures 8.1.1 to 8.1.4. Because of rain in February and early March, the best results were obtained in the first half of March during the 1989 season. From figure 8.1.1 one can see that the stress block showed positive values compared to the control block which was mostly negative. On the 14 March (day 73), the stress blocks showed a high ΔT- value. Rain on the following day caused the ΔT to decrease again to zero. ΔT remained much the same for the well watered blocks and never increased to values over 1. When studying the 1990 season, ΔT remained below the zero line for most of the time because of abundant rain which fell during February and March (figure 8.1.2). The only day when some stress condition did occur on stress block 1, was on the 27 February (day 58). Figure 9.1 shows the relative moisture level of the soil at 0-20 cm depth during the 1990 season. Some differences occurred between stress- and control blocks but were not always reflected in the ΔT- values. The period around day 55 when soil moisture was low for the stress block showed higher ΔT- values for the soybean. Figure 8.1.3 shows ΔT during late February and early March 1991. After some rain, the ΔT values on the stress blocks started to increase above the zero line from 6 March (day 66) to 13 March (74). The control blocks which received enough irrigation, remained well below the zero line. When these figures are compared with the relative soil moisture in fig. 9.2, a decline of soil moisture was also experienced on the stress blocks. Because of the hot conditions experienced during 1992 season, stress conditions occurred quite rapidly as can been seen in figure 8.1.4. After irrigation the ΔT values dropped back again below the zero line and slowly increased again as the crop was utilizing soil moisture and canopy temperatures started to increase. On the 13 February (day 44), the stress block experienced a sharp increase in ΔT up to a value of 13. During the 10 days following the 13 February stress conditions was quite high because of a shortage of water. During this period, there was a breakdown in the linear irrigation system and irrigation

scheduling could not proceed normally. A double amount of water had to be applied on the 24th February (day 55) to normalize soil moisture availability. ΔT decreased again to the zero line following this irrigation application.
When comparing all the graphs for the different seasons in figure 8.1, one can see that during hot dry seasons (1991 and 1992), ΔT gave the best indication of when stress conditions started to occur on soybean.

3.2.3.2 ΔT on Wheat

Figures 8.2.1 to 8.2.4 presents the Tc-Ta information of wheat during the 1989 to 1992 seasons. During the 1989 season, ΔT on the stress block 1 remained above the zero line. The control block gave negative ΔT values and remained below the zero line. The difference in ΔT values between stress block 1 and 2 was mainly the cause of different soil types. Soil under stress block 1 had a lower water holding capacity. ΔT values decreased normally after irrigation and slowly increased again as the Tc increased. During the 1990 season (figure 8.2.2), the SDD values showed the same pattern. ΔT started to increase until the time of irrigation. ΔT values in the most cases (except for stress block 1) never exceeded the zero line. During the 1991 season (figure 8.2.3), more or less the same pattern occurred. A substantial increase in ΔT was experienced on stress block 1 on the 13th September (day 256). The relative soil moisture values also showed a decline in soil moisture from 26 August (day 238) to 7 September (day 250). During the 1992 season, the ΔT values (figure 8.2.4), stayed most of the time below the zero line except for stress block 1. This type of pattern was also experienced in the previous year. When all the graphs in figure 8.2 are compared with one another, one can draw a conclusion that wheat is more resistant to moisture stress conditions. This could probably be a result of the colder winter conditions than the hotter conditions in which soybean is growing. The ΔT methods of detecting moisture stress was not so effective with wheat.

3.2.3.3 ΔT on Maize

Maize was only planted commercially in 1989. The ΔT graph in figure 8.2.5, gave a much better presentation of the development of stress conditions in this crop. Both stress and control blocks showed a rapid increase in ΔT. After irrigation, ΔT decreased back to the zero line. February gave the best results seeing that the maize was still growing actively towards the tassel stage. Because of thunder storms on some days, flying conditions were poor and measurements could not always be made. It was also difficult to measure the Tc of maize on the ground because of the height of the crop. At a young stage, the maize did not completely cover the ground and the soil itself influenced the IRT measurements.

3.2.4 Evaluation of Temperature Stress Difference (TSD) on crops

The TSD presents the difference in Tc between the stressed- and well watered (control) blocks. When measuring TSD, the reference plot that is well watered must be in close proximity to a field that is stressed. The TSD compensates for environmental effects such as vapour pressure deficit in air temperature with the use of the well watered plot as a reference. Not enough data was available to analyse TSD on maize.

3.2.4.1 TSD for Soybean

The TSD for soybean during the 1989 season (figure 10.1.1), showed sharp differences between irrigation periods. During 14 March (day 73), the TSD increased to 6+ and decreased again to 0.3 after sufficient rain fell. During the 1990 season (figure 10.1.2), the same differences was experienced between the irrigation treatments especially on replicate 1. On the 27 February (day 58), the TSD increased on replicate 1 to 5.1. In comparison with the SDD in figure 8.1.2, a high stress condition existed on this replicate at that date. In figure 10.1.3 which presents the TSD for the 1991 season, a gradual increase of the

TSD was experienced on the two soybean replicates. Replicate 1 increased to a value of 7.1 on the 13 March which was mainly due to the large difference in Tc between the stress- and well watered blocks. When comparing TSD with the soil moisture values in figure 9.2, the soil moisture started to decrease while TSD increased up to 13 March (day 72). During the 1992 season (figure 10.1.4), the TSD of the soybean showed relative high values from 1 February to 13 February (day 30 to 44). Afterwards the TSD decreased again to lower values up to the end of February. During early February, the air temperature fluctuated and increased to a maximum of 37°C on the 5th February (day 36). It declined again sharply on the 13th February (day 44) to 28°C and stayed low for a while up to the 23rd February when it started to rise again. This change in temperature with added irrigation caused the dip in the TSD on figure 10.1.4 between day 44 and day 64. Comparing all the seasons in figure 10.1, the TSD was able to differentiate between different days of irrigation and developing stress conditions.

3.2.4.2 TSD for Wheat

TSD data obtained for wheat during seasons 1989 to 1992, is recorded in figures 10.2.1 to 10.2.4. As in the case of soybean, irrigation and developing stress conditions played a significant role in effecting the TSD value for the different seasons. Minimum values of up to -0.5 and maximum values of up to 6.7 were reached during the different seasons. During the 1991 and 1992 seasons, the TSD gave a good indication of when to start with irrigation applications. In figure 10.2.3 and 10.2.4 especially on replicate 1, stress conditions could be differentiated from non-stress conditions if one studies the irrigation history of each season. Comparing the TSD with ΔT, there seems to exist some relationship between the two indices on wheat. When studying figure 10.2.3 and 8.2.3 of the 1991 season, the TSD, especially on replicate 1, followed the same trend as the ΔT. Differentiation on different days following irrigation was much clearer as in the case of ΔT. The same also applied to most of the other seasons. As in the case of ΔT, the TSD only helped in differentiating stress and non stress conditions in wheat, but still has to be further evaluated to find a cut-off point for irrigation scheduling.

3.2.5 Crop Water Stress Index (CWSI)

Because of the availability of measurements of air vapour pressure deficit during the 1991 season, the CWSI was evaluated for both soybean and wheat crops. The CWSI values are presented in figures 11.1 and 11.2 and were calculated using the baseline equations in figures 12.1 and 12.2 for soybean and wheat respectively. The procedure is described in 2.4.2.

3.2.5.1 CWSI on Soybean

After all the treatments received irrigation on day 56, the CWSI for both treatments remained below the zero line for eight days (Figure 11.1). Thereafter, on day 66, the CWSI for the stress blocks increased gradually above the zero line up to day 72 while the control blocks remained below the zero line. Comparing these results with soil moisture in figure 9.2, the soil moisture was depleted as CWSI increased. The control blocks remained in the high moisture zone while the CWSI remained below the zero line. Comparing these results with ΔT and TSD, the same trend was followed by the CWSI. The CWSI values varied between -0.25 and -0.1 (stress blocks) and -0.45 and -0.25 (control blocks) during the first eight days of available soil moisture. After this period, the CWSI values varied between -0.1 and 0.55 (stress blocks) and -0.53 and -0.28 (control blocks) for the next eight days. As in the case of previously discussed indices, the CWSI gave a good indication of developing stress conditions on soybean and a value above zero could be used for irrigation scheduling. When the CWSI was correlated against Julian days over the 16 days, regression analysis gave a correlation coefficient of 0.70.

3.2.5.2 CWSI on Wheat

Figure 11.2 and 12.2 represents the CWSI and water-stressed baseline for wheat during the period August to September 1991. CWSI values stayed well below the zero line except for stress block 1 from day 238 to 252. From day 254 there was a sharp increase in CWSI on stress block 1 reaching a value of 0.44 on day 256. After irrigation the CWSI decreased again to 0.06. The difference between the two stress blocks was the result of different soils underlying the blocks as previously explained. On the control blocks, the CWSI stayed below zero and varied between -0.61 and -0.09. When comparing the CWSI on wheat with ΔT on wheat in figure 8.2.3, both indices followed more or less the same pattern. On day 250 the relative soil moisture value in figure 12.2 showed lower values than on day 238. The CWSI also differed on the different treatments during these days.

3.2.6 Regression analysis of treatments on soybean and wheat for the different seasons

All the data collected for TSD, Tc and ΔT were tabled and statistically correlated. The Tc and ΔT presented the stress blocks.

Except for 1990 season, the TSD correlated significantly with canopy temperature (Tc) and ΔT. Tabling all the results and running a regression analysis, also showed that TSD correlated highly significantly with Tc and ΔT. The same applied when all the results were totalized over the 1989-92 season. TSD correlated significantly with Tc and ΔT (Table 1).

Table 1 Correlation and regression coefficients for TSD vs TC and ΔT on soybean- and wheat stress blocks

Crop	Season	Coeficient of Determination (r^2)	
		TSD/Tc	TSD/ΔT
SOYBEAN	1989	0.95**	0.90**
	1990	0.05	0.42**
	1991	0.91**	0.90**
	1992	0.74**	0.36*
	1989-1992	0.51**	0.47**
WHEAT	1989	0.52**	0.19
	1990	0.47**	0.74**
	1991	0.45**	0.64**
	1992	0.05	0.27
	1989-1992	0.15	0.47**

** **Highly significant .01 level**
* **Significant .02 level**

From these results it can be concluded that the indices TSD and ΔT can be used with confidence to estimate moisture stress conditions on crops such as soybean and wheat. It should be mentioned that quantifying the absolute values for irrigation needs, was not expected of the current research program .

3.2.7 Colour Infrared Photography (CIR)

Colour infrared film has been shown to be sensitive in both visible (0.5μm - 0.75μm) and near-infrared (0.75μm - 0.9μm) spectrum regions for plant stress. The aim of the study with infrared photography was to assess moisture stress in crops by image processing on computer and compare the results with canopy temperatures as measured with an infrared thermometer. The computer processed image was classified by supervized image processing (MIPS), into different categories viz. low moisture stress (green) medium moisture stress (red) and high moisture stress (blue) using image processing software.

3.2.7.1 Moisture stress conditions on soybean as classified by image processing

The experimental area as described in ¶ 2.3 was used as the surveillance site for CIR aerial photography. The 1991 season for soybean was used for this investigation. CIR photographs were taken of the crop at an altitude of 200 m on different dates under different irrigation treatments. Figure 13.1 shows the experimental layout of the treatments. The photographs were taken more or less a week apart. These images were computer processed so that a classification map containing three moisture stress categories could be plotted on a colour image printer. The various stages of moisture stress in the experimental blocks were compared to the canopy temperature and the ΔT in figure 8.1.3 by using supervized image processing.

(i) Day 61 - 28 February 1991

In the beginning of the period of the study, which stretched from 26 February to 13 March, all experimental blocks received irrigation. Figure 13.2, which presents the classification map on Day 61, showed that the control blocks were under low moisture stress. The moisture stress blocks were divided into some moderate stress and low stress conditions. Stress block 1 showed more stress development than stress block 2. Comparing this with ΔT in figure 8.1.3, one can see that the stress blocks had lower negative values than the control blocks. Both the treatments had ΔT values below the zero line. Canopy temperatures for the control blocks were averaging around 26°C while the stress blocks were around 27.3°C.

(ii) Day 68 - 6 March 1991

About a week later, the ΔT values of the stress blocks increased with stress block 1 reaching a value of 1 (figure 8.1.3). Figure 13.3 showed that moisture stress had spread in the stress blocks with both blocks 1 and 2 having larger areas of moderate stress. Some high stress areas also appeared in stress block 1. When measuring the canopy temperature (Tc) of these high stress areas, they appeared to be around 33.5°C which was well above the moderate stress areas of 27.9°C to 28.4°C. The control blocks which were mostly classified as low moisture stress, registered much lower Tc-values of 23.5°C to 24.9°C. Compared to figure 13.2, moisture stress developed over a larger area in figure 13.3. This trend could also be seen in the increasing ΔT-value of figure 8.1.3.

(iii) Day 74 - 13 March 1991

Figure 13.4 shows a much larger area to be under moisture stress, especially stress block 1. Moderate stress conditions also started to develop in control block 1. High moisture stress also spread over a large area in stress block 1 compared to stress block 2. The reason for stress block 1 being under larger stress conditions, was due to difference in underlying soil having a lower moisture holding capacity. Figure 8.1.3 showed that the ΔT-values also correlated well with the developing stress conditions in the classified map. The difference between the stress blocks can also be seen in Figure 10.1.3 which presents the TSD value for the different treatments.

3.2.7.2 Quantification of moisture stress areas on soybean using image processing

Table 2 presents the percentage area occupied by the different class categories as measured on 6 and 13 March 1991. Although the variation between the two replicates was high, the stress blocks showed higher areas of moisture stress after a week. On especially the stress block 1, high moisture stress occupied 48.7% of the total area of the experimental block while in the control block 1, only 6.9% of the total area was occupied by high moisture stress.

Table 2 Percentage moisture stress area of soybean occupied on the classified image for 6 and 13 March 1991

Treatment	Percentage of moisture stress - class category					
	6 March			13 March		
	Low	Moderate	High	Low	Moderate	High
Control 1	27.3	70.7	2.3	18.9	74.1	6.9
Control 2	88.8	10.7	0.5	53.3	43.9	2.7
Stress 1	5.1	85.6	9.4	0.0	50.9	48.7
Stress 2	37.9	59.3	2.9	23.2	70.7	6.1

After assessing the stress conditions of soybean in the field, it seemed that some other factor also contributed to the incidence of high moisture stress on block 1. A count of fungi was found to be exceptional high in this block. With higher moisture stress conditions, the fungi population increased, enhancing the stress conditions on soybean.

3.2.7.3 Moisture stress conditions on wheat as classified by image processing

The 1992 season for wheat was used because of a better quality CIR photograph produced during this season. Figure 14.1 shows the layout of the wheat experiment with different treatments. The various stages of moisture stress on the different treatments, were also compared with canopy temperature and ΔT values given in figure 8.2.4.

(i) Day 218 - 5 August 1992

Irrigation was applied to all the treatments on this day. The classification map in figure 14.2 shows that all the treatments were under low moisture stress conditions. When compared with figure 8.2.4, the ΔT values for all treatments were below the zero line. Canopy temperatures for the different treatments were more or less the same at 17.2 to 17.9°C. Stress block 1 gave a slightly higher Tc of 17.9°C.

(ii) Day 226 - 13 August 1992

About a week later, some stress conditions started to occur on the stress blocks. Figure 14.3 shows the spatial coverage of these stress conditions for the treatments. Stress block 1 showed the major difference with moderate stress being quite extensive. High stress conditions also started to occur at the bottom end of stress block 1. Stress block 2 showed only a small amount of moderate stress occurring on this treatment. Control block 2 showed more moderate stress conditions occurring at the bottom left end. These differences between the two replicates were explained earlier as being caused by soil types. Comparing this with figure 10.2.4 which presents the TSD values of the two replicates, these differences are clearly defined on day 226. The ΔT values in figure 8.2.4 also shows a difference between the different treatments which was found on the processed CIR image.

3.2.7.4 Quantification of moisture stress areas on wheat using image processing

From the percentage area of each category class occupied on the processed image of 5 August, one can see in table 3 that low moisture stress was more or less the same for all treatments. On this day, all treatments received irrigation water after some stress conditions existed the previous weeks. Moderate and high stress conditions were low on all the treatments. After a period of a week (on 13 August) the spatial variation of moderate and high stress conditions occupied a larger area in stress block 1.

Table 3 Percentage moisture stress area occupied on the classified images for wheat on 5 and 13 August

Treatment	Percentage of moisture stress class category					
	5 August			13 August		
	Low	Moderate	High	Low	Moderate	High
Control 1	90.6	6.0	3.4	83.2	13.8	2.9
Control 2	91.3	7.0	1.6	95.8	2.9	1.2
Stress 1	82.4	5.2	12.4	29.3	44.2	26.5
Stress 2	90.8	4.5	4.7	88.1	9.1	2.8

Conditions on the other treatments remained more or less the same. Stress block 1 showed an area of 44.2% occupied by a moderate stress class. On stress block 2, only 9.1% area was occupied by the moderate stress class. This again showed the effect of underlying soil playing a role in supplying available water as discussed previously. The ΔT values in figure 8.2.4, also followed the same trend on these two days.

3.2.8 Videography

The major disadvantage of video-imagery is its relative low resolution when compared with CIR film. Because the use of multispectral videography in South Africa is still new, especially for evaluating moisture stress, much testing had to be done to obtain usable results. The multispectral video camera was tested on two crops during the beginning of the 1993 season. These were maize and soybean. Unfortunately, due to poor weather conditions and problems with the RPA-5, the best results were obtained only on 28 January 1993 for both maize and soybean. In comparing all the images by using different filters as explained in ¶2.2.3, the best resolution to moisture stress on the crops were obtained with filter 853 nm and >853 nm. Both these filters operated in the near infrared range. After images were obtained on video tape, they were scanned into the computer and framegrabbed. These images were stored on the hard disc of the computer. The images were processed using the suitable software. Colour maps were made in which percentage moisture class categories were mapped out. These categories were low stress - green ; moderate stress - red and high stress - blue. The area of each class category were calculated as a percentage of the total area of an experimental block. These values were tabled and compared with the different filters used on the video camera.

3.2.8.1 Moisture stress conditions on soybean as classified from the video images using the 853 nm and >853 nm filters

Colour classification maps of soybean on 28.1.93 are presented in figures 15.1 and 15.3 for the filters 853 nm and >853 nm respectively. From these images one can see that the video camera was sensitive enough to differentiate between the well watered and stress blocks planted to soybean. The canopy temperature (Tc) also differed with about 5°C between the control and stress blocks.

Table 4 Percentage moisture stress area occupied on the classified images for soybean using 853 nm and >853 nm filters

	Percentage of moisture stress class category					
	Filter 853 nm			Filter >853 nm		
Treatment	Low	Moderate	High	Low	Moderate	High
Control block	91.7	7.5	0.8	80.7	18.3	1.0
Stress Block	6.5	88.6	4.4	7.5	60.3	32.3

When studying the percentage moisture class categories in table 4, it seems that the control block gave more or less the same percentage spatial coverage for both two filters used on the multispectral camera. On the stress block there was some difference between the two filters. The filter > 853 nm detected a larger high stress category than the 853 nm filter viz 32.3% against 4.4%. It could be that the computer classified some of the categories in separate classes. When looking at stress conditions as a moderate class, both the total value on the stress block differed. (88.6% - 853 nm and 60.39% - >853 nm.

3.2.8.2 Moisture stress conditions on maize as classified from the video images using the 853 nm and > 853 nm filters

The colour classification maps are represented in figure 15.2 and 15.4 for the >853 nm and 853 nm wavelengths respectively. When studying the colour maps, it seems that the 853 nm filter detected a larger low stress (green) condition than the >853 nm filter on both control and stress blocks. Image 15.2 was photographed at a higher altitude than image 15.4. It could be that the multispectral camera was more sensitive to stress conditions at a lower altitude. This condition was also found when photographing on CIR film. High altitudes produced lesser sensitivity than lower altitudes. Nevertheless, both filters were still able to differentiate between the stress and control blocks. (Compare figures 15.2 and 15.4)

Table 5 Percentage moisture stress area occupied on the classified images for maize using 853 nm and >853 nm filters

	Percentage of moisture stress class category					
	Filter 853 nm			Filter >853 nm		
Treatment	Low	Moderate	High	Low	Moderate	High
Control Block	70.9	25.9	3.1	55.6	40.8	3.5
Stress Block	18.8	46.5	34.6	2.1	68.6	28.3

From table 5, it appears that a higher percentage of the moderate category class (red) is found on the >853 nm image than the 853 nm in both the control and stress block. It is interesting to see that the high stress categories do not differ much between the two filters.

CHAPTER 4

OTHER APPLICATIONS

Allthough not in the terms of reference for this project, assessment of other conditions and related parameters on crops by colour infrared photography and image processing were investigated.

4.1 Assessment of stress conditions on tree crops

Estimating environmental stress conditions of agricultural crops can sometimes be difficult on large cropping areas. Aerial imaging systems have been effectively utilized in the past for monitoring crop conditions (Myers et al.,1983). Hoffer (1989) evaluated the versatility of CIR aerial photography for resource managers to assess various crop conditions. Chlorosis on citrus groves, which indicated nutrient disorders, was also detected by Hart et al. (1988) using CIR photography and videography. Stutte et al. (1988) used infrared reflectance data to assess cumulative stress in fruit trees. They found that percentage leaf nitrogen content of individual peach leaves and orchards correlated well with their infrared image intensities. Blazquez (1989) used spectral densitometer measurements and computer processing on CIR transperancies of citrus orchards to distinguish between healthy, diseased and dead trees.

The use of low altitude aerial photography using remotely controlled aircraft carrying a camera system has been reported to be an inexpensive method for obtaining good quality CIR aerial photographs for photo interpretation (Fouche' and Booysen, 1989). Visual photo interpretation however, can sometimes be labourious and tedious especially of citrus orchards which could contain a few thousand trees. This report therefore evaluates the application of low altitude photography from remotely controlled aircraft and image computer processing techniques as a quick method to classify and quantify stress areas in crops such as citrus, avocado and cashew nut.

4.1.1 Citrus affected by Rootrot disease.

A 15 year-old lemon orchard was photographed from an altitude of 50 m using the RPA-2 unit. The area coverage by a single transparency was 2.0 hectare. Groundtruth of the grove showed that the trees were severely stressed because of rootrot infestation (Phytophthora sinensis). Two rows of trees (14 per row) having both healthy and stressed trees were selected for analysis. The total perimeter and area of each tree was measured on the CIR image and recorded in a text file. These areas were also measured in square meters and subtracted from the total area to estimate the tree area affected by rootrot disease. Healthy areas of each tree were classified by using MIPS-feature mapping. Tree canopy was taken as a flat polygon on the image. The whole image was then feature mapped by image processing and coloring all "healthy" areas in blue (see figure 16). In this process a healthy tree, No. 8, was used as a control for pixel colouring.

Healthy areas of trees classified as blue polygons were measured using a sub-program in MIPS and stored in a text file. Tree health on the ground was rated according to a disease index of 0 (healthy) to 10 (dead) as described by Darvas et al. (1984) for avocado trees. Two rows of trees were numbered 1 to 28 and analysed by measuring their total surface area on the image. These areas were also stored in a text file. In Table 6, the percentage rootrot affected surface area of a tree was calculated by subtracting the healthy area from the total area and expressing this value as a percentage of the total tree area. From Table 6 it is evident that most of the trees were severely stressed because of Phytophthora sinensis, with some trees as high as 89%. A ground check showed that the predicted value of % rootrot affected area by image processing, correlated significantly (R=0.88) with the tree health index.

Table 6 Computer printout of a lemon grove showing tree number, total canopy area, healthy canopy area and percentage rootrot affected area on trees.

Tree No.	Total canopy area (sq.m.)	Healthy canopy area (sq.m.)	Rootrot affected area sq. m.	%
1	17.75	9.37	8.38	47.2
2	25.55	21.48	4.07	15.9
3	13.35	6.64	6.71	50.3
4	22.98	15.43	7.55	32.9
5	24.63	20.65	3.98	16.2
6	11.11	4.64	6.47	58.2
7	11.20	6.05	5.15	46.0
8	**22.98**	**19.74**	**3.24**	**14.1**
9	14.27	8.05	6.22	22.9
10	19.16	11.94	7.22	37.7
11	20.16	10.53	9.63	47.8
12	20.32	11.28	9.04	44.5
13	24.30	17.50	6.80	28.0
14	14.93	9.04	5.89	39.5
15	9.87	2.74	7.13	72.2
16	13.19	4.06	9.13	69.2
17	22.98	13.44	9.54	41.5
18	12.94	5.47	7.47	57.7
19	11.70	2.65	9.05	77.4
20	10.78	2.65	8.13	75.4
21	21.07	11.94	9.13	43.4
22	15.51	5.81	9.70	62.5
23	**9.46**	**1.00**	**8.46**	**89.4**
24	**8.71**	**1.41**	7.30	83.8
28	17.34	14.35	2.99	17.2

4.1.2 Phytophthora stress on Avocado

CIR photographs were obtained by photographing two blocks of an Avocado orchard infested by rootrot disease (**Phytophthora cinnamomi**) at an altitude of 150 m. The images were processed by MIPS software to estimate the percentage Phytophthora infestation in the orchard. The orchards were classified into a normal- and stressed category.Canopy area of the two classes were calculate into hectare and percentage.

Table 7 Percentage area of avocado orchards affected by Phytophthora disease

	Total canopy area (ha)		**Rootrot affected area (%)**	
Tree condition	**blk A**	**blk B**	**blk A**	**blk B**
Normal	2.5	3.8	57.7	56.7
Stressed	1.8	2.9	42.5	43.2

From Table 7, which presents the percentage canopy surface area affected by the rootrot disease, it is evident that about 42.5% of the surface area of the trees in block A and 43.2% in block B were infested with this disease. This gave a good and quick indication of areas that need to be treated by fungicide to control the disease.

4.1.3 Evaluation of fungicide treatment on cashew nut.

Part of a cashew nut orchard which suffered from a root disease, was treated with injections of a fungicide to control the root disease. Trees which received chemical treatment were compared with untreated trees by using remote sensing and image processing. Images were processed into two categories and the canopy surface area of healthy and unhealthy areas calculated.

Table 8 Observations on chemical control or root disease in a cashew nut orchard.

Treatment	healthy canopy area sq.m.	%	rootrot affected canopy area sq.m.	%
Untreated trees(10)	612	60.0	404	40.0
Treated trees(10)	907	81.3	207	18.6

The processed image showed that that part of the orchard was affected to a certain degree with rootrot disease. Seven rows of the trees were subsequently treated with fungicide and the entire area was photographed after six months. In table 8 the treated trees showed a lower incidence of the disease (18.6%) compared to the untreated trees (40.0%). From this study it could be concluded that chemical treatment by fungicide injection improved tree condition and the stress condition could be assessed by remote sensing.

4.2 Nutrient disorders on crops.

4.2.1 Phosphorus fertilizer trial on wheat.

A soil known to have a P-deficiency was fertilized with different P-carriers and planted with wheat. The P-carriers used were superphosphate (calcium rich phosphate), calmafos (magnesium rich phosphate) and langfos (sedimentary rock phosphate). Each P-carrier was applied at rates of 50, 100, 150 and 200 kg/ha on blocks measuring 10 x 10 m. A control treatment which received no phosphorus fertilizer was also included in the field trial. A blanket treatment of 25 kg K/ha and 50 kg N/ha was applied to all the blocks. Treatments were triplicated and randomized into 40 blocks. Since the experimental site was large, a part consisting of 24 blocks in which each treatment was duplicated, was used for aerial CIR photography and computer processing. The experimental site was photographed at an altitude of 50 m and transparencies scanned into the computer for processing by MIPS. Crop yield and soil-P analysis were also recorded.

Table 9 The affect of different phosphorus-fertilized treatments on the yield of wheat and soil - P status.

Phosphorus Fertilizer	Treatment		Yield (kg / ha)	Extractable Soil - P (ppm)
	No	Kg/ha		
Control	1	0	860	5
Superphosphate	2a	50	<u>**4 320**</u>	<u>**16**</u>
	2b	100	<u>**4 721**</u>	<u>**28**</u>
	2c	150	<u>**5 032**</u>	<u>**19**</u>
	2d	200	<u>**4 361**</u>	<u>**78**</u>
Calmafos	3a	50	2 262	12
	3b	100	2 981	21
	3c	150	3 034	36
	3d	200	2 722	29
Langfos	4a	50	1 870	11
	4b	100	1 821	15
	4c	150	2 453	29
	4d	200	2 911	42

Differences could be clearly seen between all treatments in the computer classification of the CIR image. From Table 9 it is evident that the superphosphate fertilized treatments gave the best response in total yield of wheat and also increased P in the soil. The CIR image also showed superphosphate to affect the wheat foliage color, giving it a more reddish color.

Table 10 Percentage area of each P-category occupied in the classified images of the different P - treatments.

P-treatment		% P-Category		
		Low-P class	Med-P class	High-P class
Control		90	8	2
Super-P	50kg/ha	3	19	78
	100kg/ha	2	40	58
	150kg/ha	5	28	67
	200kg/ha	8	27	65
Calmafos	50kg/ha	15	63	22
	100kg/ha	18	45	37
	150kg/ha	12	46	42
	200kg/ha	14	46	40
Langfos	50kg/ha	28	46	26
	100kg/ha	19	63	18
	150kg/ha	21	43	36
	200kg/ha	16	45	39

On the classified image, three categories were identified viz. high - P (green), medium - P (red) and low - P (blue). In Table 10, which presents the % area of each P-category occupied in the classified image, the superphosphate treatment gave the highest % area occupied by the "High-P class" category when compared to the other treatments. When the % "High-P class" in each P-fertilizer treatment was correlated with the yield of wheat, a significant correlation coefficient (R=0.95) was found. The "Low-P class" again showed a negative correlation with wheat yield.

CHAPTER 5

CONCLUSIONS AND RECOMMENDATIONS

5.1 The use of radio control aircraft

Low altitude large scale reconnaissance by remote control aircraft has shown to be an economical way for aerial surveillance of crop moisture stress and other related stress conditions on different agricultural crops. The use of remotely piloted aircraft for aerial surveillance is also much cheaper than conventional aircraft. Small isolated areas can quickly be covered and visual information obtained by aerial video- or photography. The RPA's which have been described in this report are relative inexpensive, small and easily transported by truck or trailer to the area to be surveyed. Using failsafe systems such as an onboard parachute, autopilot and selfstarter, flying these aircraft is safer and easier. Experienced radio control pilots are available at radio control flying clubs all over the country and can be used at reasonable rates to fly radio control aircraft as research tools.

5.2 Assessment of moisture stress on crops

Under moisture stress conditions, plants produce changes in their physiological status which result in shifts in the infrared spectral reflectance of the canopy. Spatial variation of moisture stress can be detected in the prevailing crop by colour infrared aerial photography and image processing on computer. The infrared images are classified into mosture stress classes using an image processing software program (MIPS). Classification is done under supervised image intrepretation by comparing images of a well watered crop with moisture stressed crops. By comparing the results of infrared photograph image processing to canopy temperature related indices, such as Δ T, CWSI and TSD, areas of moisture stress, can be assessed on different short term crops for their crop water requirements. By refining this method, especially with the use of infrared videography, a more timely assessment of crop water stress development can be made. Combining videography with infrared thermometry may well be a useable tool in the future for irrigation scheduling.

5.3 Nutrient and disease stress on crops

Using inexpensive 35 mm colour infrared photography at low altitude by remote control aircraft, a good quality positive transparency is produced which can be scanned into a desktop computer for image processing with low cost image processing software such as MIPS. Screening and monitoring long term crops such as citrus and avocado, can be done to detect nutrient and disease disorders. Aerial infrared images of different crops on farms can be kept and compared over time for maximum crop use efficiency such as plant density, crop growth, nutrient disorders, irrigation efficiency, crop yield, fertilizer, insecticide application etc. With the availability of low cost colour super VGA computers today, the farmer can also link relevant information of crops to the aerial infrared image by using GIS software on the computer. Crop monitoring can also be done on a timely basis to estimate crop productivity and yield.

5.4 Recommendations for future research

Results of the study indicate that the use of low altitude aerial colour infrared photography obtained from remotely controlled aircraft and image processing computers, can be a relative inexpensive technique to assess crop stress conditions.

It is hoped that the applications generated by the project will continue along two distinct paths, viz:

5.4.1 Technology transfer

The use of remote controlled aircraft as a platform for remote sensing should by used in practice because of its inexpensiveness and ablity for low altitude aerial surveillance properties. This should fill the gap between large aircraft used for high altitude aerial surveillance and remote satellite imagery. The technology lends itself for practical use in assessment of stress conditions on crops grown on small areas viz 5 to 50 hectare for example on the following:

* Assessment of crop water stress development on centre pivot irrigation systems by using infrared videography combined with infrared thermometry for timely irrigation scheduling or testing existing irrigation scheduling models.

* Checking tree crops such as citrus or avocado by infrared aerial photography for root related diseases resulting from over irrigation and poor soil drainage.

* Monitoring the effectiveness of distributing water soluble fertilizers such as nitrogen through irrigation systems on short term crops viz maize, soybean and wheat by colour aerial videography.

* Using computer processed aerial infrared images of long term tree crops such as citrus as a useable tool for recording orchard condition over different seasons.

* Infrared aerial videography can be used to monitor pollution of dams over time.

* Water leakage from underground pipes could be observed at low altitudes using infrared photography and computer processing.

* Soil erosion and donga formation could be studied and monitored effectively at low altitudes and recorded by video for soil conservation.

* Areas of soil salinization especially on crops such as irrigated sugar can be aerial photographed by infrared cameras and mapped out using computer processing.

5.4.2 Recommended future research.

* To develope a cost effective irrigation scheduling system using aerial surveillance by near-, mid- and thermal infrared video cameras.

* To compare results of crop water stress as observed by infrared video cameras and Landsat TM satellite data.

* To evaluate new aerial photographic platforms such as remote controlled balloons.

CHAPTER 6

REFERENCES

BENZON, G.J. 1983. An improved remote piloted aircraft for ultra low volume aerial application. MS. Thesis. Univ. of Delaware. Newmark. USA.

BERRY, C. 1991. Cyclops RPV system. RCM modeler, Nov. 1991., pp 138-144.

BOYER, M., MILLER, J., BELANGER, M., HARE, E., and WU, J. 1988. Senescence and spectral reflection in leaves of northern pin oak. *Quercus polustris muenchu.* Remote sensing Environ., 25 : 71-87.

BLAZQUEZ, C.H. 1989. Computer based image analysis and tree counting with aerial colour infrared photography. Proc. of the 12th Biennial Workshop on Colour Aerial photography and Videography in Plant Sciences. ASPRS., pp 149-163.

DARVAS, J.M., TOERIEN, J.C., and MILNE, D.L. 1984. Control of avocado rootrot by trunk injection with Phosethyl-Al. Plant Disease, 68 : 691-693.

DOMMERT, K.R., MAILANDER, M.P. and SISTLER, F.E. 1988. Remote sensing of waterflow patterns in shallow ponds using drones. First workshop on Videography. ASPRS., Falls church, Virginia. pp 248-255.

ESCOBAR, D.E., EVERITT, J.H. and DAVIS, M.L. 1988. Potential of mid infrared video imagery for use in irrigation management studies. Proc. first Workshop on Videography. ASPRS., Falls church, Virginia, pp 248-255.

EVERITT, J.H., ESCOBAR, D.E., ALANTZ, M.A. and DAVIES, M.R. 1987a. Using airborne mid-infrared video imagery for distinguishing plant species and soil conditions. Remote sens. Environ., 22 : 423-428.

EVERITT, J.H., ESCOBAR, D.E. and VILLARREAL, R. 1988b. Evalu ation of single band video and video band indices for grassland phytomass assessment. PE & RS., 54 : 1177-1180.

EVERITT, J.H., ESCOBAR, D.E., VILLARREAL, R., NORIEGA, J.R. and DAVIS, M.R. 1991a. Airborne video systems for agricultural assessment. Remote Sensing Environment, 35 : 231-342.

FOUCHÉ, P.S. 1986. Landbou navorsing met model vliegtuie. Landbou weekblad, 415, 30-32.

FOUCHÉ, P.S. and BOOYSEN, N.W. 1989. Remotely piloted aircraft for low altitude aerial surveillance in agriculture. Proc. 12th Biennial Workshop on colour aerial photography and videography in Plant Sciences. ASPRS., pp 277-283.

FOUCHÉ, P.S. and BOOYSEN, N.W. 1991. Assessment of crop stress conditions using low altitude aerial colour infrared photography and computer processing. Proc. 13th Biennial Workshop on colour aerial photography and videography in Plant Sciences. ASPRS., pp 18-27.

FOUCHÉ, P.S. 1993. Estimation of crop water stress on short term crops using low altitude aerial infrared thermometry and colour infrared photography. Proc. 14th Biennial Workshop on colour aerial photography and videography in Plant Sciences. ASPRS., (in press).

FUCHS, M. 1990. Infrared measurement of canopy temperature and detection of plantwater stress. Theor. Appl. Climatol., 41 253-261.

GARDNER, B.R., BLAD, B.L., GARRITY, D.P., and WATTS, D.G. 1981. Relationships between crop temperature, grain yield, evapotranspiration and phenological development in two hybrids of moisture stressed sorgham. Irr. Sc., 2 : 213-224.

GATES, D.M., KEEGAN, H.J., SCHLETER, J.C. and WEIDNER, V.R. 1965. Spectral properties of plants. Appl. Opt., 4 : 11-20.

GEISER, K.M., SLACK, D.C., ALLRED, E.R. and STRANGE. 1982. Irrigation scheduling using crop canopy minus air temperature differences. Trans. ASAE., 25 : 689-694.

GRANT, L. 1987. Diffuse and specular characteristics of leaf reflectance. Remote Sens. Environ., 22 : 309-322.

GOTTWALD, T.R. and TEDDES, W.L. 1986. MADDSAP - 1, A versatile remotely piloted vehicle for Agricultural research. J.of Econ. Entomol., 79 : 857-863.

HART, W.G., EVERITT, J.H., ESCOBAR, D.E., DAVIS, M.R., and GARZA, M.G. 1988. Comparing imaging systems for assessment of diverse conditions of agricultural resources. Proc. of the first workshop on Videography, ASPRS., pp 160-165.

HOFFER, R.M. and JOHANNSEN, C.J. 1969. Ecological potentials in spectral signiture analysis. Remote sensing in Ecology (P.L.Johnson Ed.) Univ. of Georgia Press, Athens. GA. USA.

HOFFER, R.M. 1989. Colour and colour infrared photography for vegetation assessment. Proc. of the 12th Biennial Workshop on colour aerial photography in Plant Sciences, ASPRS., pp 1-5.

HORLER, D.N.H. and BARBER, J. 1981. Principles of remote sensing of plants - in Plants and the Daylight Spectrum. (H.Smith, Ed.) Academic Press, New York.

HOWELL, T.A., HATFIELD, J.L., YAMADA, H., DAVIES, K.R. 1984. Evaluation of cotton canopy temperature to detect crop water stress, Trans. ASAE., 27 : 84-88.

IDSO, S.B., JACKSON, R.D. and REGINATO, R.J. 1977. Remote sensing of crop yield. Science, 196 : 19-25.

IDSO, S.B., JACKSON, R.D., PINTER, P.J., REGINATO, R.J. and HATFIELD, J.L. 1981a. Normalising the stress degree day parameter for environmental variability. Agric. Meteorol., 24 : 45-55.

IDSO, S.B., REGINATO, R.J., REICOSKY, D.C. and HATFIELD, J.L. 1981b. Determining soil induced plantwater potential depressions in alfalfa by means of infrared thermometry. Agron. J., 73 : 826-830.

JACKSON, R.D., REGINATO, R.J. and IDSO, S.B. 1977. Wheat canopy temperature : A practical tool for evaluating water requirements. Water Resources Res., 13 : 651-656.

JACKSON, R.D., IDSO, S.B., REGINATO, R.J. and PINTER, P.J. 1981. Canopy temperature as a crop water stress indicator. Water Resource Res., 17 : 1133-1138.

JACKSON, R.D., 1982. Canopy temperature and crop water stress. In : D.Hillel (Ed.). Advances in irrigation. Vol. 1. Academic press, New York, pp 43-85.

JACKSON, R.D., 1986. Remote sensing of biotic and abiotic plant stress. Ann. Rev. Phytopathol, 24 : 265-287.

KNIPLING, E. 1970. Physical and physiological basis for the reflectance of visible and near infrared radiation from vegetation. Remote Sens. Environ., 1 : 155-159.

MAUSEL, P.W., EVERITT, J.H., ESCOBAR, D.E. and KING, D.J. 1992. Airborne Videography : Current status and future perspectives. Photogram. Eng. and Remote Sensing Vol. 58, No. 8, pp 1189-1195.

MYERS, V.I., BAUER, M.E., GAUSMAN, H.W., HART, W.G., SMUGGE, T.J. and WESTIN, F.C. 1983. Remote sensing applications in agriculture. In : Robert N. Colwell (Ed.), Mannual of Remote Sensing. ASPRS. Falls church, VA., pp 2111-2229.

NIELSON, D.C. and GARDNER, B.R. 1987. Scheduling irrigation for Corn with the crop water stress index. Applied Agricultural Research Vol. 2, No. 5, pp 295 - 300.

RIPPLE, W.J. 1986. Spectral reflectance relationships to leaf water stress. Photogramm. Eng. Remote Sens., 52 : 1669-1675.

STUTTE, G.W., STUTTE, C.A., and NEWELL, M.J. 1988, Quantification of water and nitrogen stress in peach trees using ICAS computer video image analysis. Proc. First Workshop on Videography. ASPRS., pp. 137-144.

RIPPLE, W.J. and SCHRUMPF, B.J. 1987. Remote sensing of leaf water status. Proc. of the Int. Conf. on measurement of soil and plantwater status. Vol. 2. Plants. Utah state University. July. Logan, UT.

SALES, J.R. 1986. Everything about R/C. Tower Hobbies, Box 778, Champaign. Ilnois, USA.

STUM, R. 1988. Camera in the Sky. RC Modeler, July, pp 228-242.

THROSSEL, C.S., CARROW, R.N., and MILLIKEN, G.A. 1981. Canopy temperature based irrigation scheduling indices for Kentucky blue grass turf. Crop Sci., 27 : 126-131.

TUCKER, C.J. 1980. Remote sensing of leaf water content in the infrared. Remote Sensing Environ., 10 : 23-32.

YUAN, X.P., KING, D.J. and VLECK, J. 1991. Assessment of sugar maple decline based on spectral analysis of multispectral aerial videography. Remote Sens. of Env., 37 (1) : 47-54.

CHAPTER 7

APPENDIX

Fig. 7.1.4 Canopy Temperature of Soybean
28 Jan - 15 March 1992

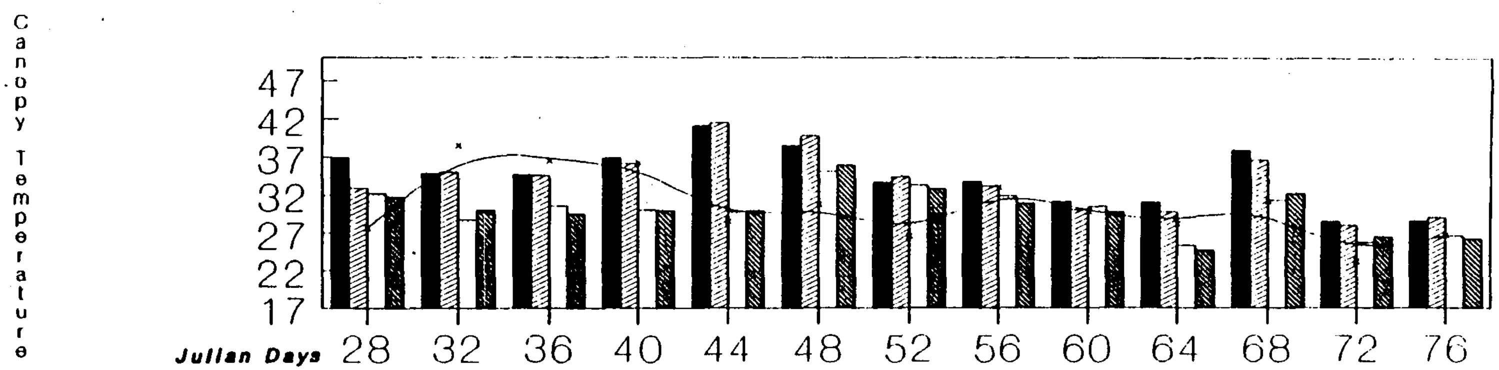

	28	32	36	40	44	48	52	56	60	64	68	72	76
STRESS Blk 1	37	34.8	34.7	36.9	41.2	38.6	33.7	33.8	31.2	31.1	38	28.6	28.7
STRESS Blk 2	32.9	35	34.6	36.1	41.5	39.8	34.4	33.2	30.1	29.8	36.7	28.1	29.1
CONTRL Blk 1	32.2	28.8	30.6	30.1	29.8	35.1	33.3	31.9	30.5	25.4	31.4	25.8	26.7
CONTRL Blk 2	31.8	30.1	29.5	30	30	36	32.8	30.9	29.8	24.7	32.2	26.6	26.3
Air-Temp	27.6	38.5	36.5	36.2	28.5	30.8	26.5	32.9	29.8	28.2	31.2	23.2	26.8

TREATMENTS

STRESS Blk 1 | STRESS Blk 2 | CONTRL Blk 1 | CONTRL Blk 2 | Air-Temp

Fig. 7.2.1 Canopy Temperature of Wheat
28 August - 14 September 1989

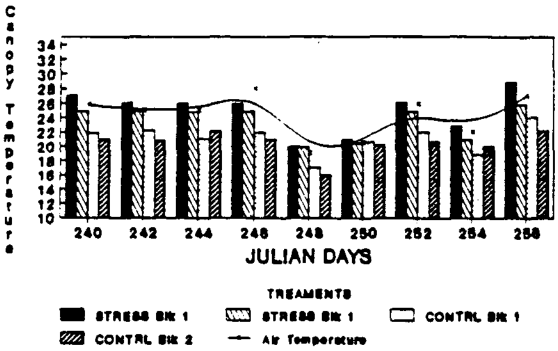

Fig. 7.2.2 Canopy Temperature of Wheat
31 July - 12 August 1990

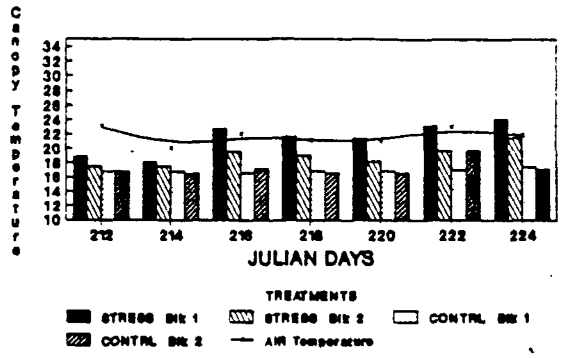

Fig. 7.2.3 Canopy Temperature of Wheat
26 August - 18 September 1991

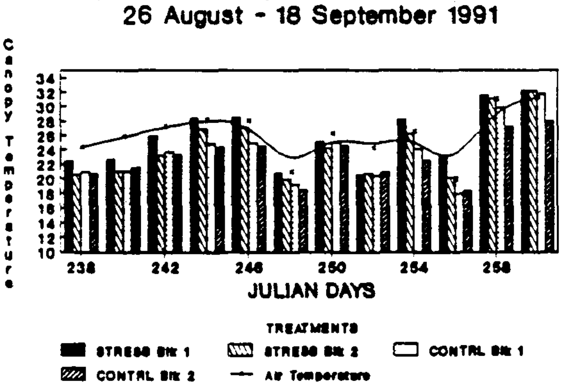

Fig. 7.2.4 Canopy Temperature of wheat
Days 5 August - 16 September 1992

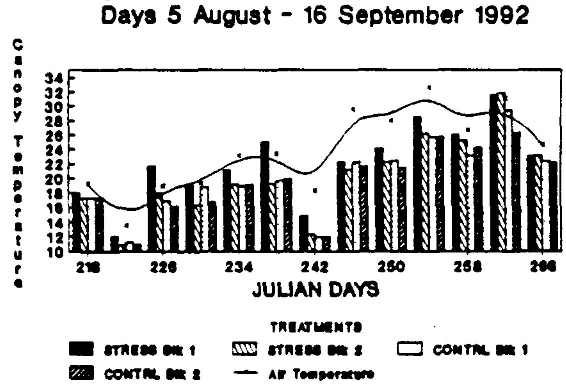

Fig. 7.2 Tc and Ta on Wheat for 1989 - 1992 seasons

Fig. 7.2.1 Canopy Temperature of Wheat
28 August - 14 September 1989

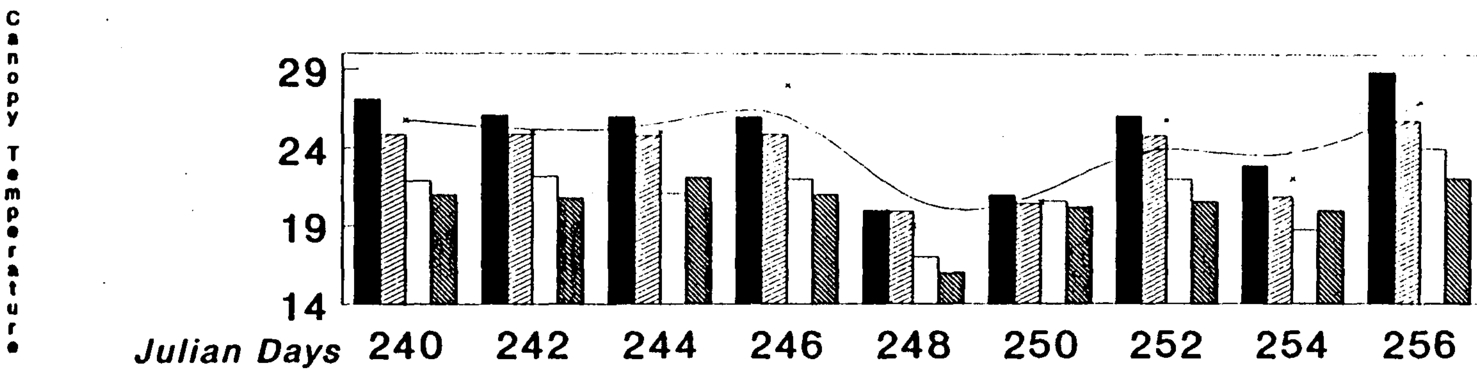

Julian Days	240	242	244	246	248	250	252	254	256
STRESS Blk 1	27.1	26.1	26	26	20	21	26.1	22.9	28.9
STRESS Blk 1	24.9	24.9	24.8	24.9	19.9	20.4	24.8	20.9	25.8
CONTRL Blk 1	21.9	22.2	21.1	22	17	20.6	22	18.8	24
CONTRL Blk 2	21	20.8	22.1	21	16	20.2	20.6	20	22.1
Air Temperature	25.8	25	25	28	19	20.5	25.8	22	27

TREAMENTS

STRESS Blk 1 — STRESS Blk 1 — CONTRL Blk 1 — CONTRL Blk 2 — Air Temperature

Fig. 7.2.2 Canopy Temperature of Wheat 31 July - 12 August 1990

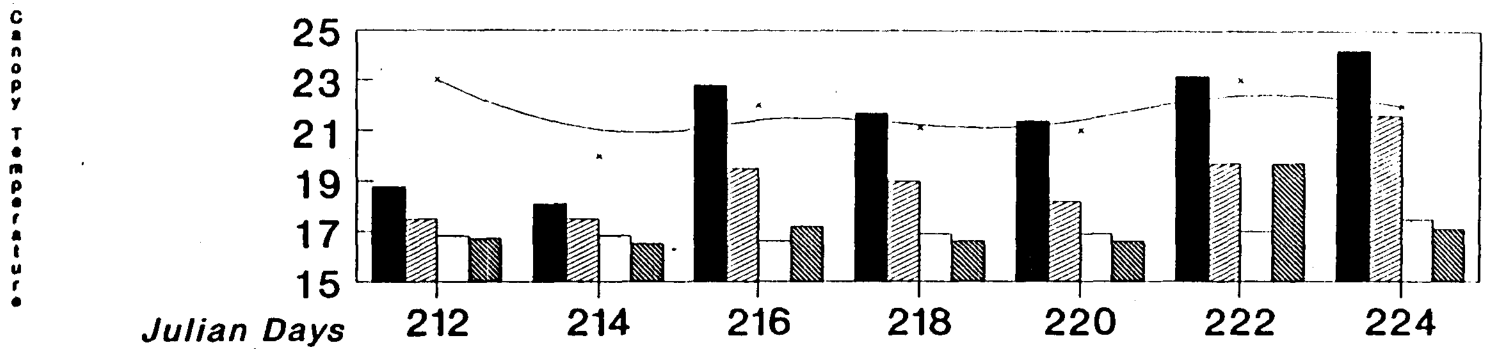

Julian Days	212	214	216	218	220	222	224
STRESS Blk 1	18.8	18.1	22.8	21.7	21.4	23.2	24.2
STRESS Blk 2	17.5	17.5	19.5	19	18.2	19.7	21.6
CONTRL Blk 1	16.8	16.8	16.6	16.9	16.9	17	17.5
CONTRL Blk 2	16.7	16.5	17.2	16.6	16.6	19.7	17.1
AIR Temperature	23	20	22	21.1	21	23	22

TREATMENTS

STRESS Blk 1 STRESS Blk 2 CONTRL Blk 1

CONTRL Blk 2 AIR Temperature

Fig. 7.2.3 Canopy Temperature of Wheat
28 August - 19 September 1991

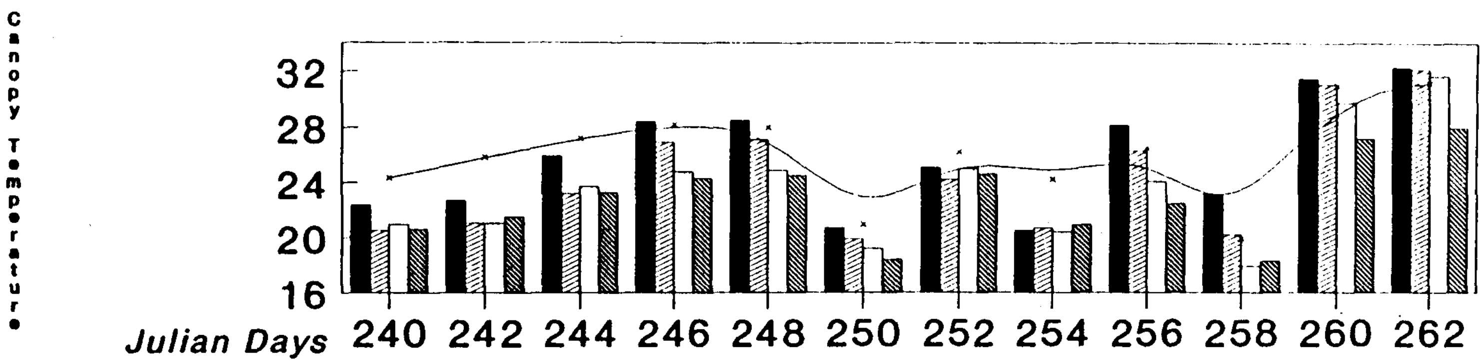

STRESS Blk 1	22.4	22.7	25.9	28.4	28.5	20.7	25.1	20.5	28.2	23.2	31.5	32.3
STRESS Blk 2	20.5	21	23.2	26.9	27.1	19.9	24.2	20.7	26.3	20.2	31.1	32.2
CONTRL Blk 1	20.9	21	23.7	24.8	24.9	19.2	25	20.4	24.1	17.9	29.8	31.7
CONTRL Blk 2	20.6	21.5	23.3	24.3	24.5	18.4	24.6	20.9	22.5	18.3	27.2	28
Air Temperature	24.3	25.8	27.2	28.2	28	20.9	26.2	24.2	26.5	19.9	31	31.2

TREATMENTS

STRESS Blk 1 STRESS Blk 2 CONTRL Blk 1

CONTRL Blk 2 Air Temperature

Fig. 7.2.4 Canopy Temperature for wheat
Days 5 August - 22 September 1992

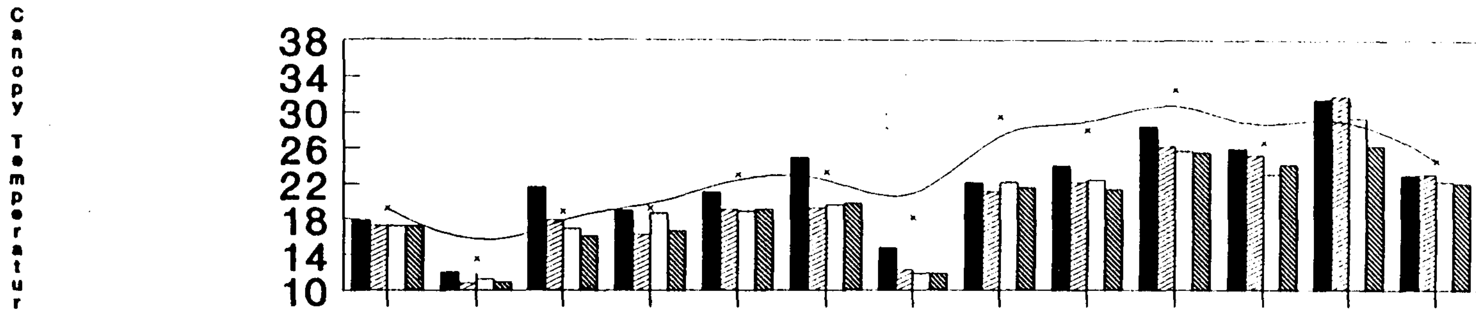

Julian Days	218	222	226	230	234	238	242	246	250	254	258	262	266
STRESS Blk 1	17.9	12	21.6	19	21.1	25	14.8	22.2	24.1	28.5	26	31.5	23
STRESS Blk 2	17.2	10.8	17.9	16.3	19.1	19.3	12.3	21.2	22.2	26.2	25.2	31.8	23.1
CONTRL Blk 1	17.2	11.2	16.9	18.7	18.9	19.6	11.9	22.2	22.4	25.7	23.1	29.4	22.3
CONTRL Blk 2	17.2	10.9	16.1	16.7	19.1	19.8	11.9	21.6	21.4	25.6	24.2	26.3	22.1
Air Temperature	19.2	13.5	18.8	19.2	23	23.3	18.2	29.5	28	32.5	26.6	31	24.6

TREATMENTS

STRESS Blk 1 STRESS Blk 2 CONTRL Blk 1

CONTRL Blk 2 Air Temperature

Fig.7.2.5 Canopy Temperature of Maize
9 February - 28 February 1989

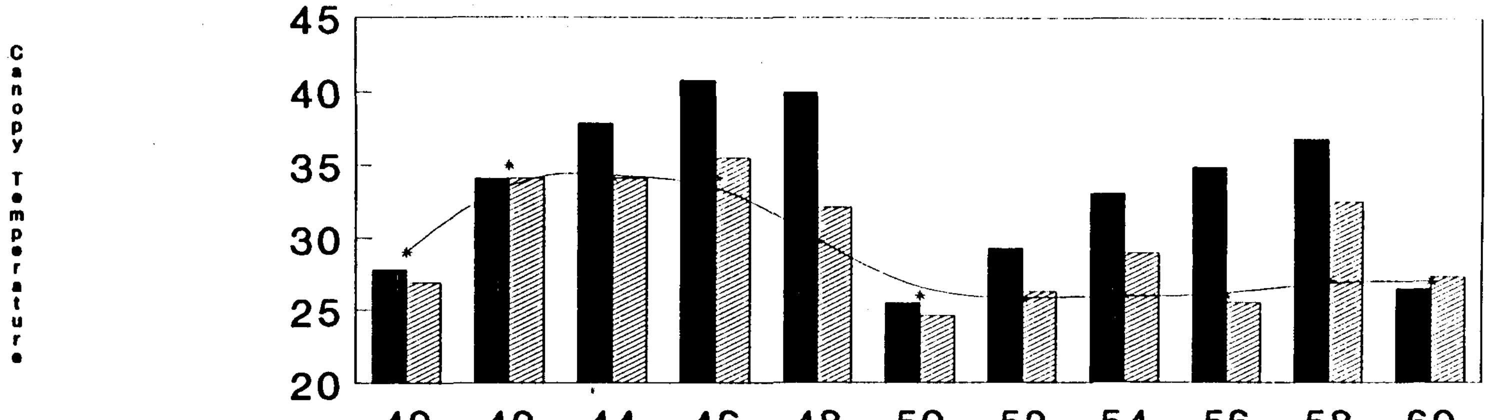

Julian Days	40	42	44	46	48	50	52	54	56	58	60
Ave.STRESS Blk	27.8	34.1	37.9	40.8	40	25.5	29.3	33.1	34.9	36.8	26.5
Ave.CONTRL Blk	26.9	34.1	34.1	35.5	32.1	24.6	26.3	28.9	25.5	32.5	27.3
Air Temperature	29	35	34.1	34.2	29.8	26	25.8	26	25.9	27.1	27

TREATMENTS

Ave.STRESS Blk   Ave.CONTRL Blk

Air Temperature

Fig. 8.1.1 ΔT of Soybean
8 March - 18 March 1989

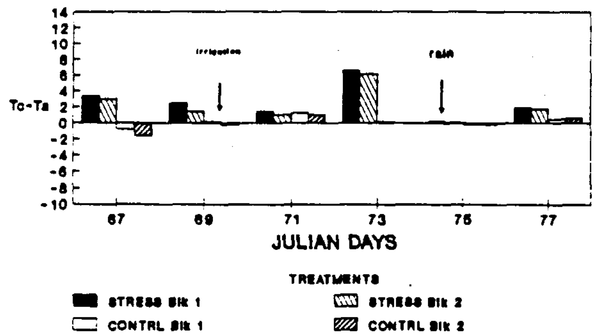

Fig. 8.1.2 ΔT of Soybean
15 February - 17 March 1990

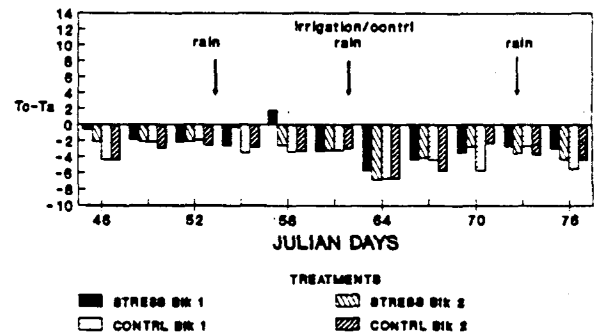

Fig. 8.1.3 ΔT of Soybean
25 February - 13 March 1991

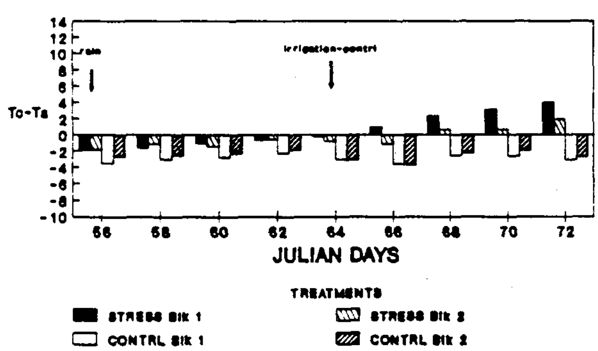

Fig. 8.1.4 ΔT of Soybean
28 Januarie - 15 March 1992

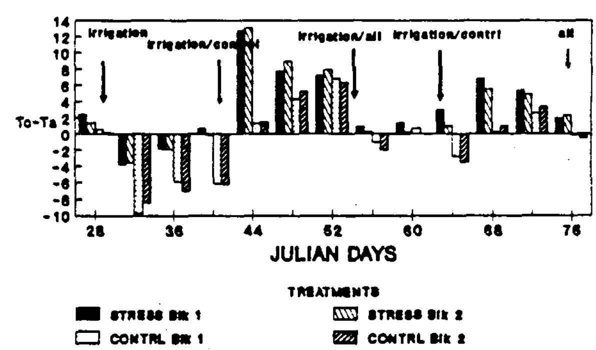

Fig. 8.1 ΔT on Soybean for 1989 - 1992 seasons

Fig. 8.1.1 ΔT of Soybean
8 March - 18 March 1989

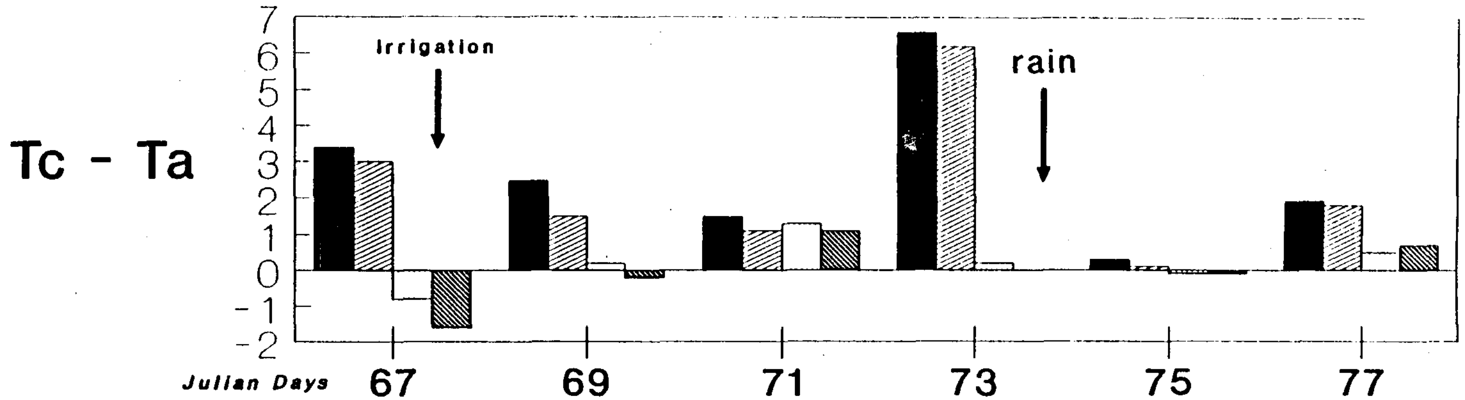

	67	69	71	73	75	77
STRESS Blk 1	3.4	2.5	1.5	6.6	0.3	1.93
STRESS Blk 2	3	1.5	1.1	6.2	0.1	1.8
CONTRL Blk 1	-0.8	0.2	1.3	0.2	-0.1	0.5
CONTRL Blk 2	-1.6	-0.2	1.1	0	-0.1	0.7

TREATMENTS

STRESS Blk 1   STRESS Blk 2

CONTRL Blk 1   CONTRL Blk 2

Fig. 8.1.2 ΔT of Soybean
15 February - 17 March 1990

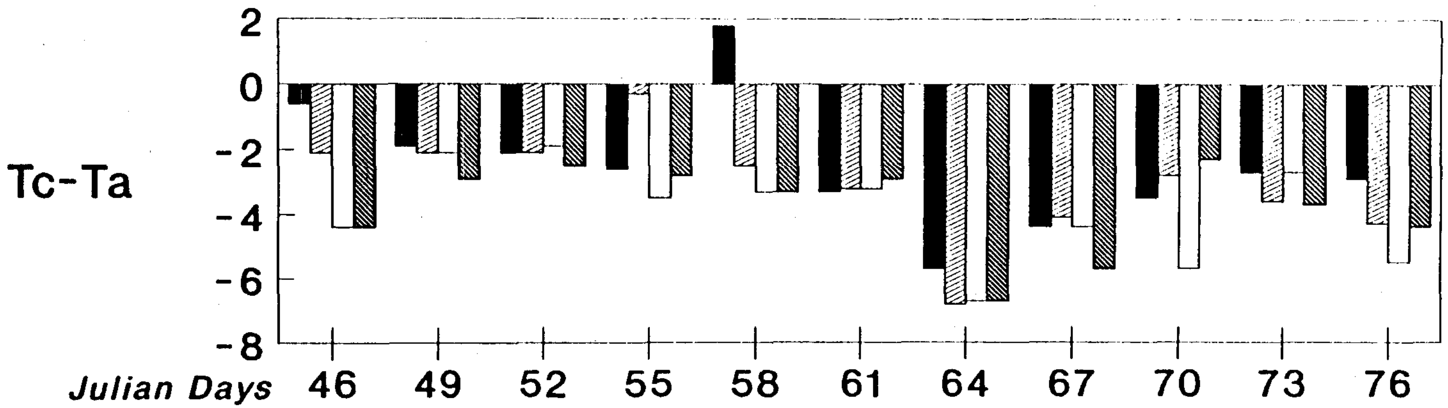

STRESS Blk 1	-0.6	-1.9	-2.1	-2.6	1.8	-3.3	-5.7	-4.4	-3.5	-2.7	-2.9
STRESS Blk 2	-2.1	-2.1	-2.1	-0.3	-2.5	-3.2	-6.8	-4.1	-2.8	-3.6	-4.3
CONTRL Blk 1	-4.4	-2.1	-1.9	-3.5	-3.3	-3.2	-6.7	-4.4	-5.7	-2.7	-5.5
CONTRL Blk 2	-4.4	-2.9	-2.5	-2.8	-3.3	-2.9	-6.7	-5.7	-2.3	-3.7	-4.4

TREATMENTS

STRESS Blk 1 | STRESS Blk 2
CONTRL Blk 1 | CONTRL Blk 2

Fig. 8.1.3 ΔT of Soybean
25 February - 13 March 1991

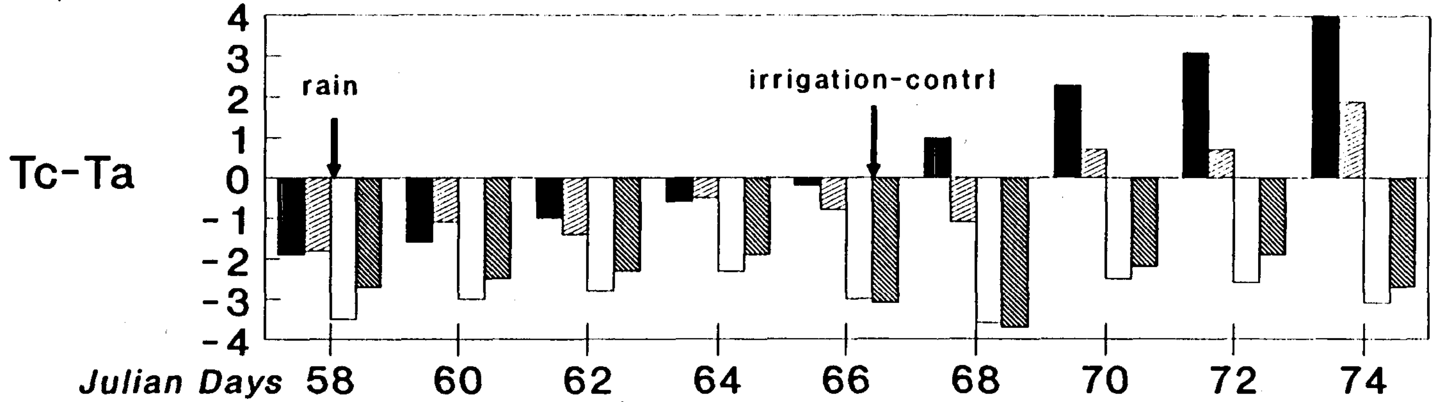

STRESS Blk 1	-1.9	-1.6	-1	-0.6	-0.2	1	2.3	3.1	4
STRESS Blk 2	-1.8	-1.1	-1.4	-0.5	-0.8	-1.1	0.7	0.7	1.9
CONTRL Blk 1	-3.5	-3	-2.8	-2.3	-3	-3.6	-2.5	-2.6	-3.1
CONTRL Blk 2	-2.7	-2.5	-2.3	-1.9	-3.1	-3.7	-2.2	-1.9	-2.7

TREATMENTS

STRESS Blk 1 | STRESS Blk 2
CONTRL Blk 1 | CONTRL Blk 2

Fig. 8.1.4 ΔT of Soybean
28 Januarie - 15 March 1992

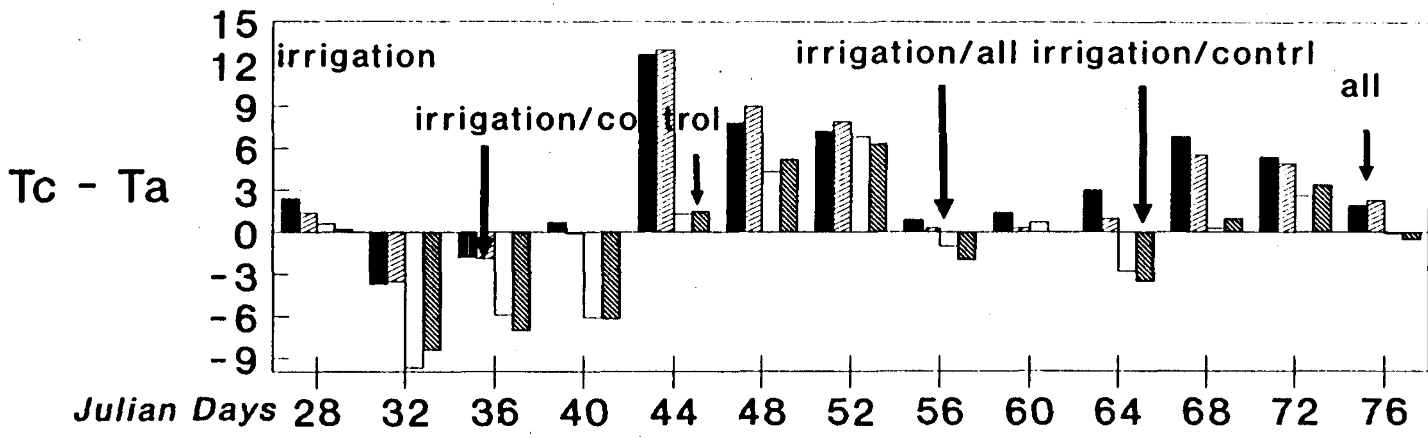

	28	32	36	40	44	48	52	56	60	64	68	72	76
STRESS Blk 1	2.4	-3.7	-1.8	0.7	12.7	7.8	7.2	0.9	1.4	3	6.8	5.4	1.9
STRESS Blk 2	1.4	-3.5	-1.9	-0.1	13	9	7.9	0.3	0.3	1	5.5	4.9	2.3
CONTRL Blk 1	0.6	-9.7	-5.9	-6.1	1.3	4.3	6.8	-1	0.7	-2.8	0.3	2.6	-0.1
CONTRL Blk 2	0.2	-8.4	-7	-6.2	1.5	5.2	6.3	-2	0	-3.5	1	3.4	-0.5

TREATMENTS

STRESS Blk 1 — STRESS Blk 2

CONTRL Blk 1 — CONTRL Blk 2

Fig. 8.2.1 ΔT of Wheat
28 August - 14 September 1989

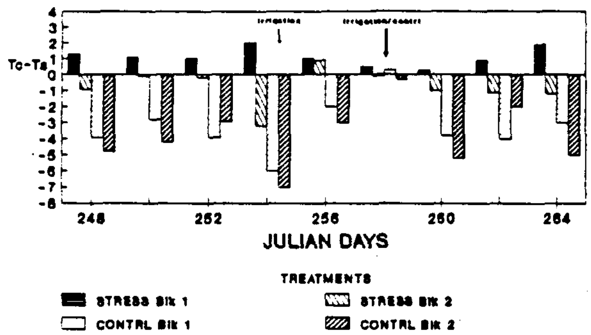

Fig. 8.2.2 ΔT of Wheat
31 July - 12 August 1990

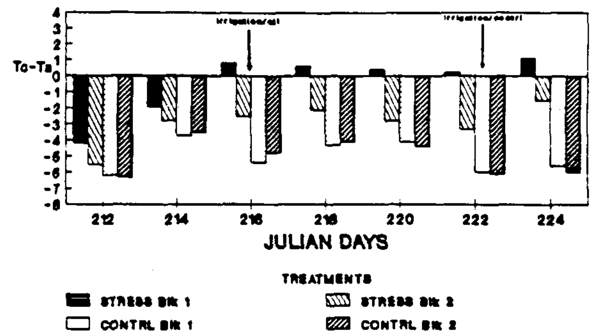

Fig. 8.2.3 ΔT of Wheat
28 August - 19 September 1991

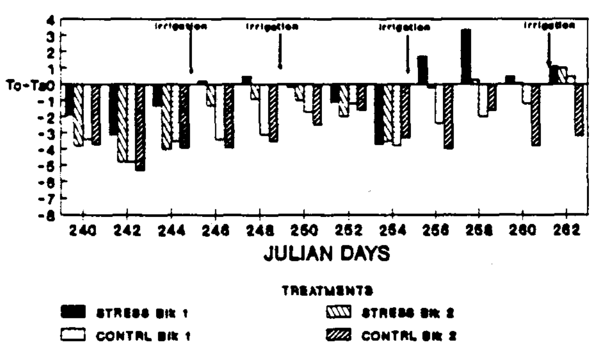

Fig. 8.2.4 ΔT of Wheat
5 August - 22 September 1992

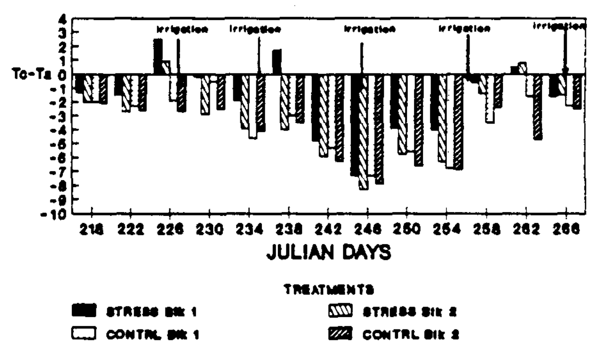

Fig.8.2 ΔT on Wheat for 1989 - 1992 seasons

Fig. 8.2.1 Δ T of Wheat
28 August - 14 September 1989

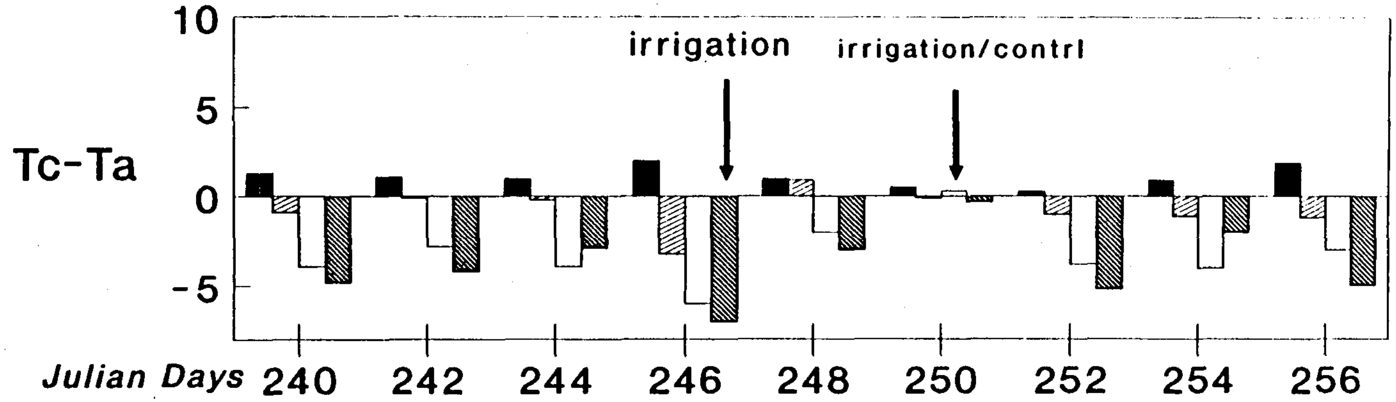

	240	242	244	246	248	250	252	254	256
STRESS Blk 1	1.3	1.1	1	2	1	0.5	0.3	0.9	1.9
STRESS Blk 2	-0.9	-0.1	-0.2	-3.2	0.9	-0.1	-1	-1.1	-1.2
CONTRL Blk 1	-3.9	-2.8	-3.9	-6	-2	0.3	-3.8	-4	-3
CONTRL Blk 2	-4.8	-4.2	-2.9	-7	-3	-0.3	-5.2	-2	-5

TREATMENTS

STRESS Blk 1 | STRESS Blk 2
CONTRL Blk 1 | CONTRL Blk 2

Fig. 8.2.2 ΔT of Wheat
31 July - 12 August 1990

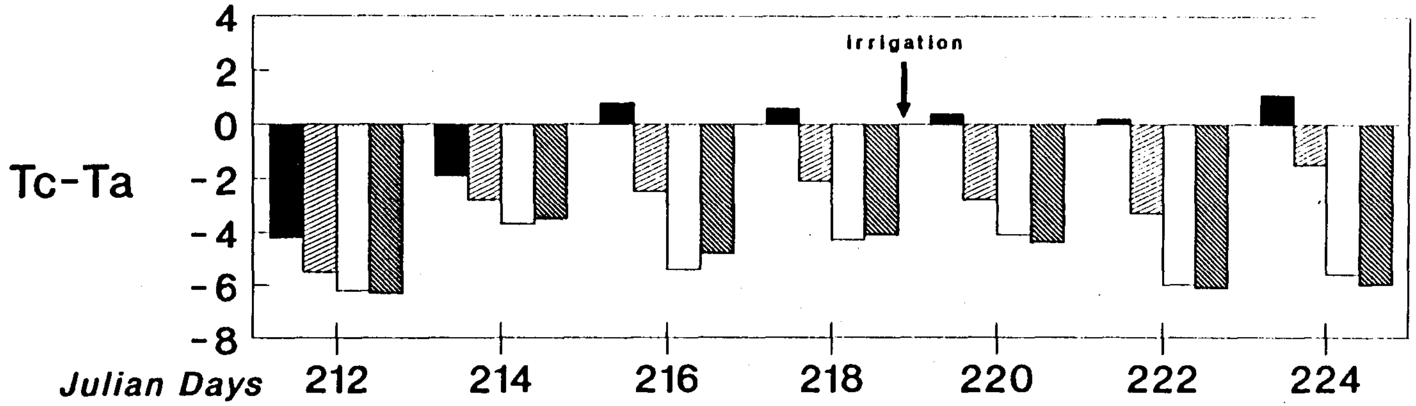

Julian Days	212	214	216	218	220	222	224
STRESS Blk 1	-4.2	-1.9	0.8	0.6	0.4	0.2	1.1
STRESS Blk 2	-5.5	-2.8	-2.5	-2.1	-2.8	-3.3	-1.5
CONTRL Blk 1	-6.2	-3.7	-5.4	-4.3	-4.1	-6	-5.6
CONTRL Blk 2	-6.3	-3.5	-4.8	-4.1	-4.4	-6.1	-6

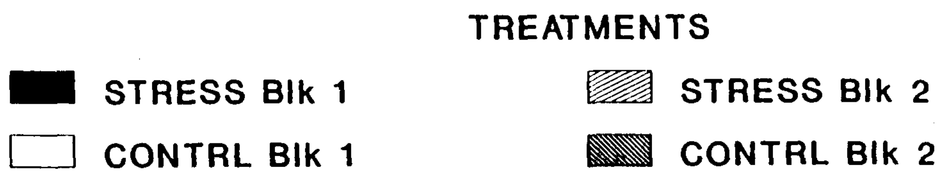

Fig. 8.2.3 Δ T of Wheat
26 August - 18 September 1991

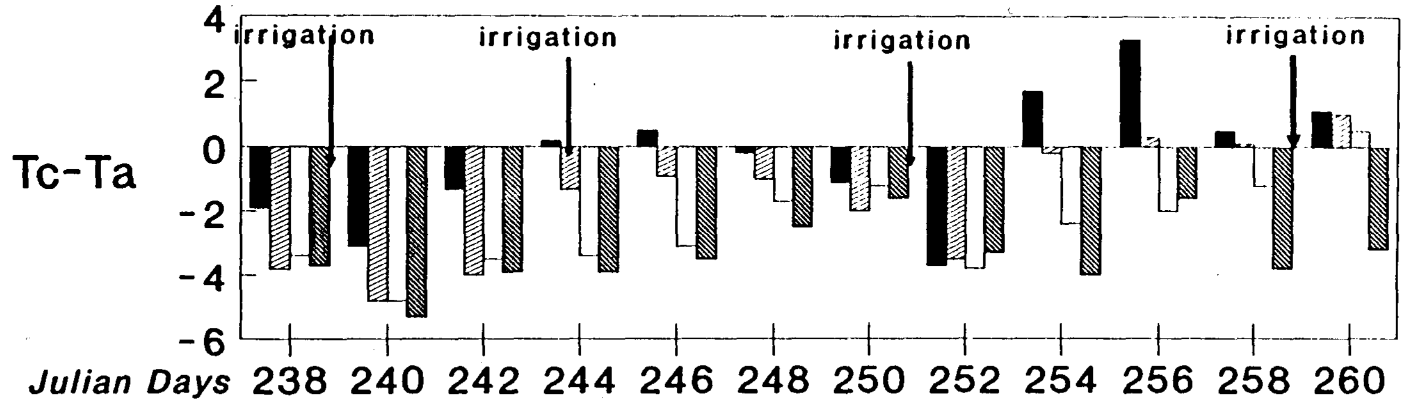

Julian Days	238	240	242	244	246	248	250	252	254	256	258	260
STRESS Blk 1	-1.9	-3.1	-1.3	0.2	0.5	-0.2	-1.1	-3.7	1.7	3.3	0.5	1.1
STRESS Blk 2	-3.8	-4.8	-4	-1.3	-0.9	-1	-2	-3.5	-0.2	0.3	0.1	1
CONTRL Blk 1	-3.4	-4.8	-3.5	-3.4	-3.1	-1.7	-1.2	-3.8	-2.4	-2	-1.2	0.5
CONTRL Blk 2	-3.7	-5.3	-3.9	-3.9	-3.5	-2.5	-1.6	-3.3	-4	-1.6	-3.8	-3.2

TREATMENTS

- STRESS Blk 1
- STRESS Blk 2
- CONTRL Blk 1
- CONTRL Blk 2

Fig. 8.2.4 ΔT of Wheat
5 August - 22 September 1992

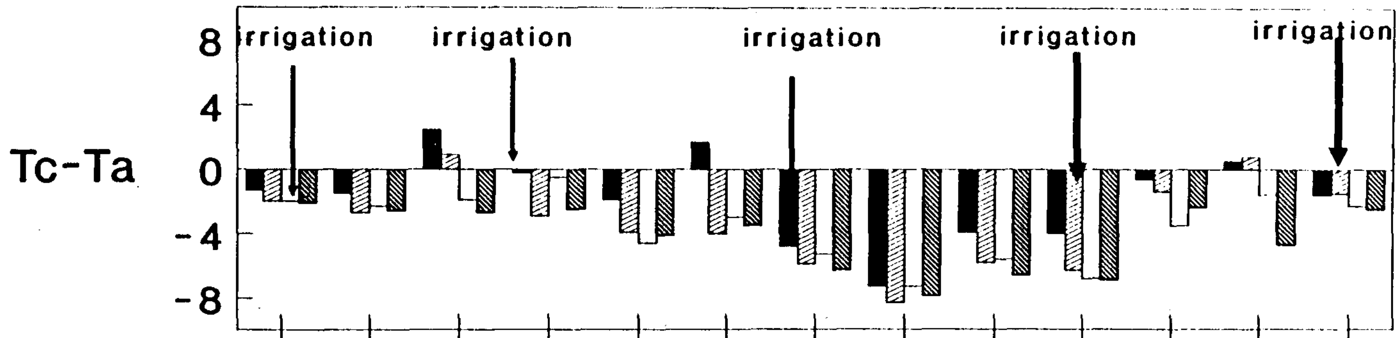

Julian Days	218	222	226	230	234	238	242	246	250	254	258	262	266
STRESS Blk 1	-1.3	-1.5	2.5	-0.2	-1.9	1.7	-4.8	-7.3	-3.9	-4	-0.6	0.5	-1.6
STRESS Blk 2	-2	-2.7	0.9	-2.9	-3.9	-4	-5.9	-8.3	-5.8	-6.3	-1.4	0.8	-1.5
CONTRL Blk 1	-2	-2.3	-1.9	-0.5	-4.6	-3	-5.3	-7.3	-5.6	-6.8	-3.5	-1.6	-2.3
CONTRL Blk 2	-2.1	-2.6	-2.7	-2.5	-4.1	-3.5	-6.3	-7.9	-6.6	-6.9	-2.4	-4.7	-2.5

TREATMENTS

STRESS Blk 1　　STRESS Blk 2

CONTRL Blk 1　　CONTRL Blk 2

Fig. 8.2.5 Δ T of Maize
9 February - 28 February 1989

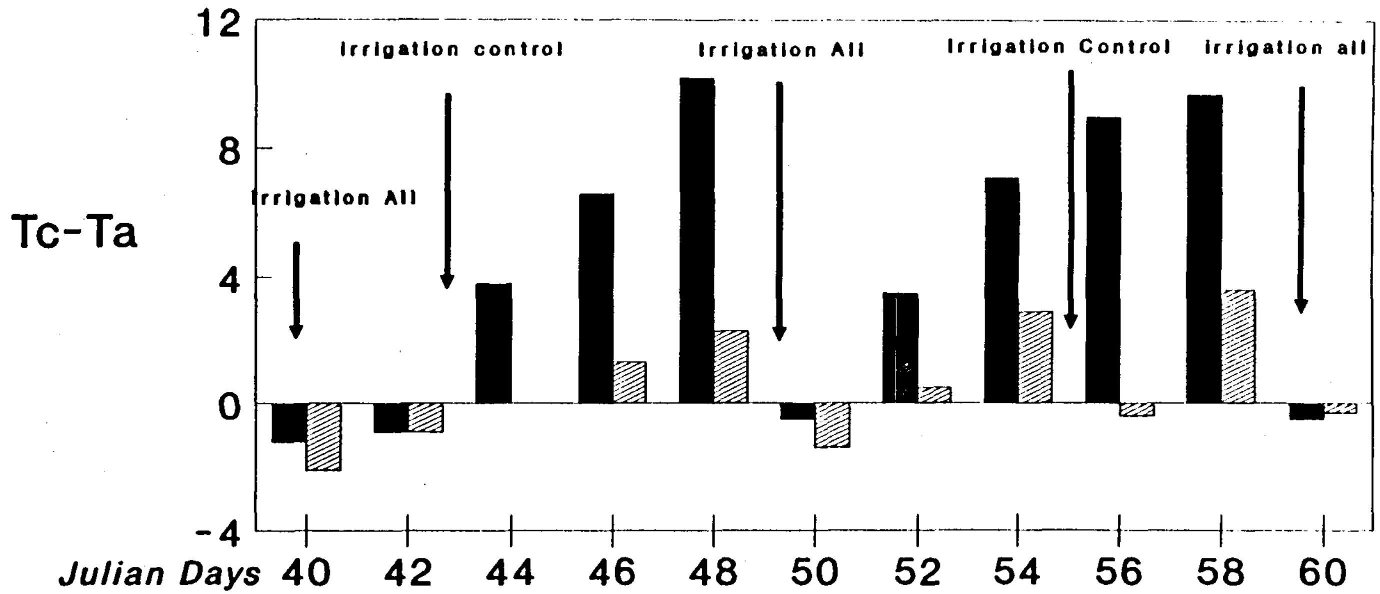

Julian Days	40	42	44	46	48	50	52	54	56	58	60
Ave.STRESS Blk	-1.2	-0.9	3.8	6.6	10.2	-0.5	3.5	7.1	9	9.7	-0.5
Ave.CONTRL Blk	-2.1	-0.9	0	1.3	2.3	-1.4	0.5	2.9	-0.4	3.6	-0.3

TREATMENTS

Ave.STRESS Blk   Ave.CONTRL Blk

Fig. 9.1 Soil Moisture - Soybean
0/20 cm Depth 16 Feb - 23 March 1990

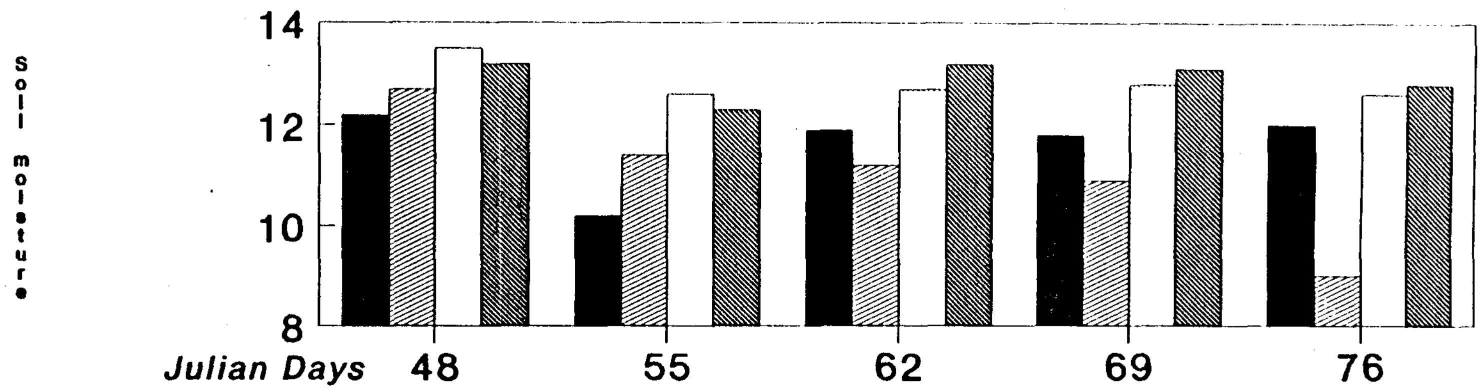

Julian Days	48	55	62	69	76
STRESS Blk 1	12.2	10.2	11.9	11.8	12
STRESS Blk 2	12.7	11.4	11.2	10.9	9
CONTRL Blk 1	13.5	12.6	12.7	12.8	12.6
CONTRL Blk 2	13.2	12.3	13.2	13.1	12.8

Fig. 9.2 Soil Moisture - Soybean
0/20 cm Depth 27 Feb. - 13 March. 1991

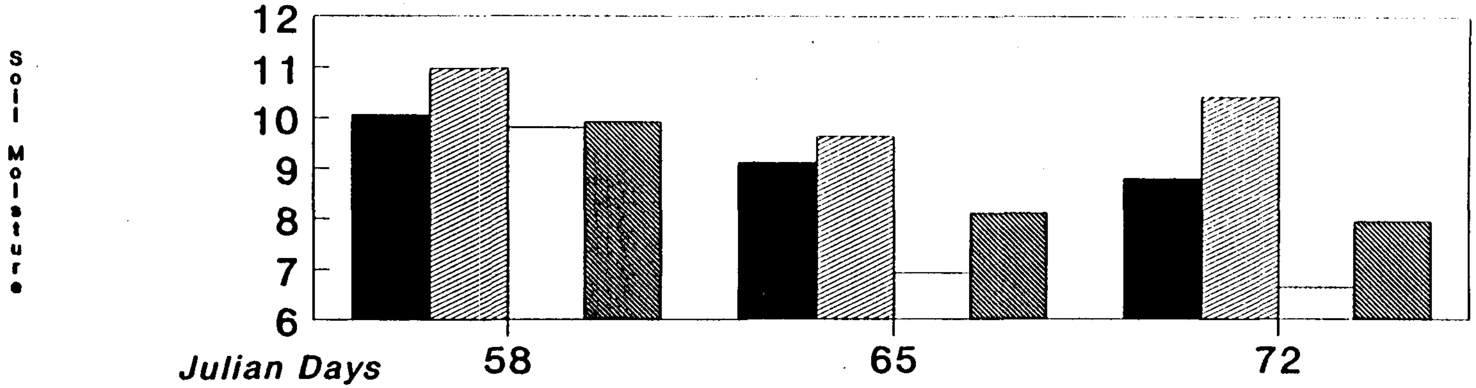

	58	65	72
CONTRL Blk 1	10.071	9.12	8.794
CONTRL Blk 2	10.98	9.636	10.426
STRESS Blk 1	9.81	6.921	6.644
STRESS Blk 2	9.93	8.1	7.957

TREATMENTS

CONTRL Blk 1 CONTRL Blk 2

STRESS Blk 1 STRESS Blk 2

Fig. 9.3 Soil Moisture - Wheat 0/20 cm Depth 3 Aug.- 15 Aug. 1990

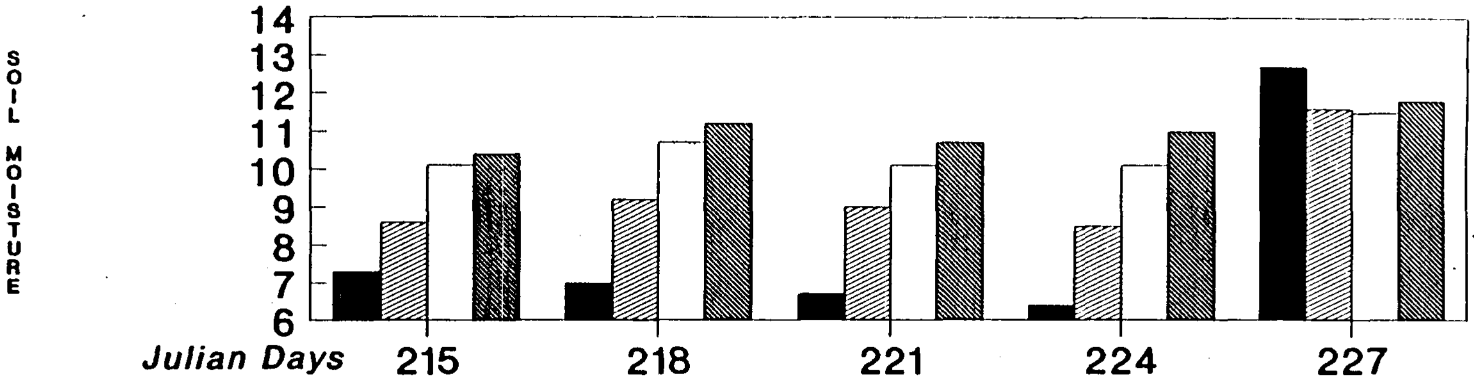

Julian Days	215	218	221	224	227
STRESS Blk 1	7.3	7	6.7	6.4	12.7
STRESS Blk 2	8.6	9.2	9	8.5	11.6
CONTRL Blk 1	10.1	10.7	10.1	10.1	11.5
CONTRL Blk 2	10.4	11.2	10.7	11	11.8

TREATMENTS

STRESS Blk 1 | STRESS Blk 2

CONTRL Blk 1 | CONTRL Blk 2

Fig. 9.4 Soil Moisture - Wheat
0/20 cm Depth 26 Aug. - 7 Sept. 1991

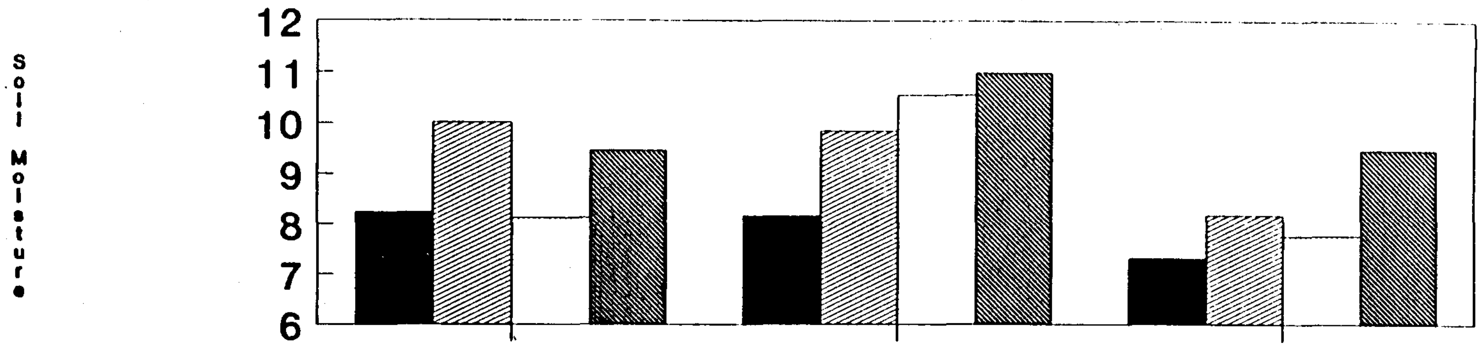

Julian Days	238	244	250
STRESS Blk 1	8.247	8.166	7.318
STRESS Blk 2	10.018	9.854	8.184
CONTRL Blk 1	8.13	10.553	7.773
CONTRL Blk 2	9.464	10.99	9.472

TREATMENTS

STRESS Blk 1 — STRESS Blk 2

CONTRL Blk 1 — CONTRL Blk 2

Fig. 10.1.1 TSD for Soybean
8 March - 18 March 1989

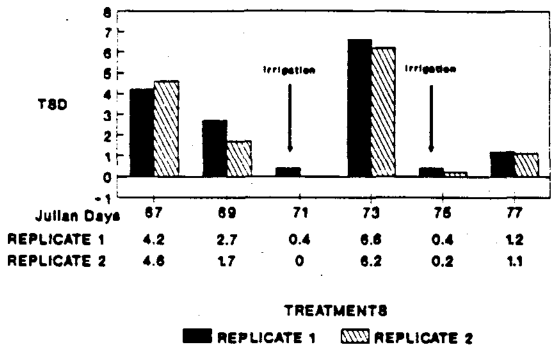

Fig. 10.1.2 TSD of Soybean
15 Feb - 17 March 1990

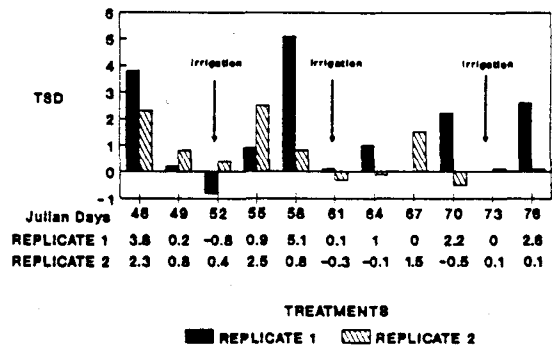

Fig. 10.1.3 TSD for Soybean
25 Feb. - 13 March 1991

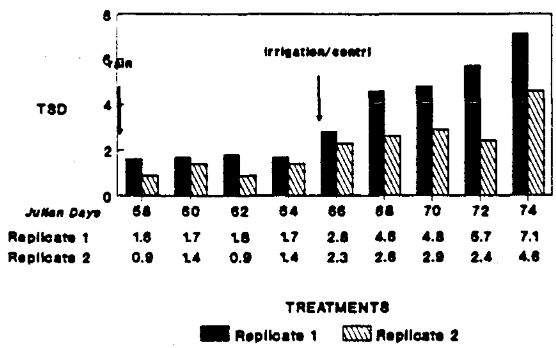

Fig. 10.1.4 TSD for Soybean
28 January - 15 March 1992

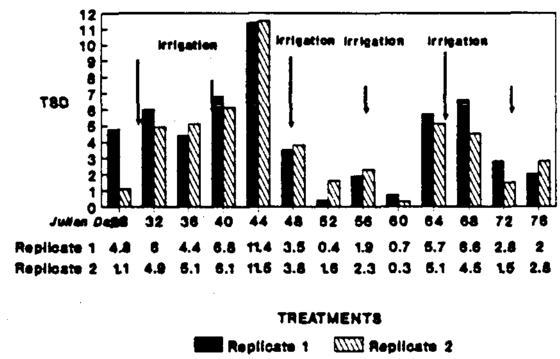

Fig. 10.1 TSD on Soybean for 1989-1992 seasons

Fig. 10.1.1 TSD for Soybean
8 March - 18 March 1989

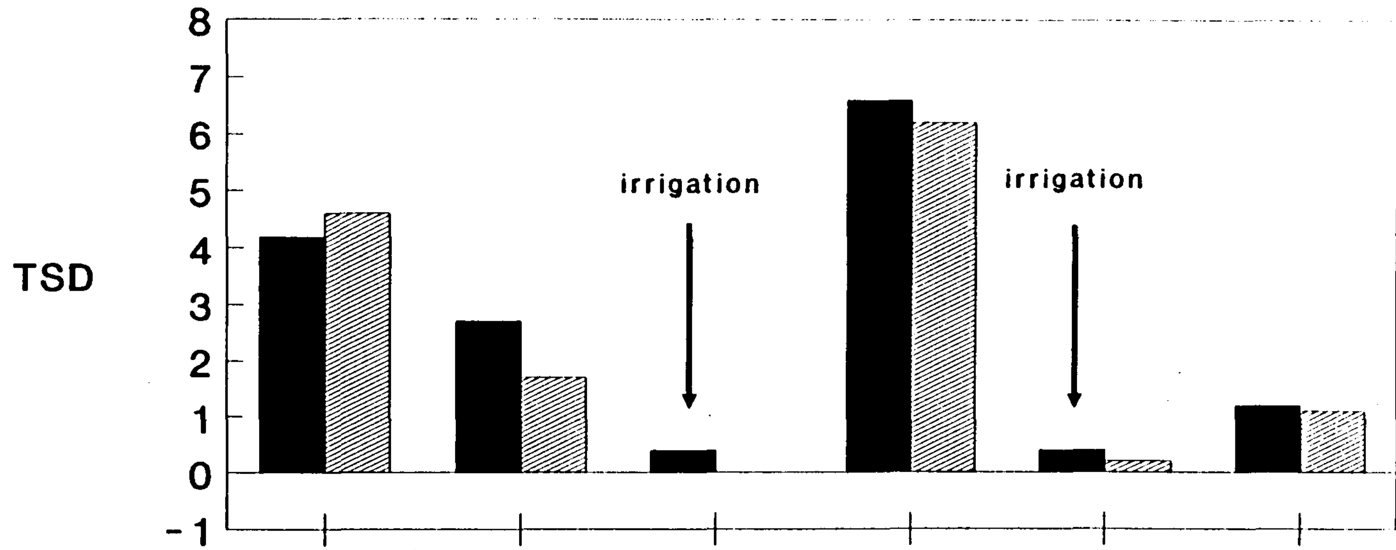

Julian Days	67	69	71	73	75	77
REPLICATE 1	4.2	2.7	0.4	6.6	0.4	1.2
REPLICATE 2	4.6	1.7	0	6.2	0.2	1.1

TREATMENTS

REPLICATE 1   REPLICATE 2

Fig. 10.1.2 TSD of Soybean
15 Feb - 17 March 1990

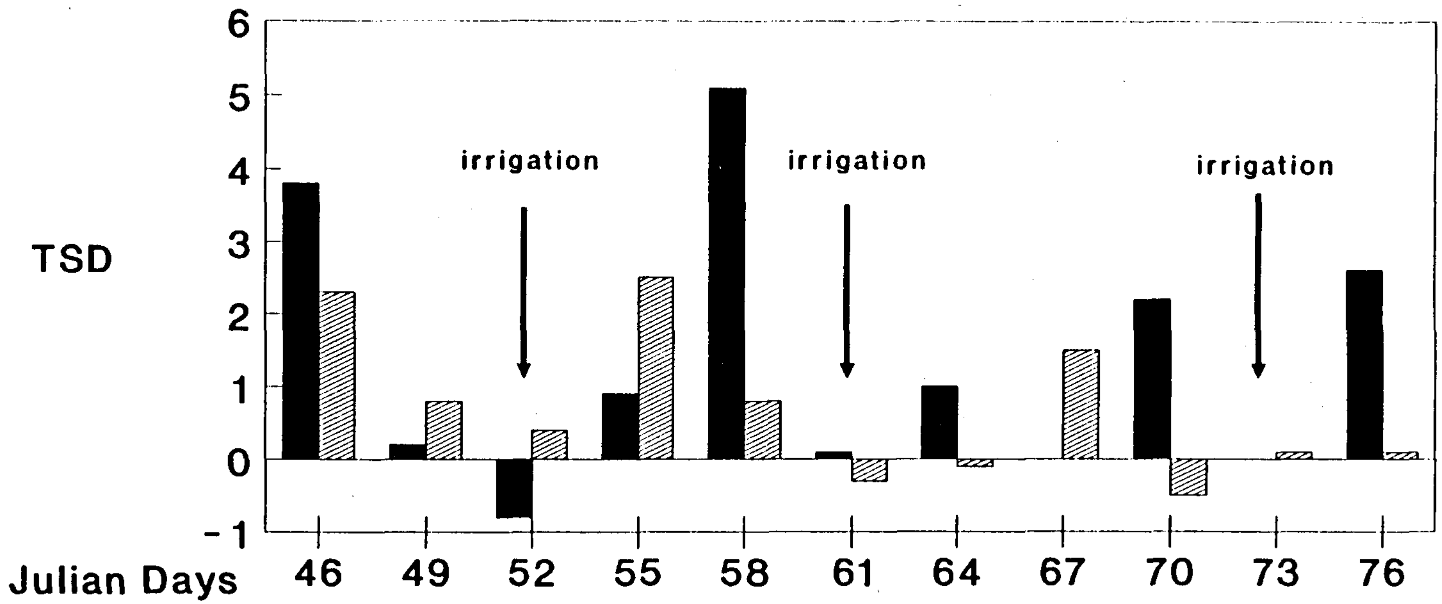

Julian Days	46	49	52	55	58	61	64	67	70	73	76
REPLICATE 1	3.8	0.2	-0.8	0.9	5.1	0.1	1	0	2.2	0	2.6
REPLICATE 2	2.3	0.8	0.4	2.5	0.8	-0.3	-0.1	1.5	-0.5	0.1	0.1

TREATMENTS

REPLICATE 1 REPLICATE 2

Fig. 10.1.3 TSD for Soybean
25 Feb. - 13 March 1991

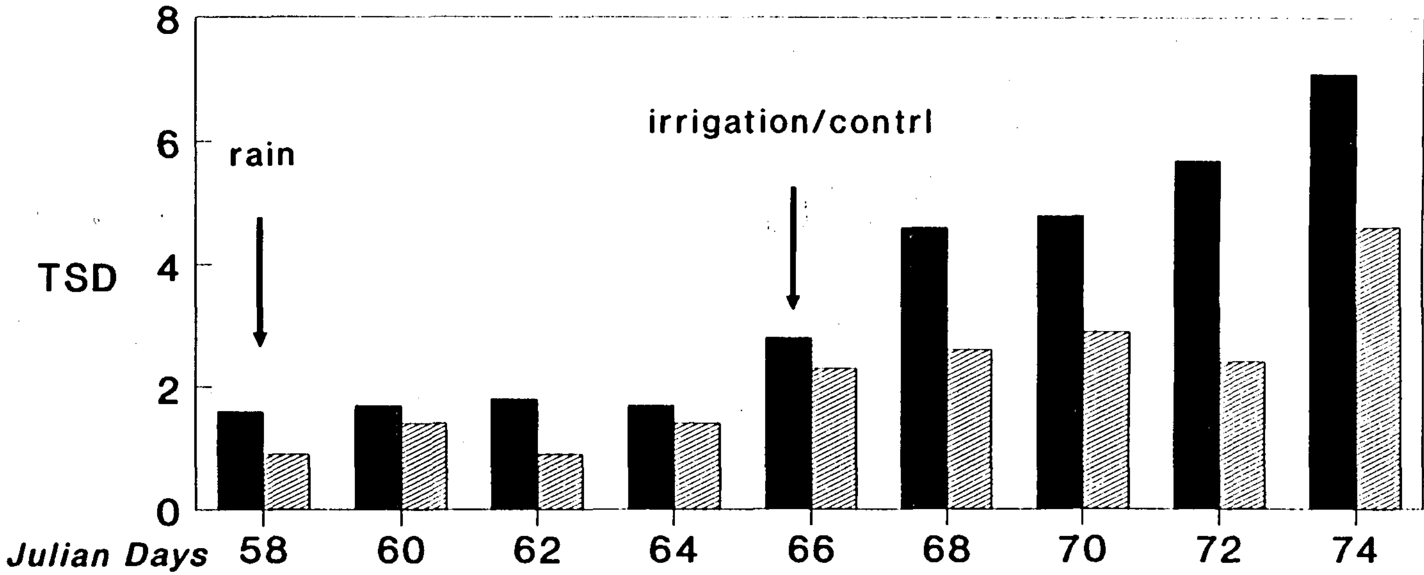

Julian Days	58	60	62	64	66	68	70	72	74
Replicate 1	1.6	1.7	1.8	1.7	2.8	4.6	4.8	5.7	7.1
Replicate 2	0.9	1.4	0.9	1.4	2.3	2.6	2.9	2.4	4.6

TREATMENTS

Replicate 1 Replicate 2

Fig. 10.1.4 TSD for Soybean
28 January - 15 March 1992

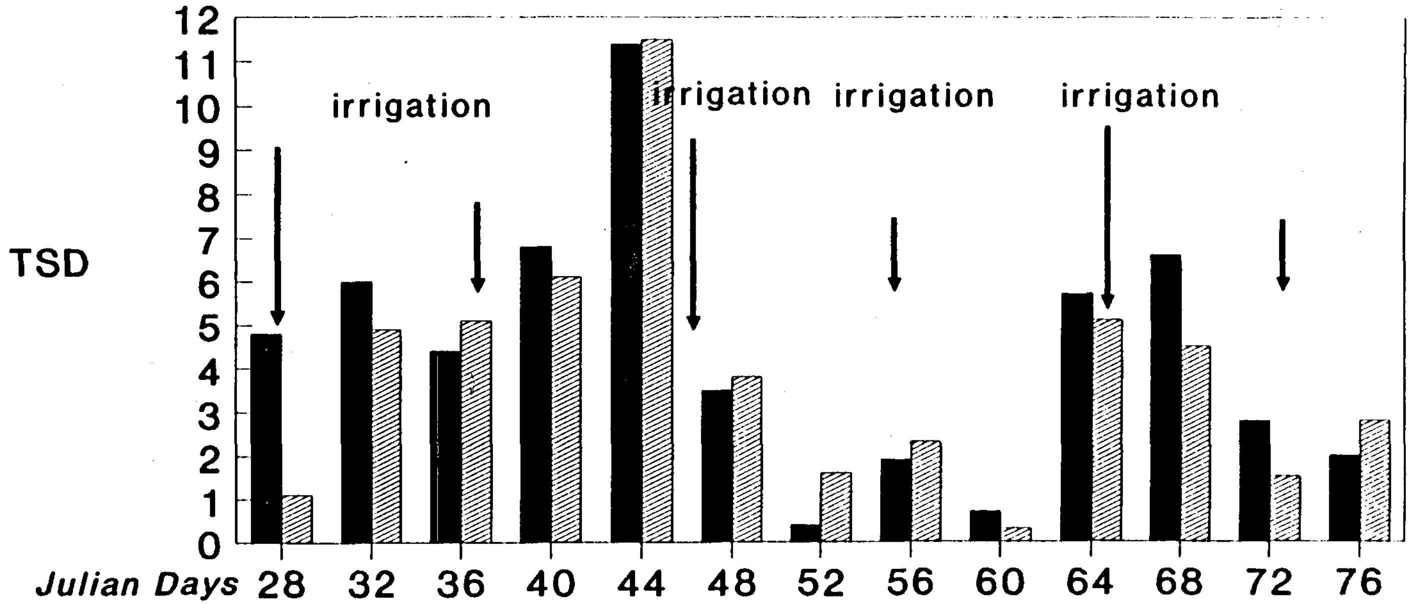

Replicate 1	4.8	6	4.4	6.8	11.4	3.5	0.4	1.9	0.7	5.7	6.6	2.8	2
Replicate 2	1.1	4.9	5.1	6.1	11.5	3.8	1.6	2.3	0.3	5.1	4.5	1.5	2.8

TREATMENTS

Replicate 1 Replicate 2

Fig. 10.2.1 TSD for Wheat
28 August - 14 September 1989

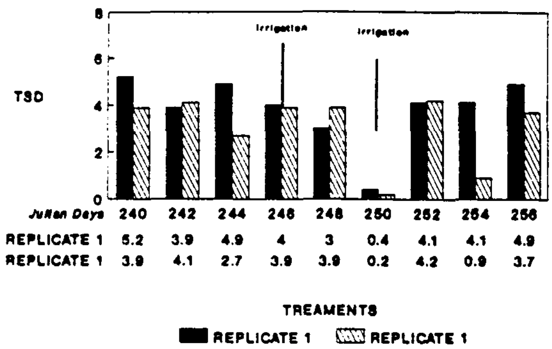

Fig. 10.2.2 TSD of Wheat
31 July - 12 August 1990

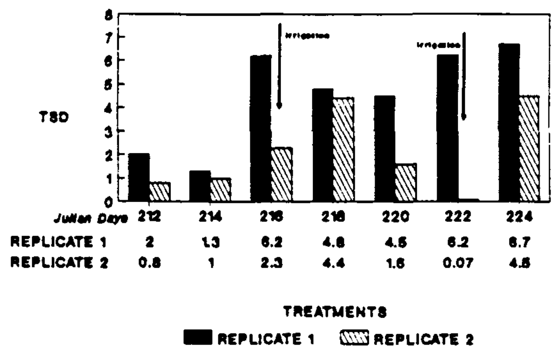

Fig. 10.2.3 TSD Wheat
26 August - 18 September 1991

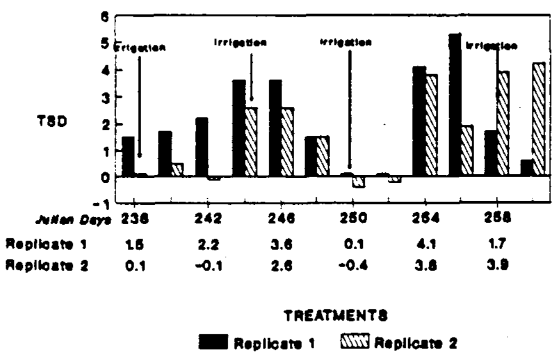

Fig. 10.2.4 TSD Wheat
5 August - 16 September 1992

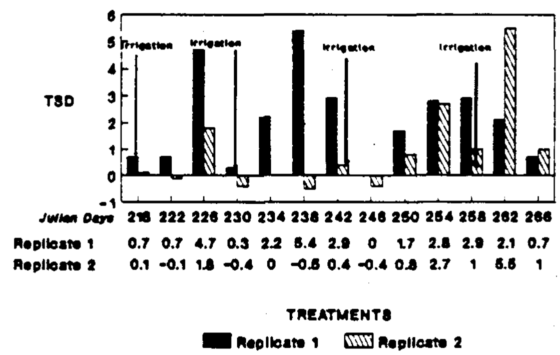

Fig. 10.2 TSD on Wheat for 1989 - 1992 seasons

Fig. 10.2.1 TSD for Wheat
28 August - 14 September 1989

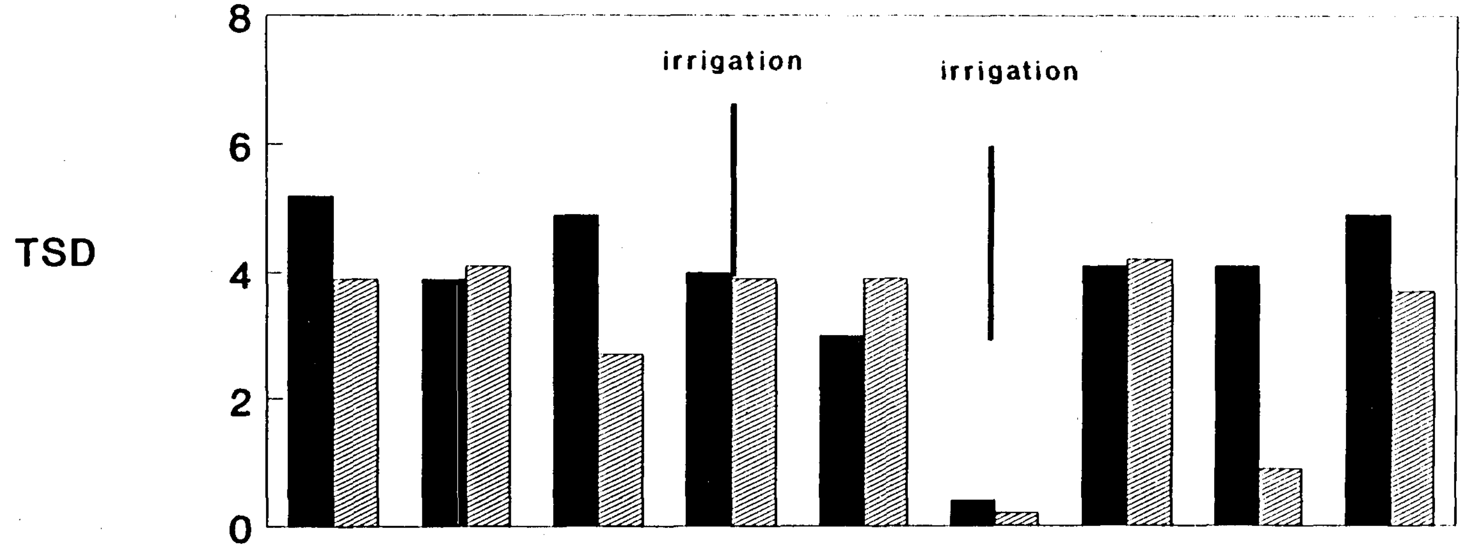

Julian Days	240	242	244	246	248	250	252	254	256
REPLICATE 1	5.2	3.9	4.9	4	3	0.4	4.1	4.1	4.9
REPLICATE 1	3.9	4.1	2.7	3.9	3.9	0.2	4.2	0.9	3.7

TREAMENTS

REPLICATE 1 REPLICATE 1

Fig. 10.2.2 TSD of Wheat
31 July - 12 August 1990

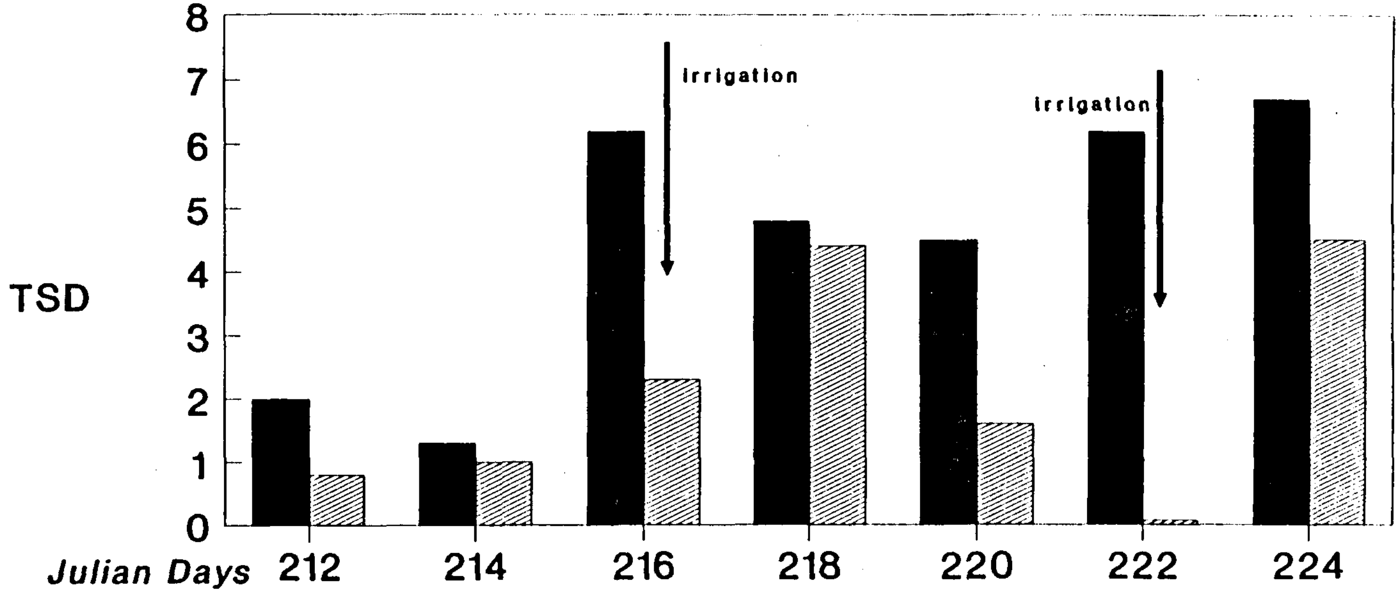

Julian Days	212	214	216	218	220	222	224
REPLICATE 1	2	1.3	6.2	4.8	4.5	6.2	6.7
REPLICATE 2	0.8	1	2.3	4.4	1.6	0.07	4.5

TREATMENTS

REPLICATE 1 REPLICATE 2

Fig. 10.2.3 TSD Wheat
26 August - 18 September 1991

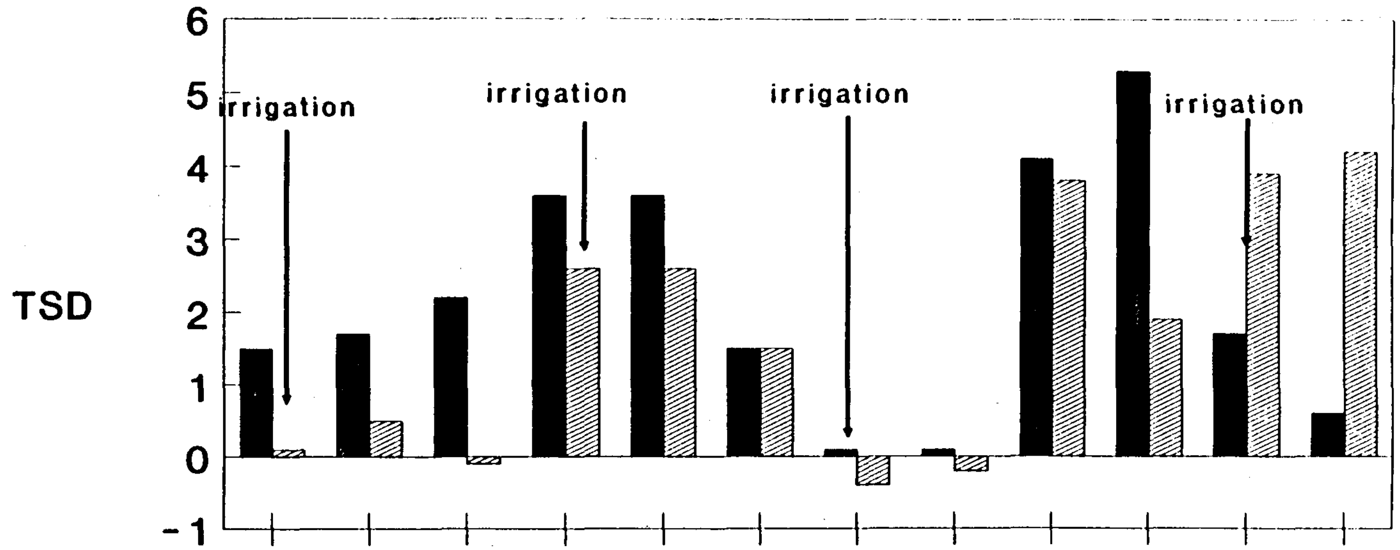

Julian Days	238	240	242	244	246	248	250	252	254	256	258	260
Replicate 1	1.5	1.7	2.2	3.6	3.6	1.5	0.1	0.1	4.1	5.3	1.7	0.6
Replicate 2	0.1	0.5	-0.1	2.6	2.6	1.5	-0.4	-0.2	3.8	1.9	3.9	4.2

TREATMENTS

Replicate 1 **Replicate 2**

Fig. 10.2.4 TSD Wheat
5 August - 22 September 1992

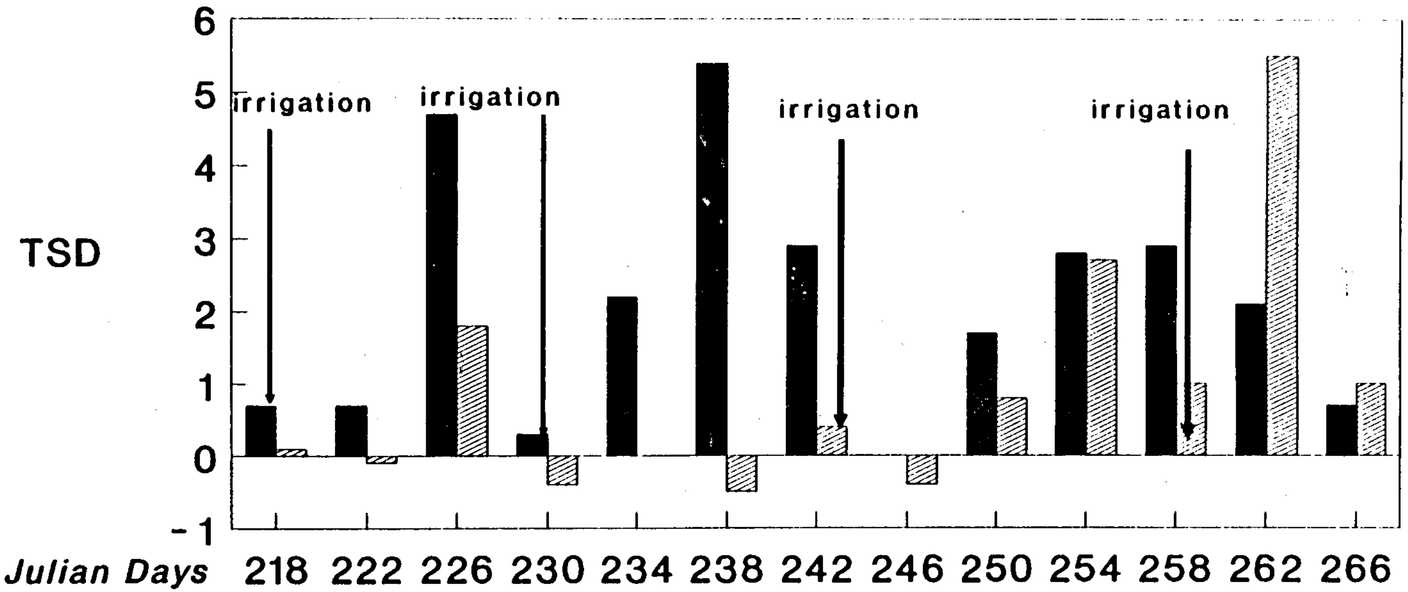

Julian Days	218	222	226	230	234	238	242	246	250	254	258	262	266
Replicate 1	0.7	0.7	4.7	0.3	2.2	5.4	2.9	0	1.7	2.8	2.9	2.1	0.7
Replicate 2	0.1	-0.1	1.8	-0.4	0	-0.5	0.4	-0.4	0.8	2.7	1	5.5	1

TREATMENTS

Replicate 1   Replicate 2

Fig. 11.1 CWSI - Soybean
25 Feb - 13 March 1991

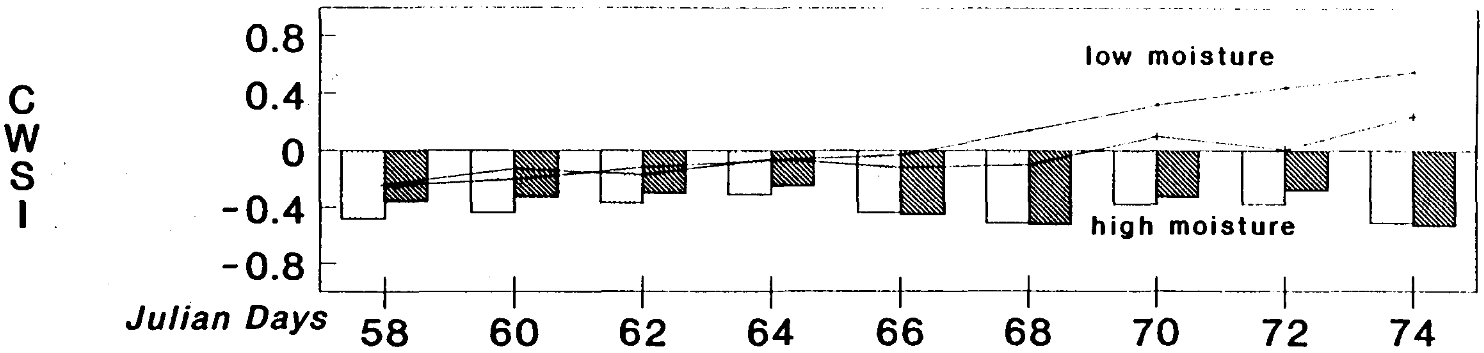

	58	60	62	64	66	68	70	72	74
STRESS Blk 1	-0.25	-0.2	-0.12	-0.07	-0.03	0.14	0.32	0.44	0.55
STRESS Blk 2	-0.24	-0.13	-0.17	-0.06	-0.12	-0.1	0.1	0.01	0.24
CONTRL Blk 1	-0.48	-0.44	-0.37	-0.31	-0.44	-0.51	-0.38	-0.38	-0.51
CONTRL Blk 2	-0.36	-0.33	-0.3	-0.25	-0.45	-0.52	-0.33	-0.28	-0.53

TREATMENTS

Fig. 11.2 CWSI - Wheat
26 Aug. - 18 Sept. 1991

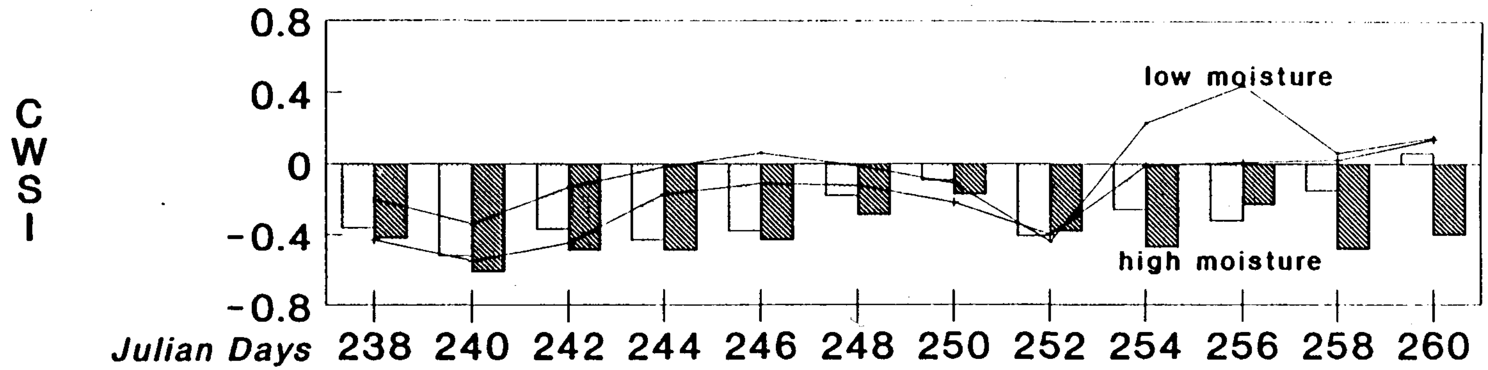

Julian Days	238	240	242	244	246	248	250	252	254	256	258	260
STRESS Blk 1	-0.2	-0.34	-0.13	-0.02	0.06	-0.01	-0.11	-0.44	0.23	0.44	0.06	0.15
STRESS Blk 2	-0.43	-0.55	-0.45	-0.17	-0.11	-0.12	-0.22	-0.4	-0.01	0.01	0.02	0.14
CONTRL Blk 1	-0.36	-0.52	-0.37	-0.43	-0.38	-0.18	-0.09	-0.41	-0.26	-0.32	-0.15	0.06
CONTRL Blk 2	-0.42	-0.61	-0.49	-0.49	-0.43	-0.29	-0.17	-0.38	-0.47	-0.23	-0.48	-0.4

TREATMENTS

STRESS Blk 1 STRESS Blk 2

CONTRL Blk 1 CONTRL Blk 2

Fig. 12.1 Water stressed baseline for Soybean - Feb. to March 1991

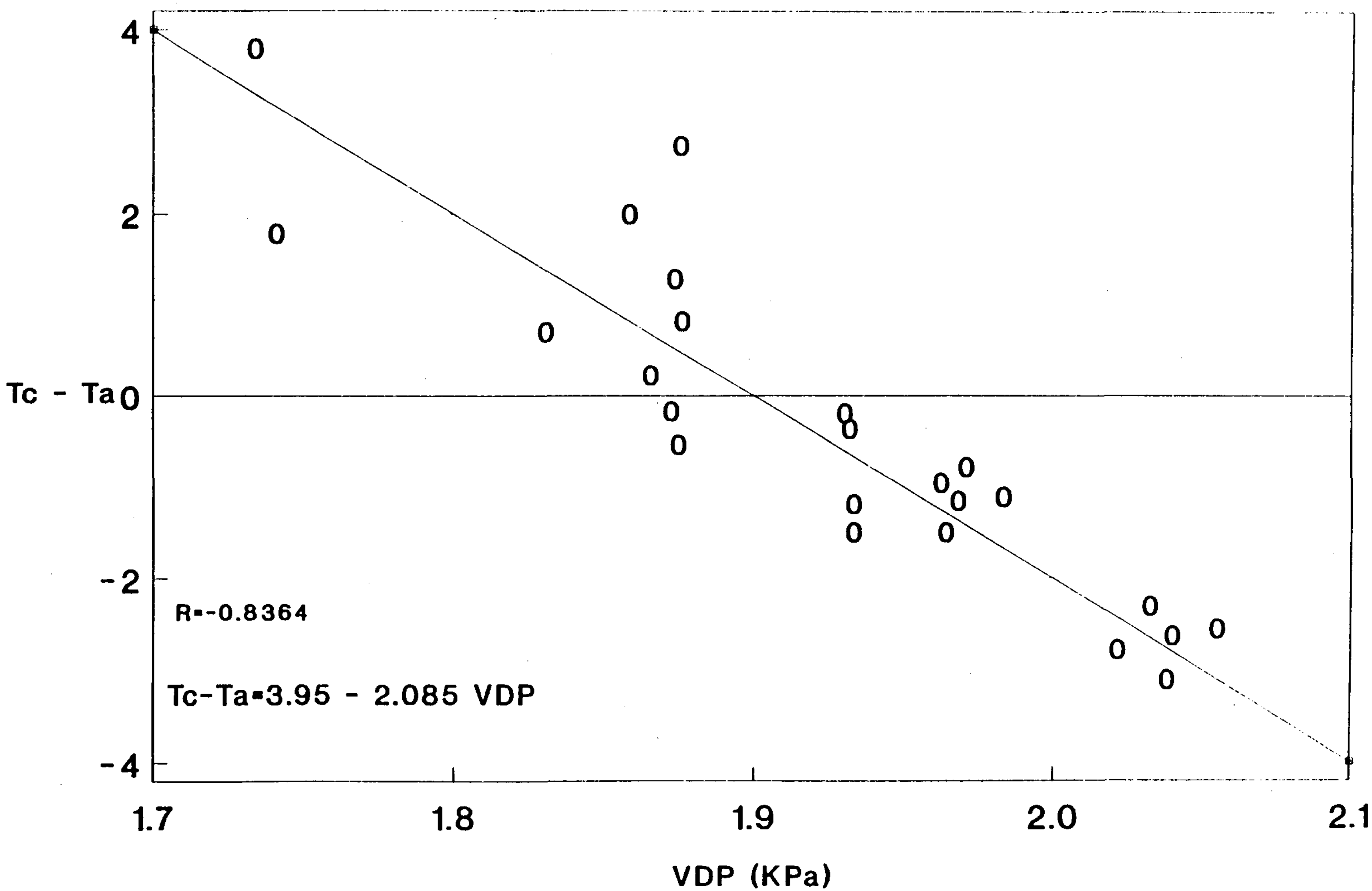

Fig. 12.2 Water stressed baseline for Wheat - Aug. to September 1991

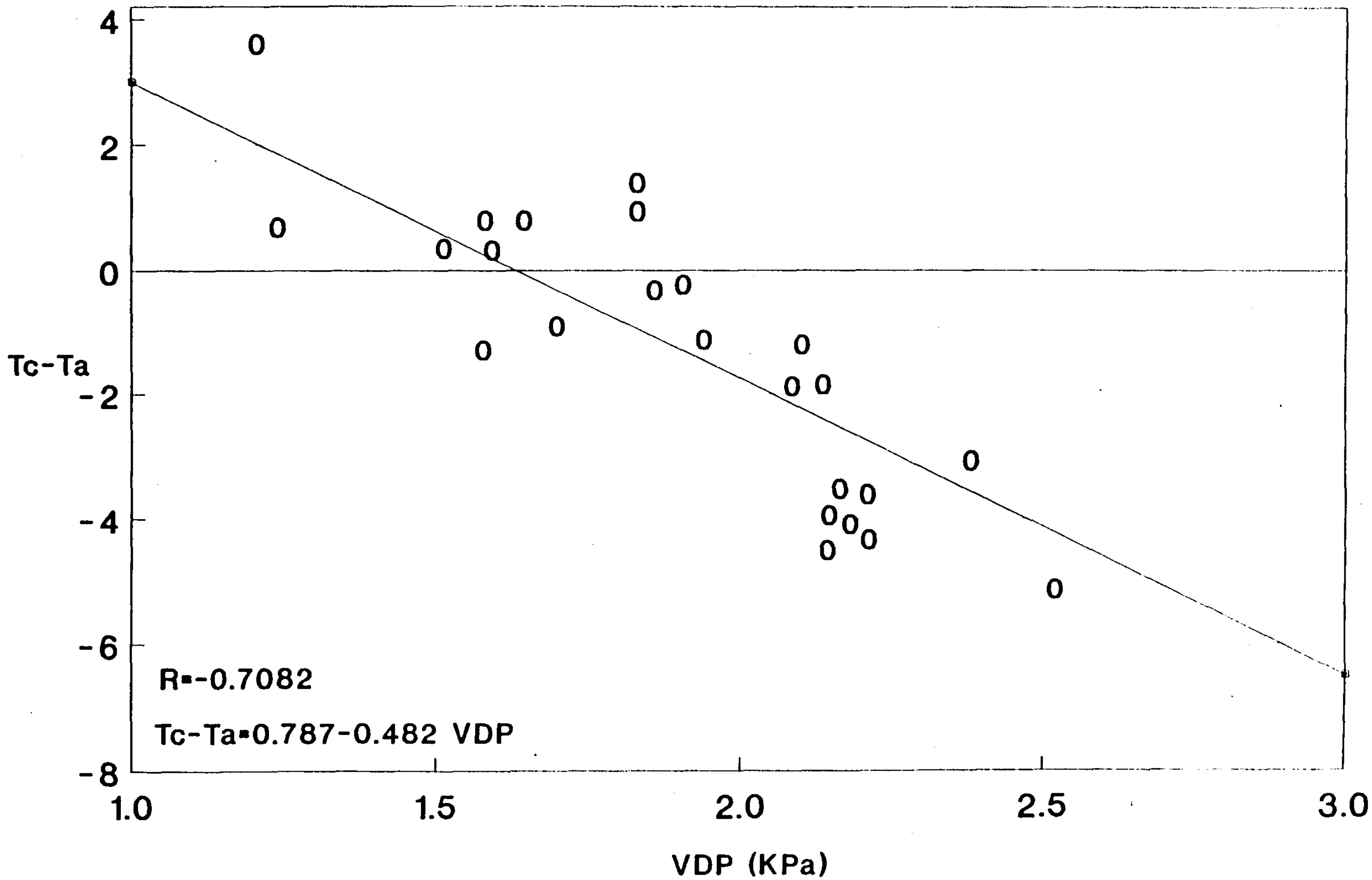

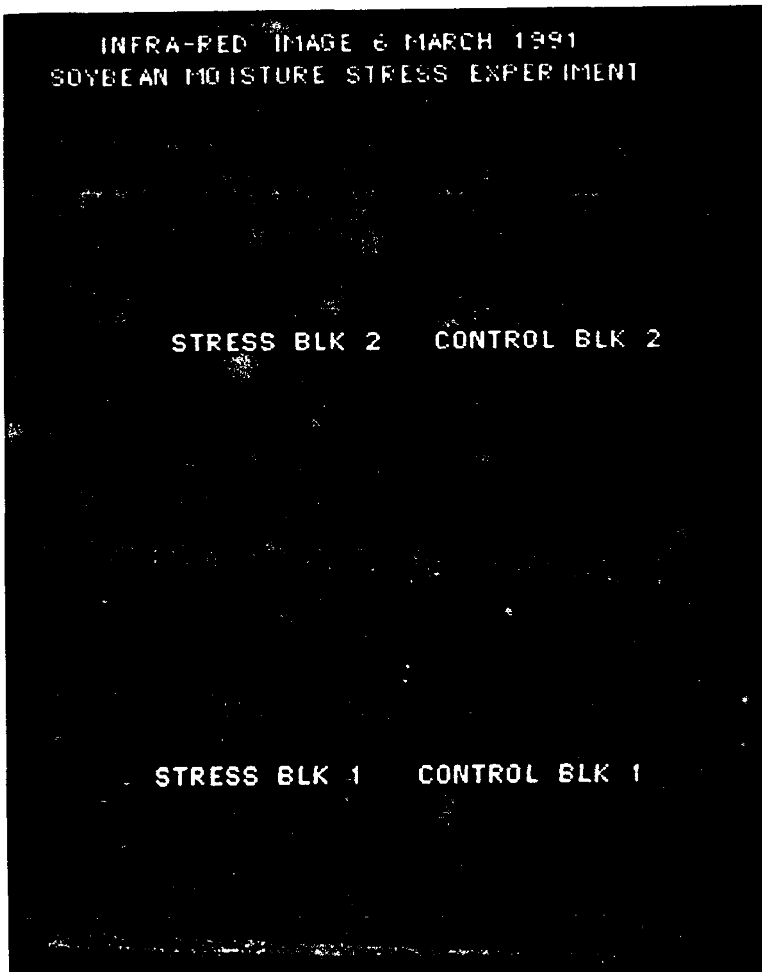

Fig.13.1 Exp. layout on soybean

Fig. 13.2 Moisture stress classification map

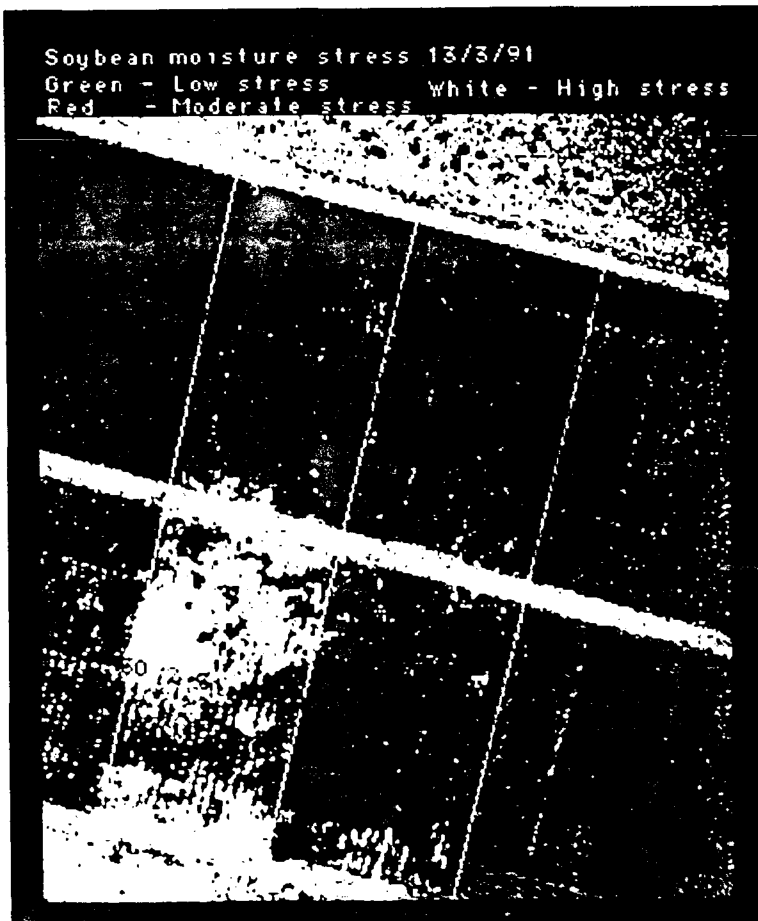

Fig. 13.3 Moisture stress classification map of soybean

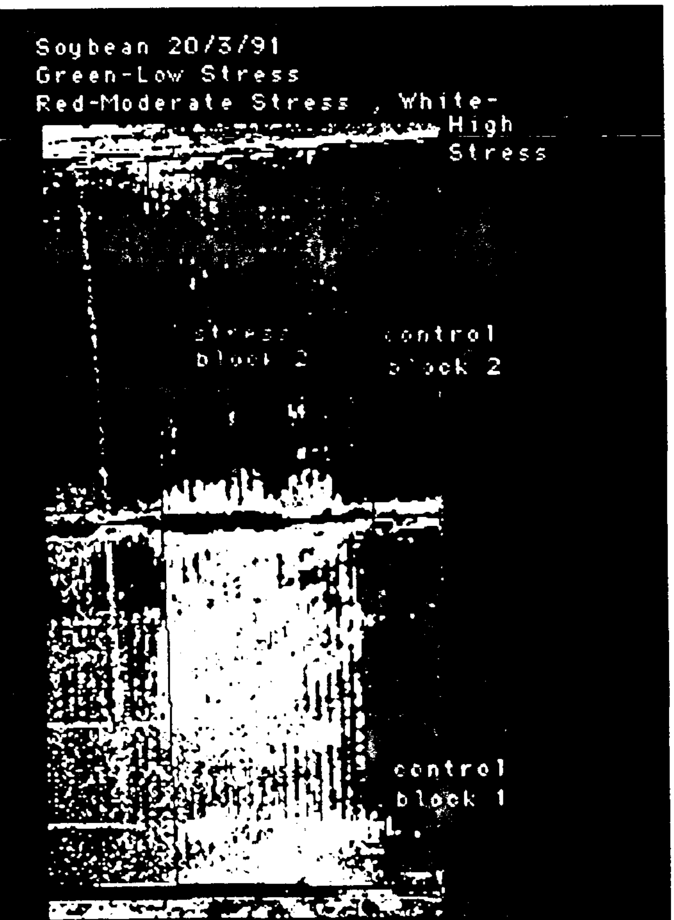

Fig. 13.4 Moisture classification map of soybean

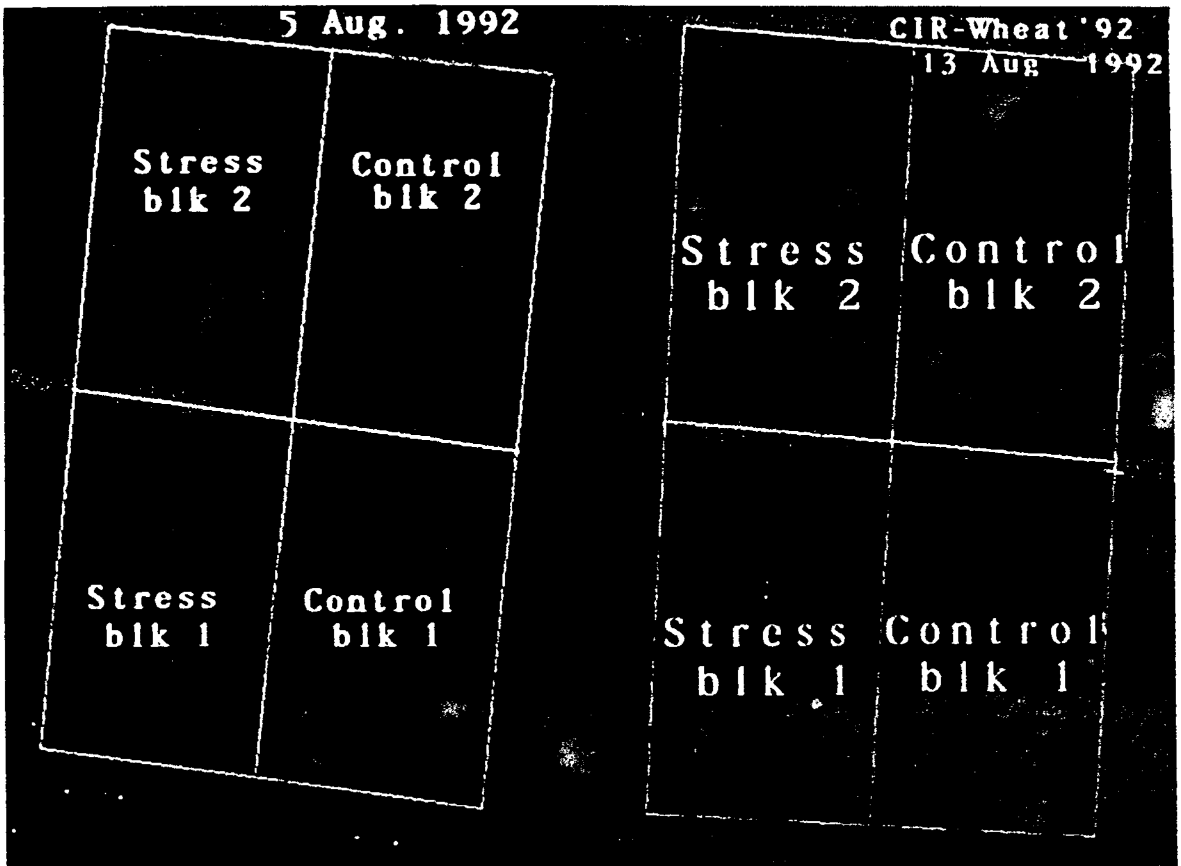

Fig. 14.1 Experimental outlay on wheat (CIR).

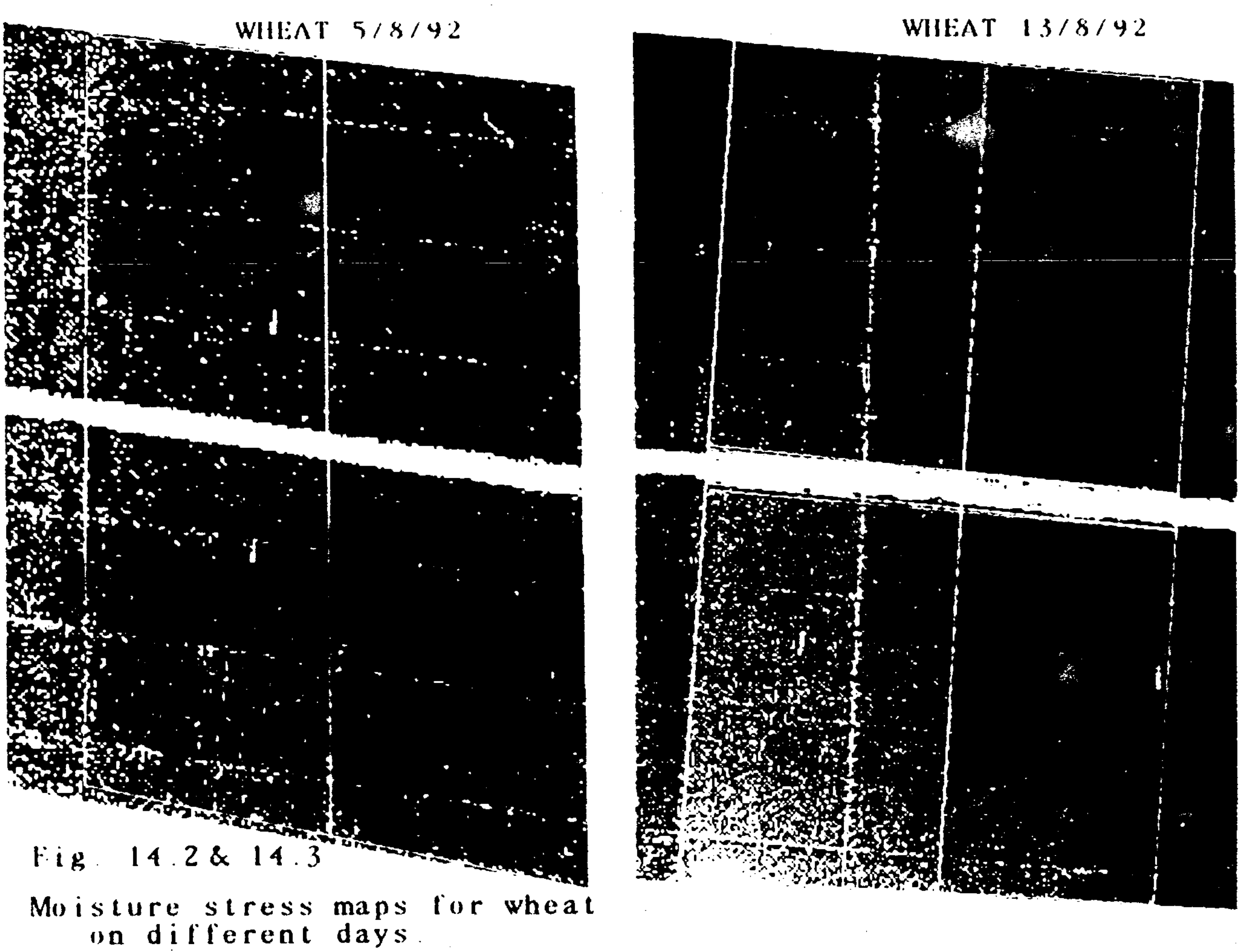

Fig. 14.2 & 14.3

Moisture stress maps for wheat on different days.

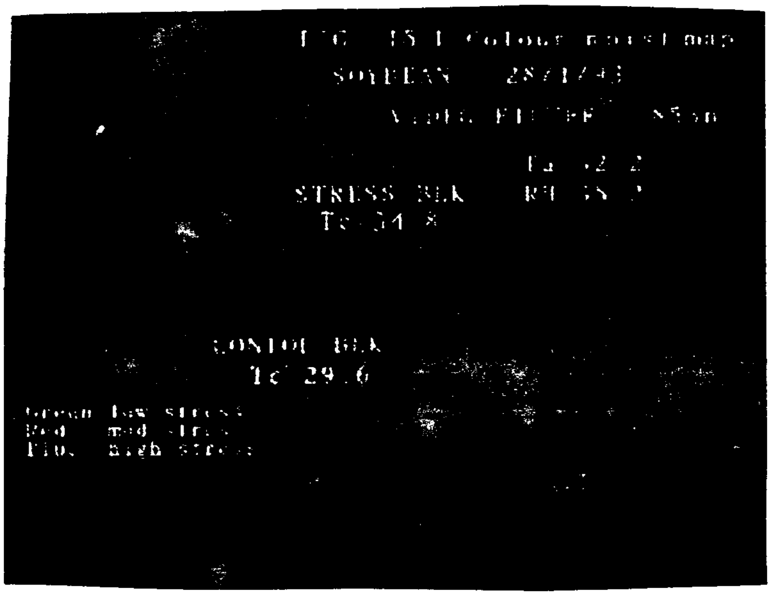

Fig. 15.1
Colour Moisture map of Soybean - Filter 853 μm

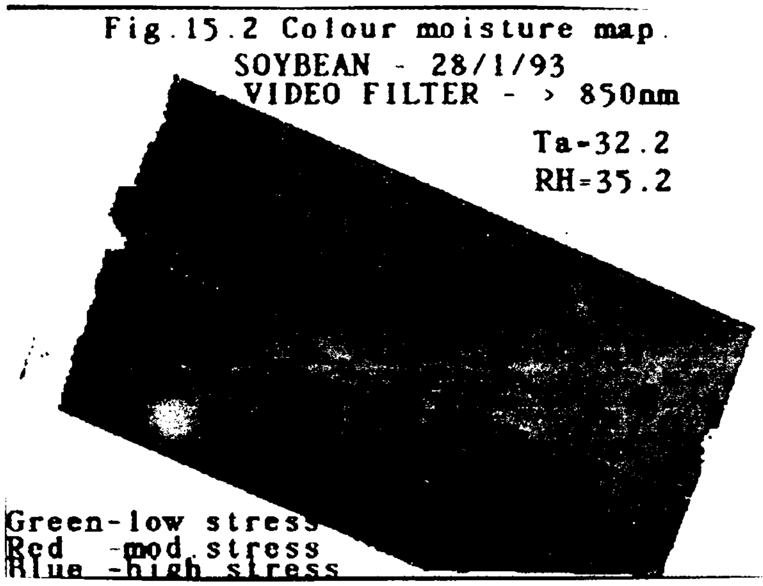

Fig. 15.2
Colour moisture map of Soybean - Filter > 853 μm

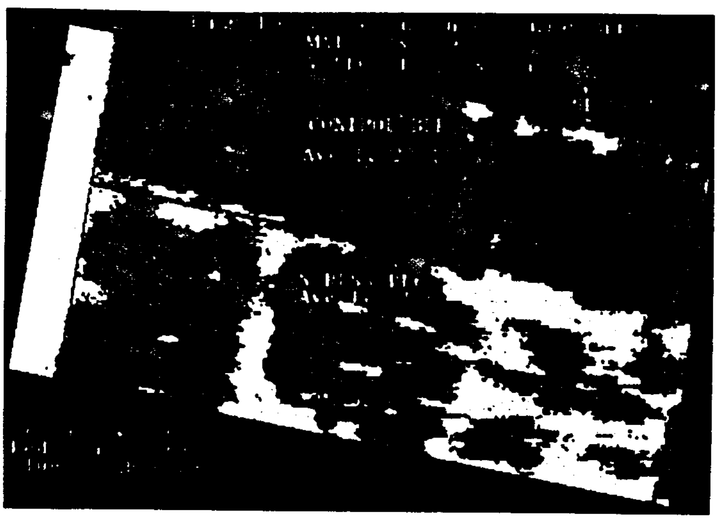

Fig. 15.3
Colour moisture map of Maize - Filter 853 μm

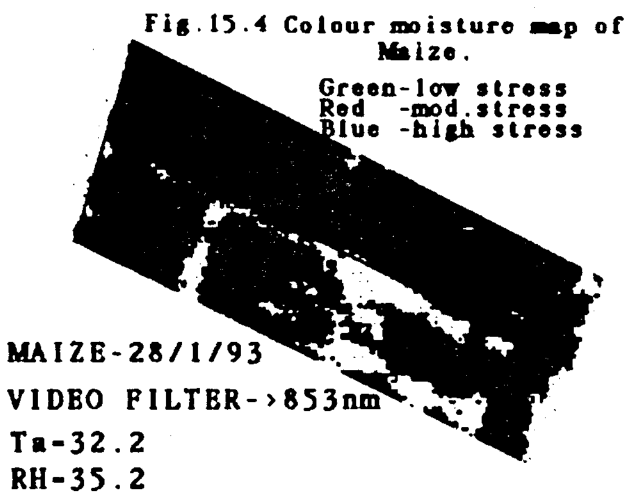

Fig. 15.4
Colour moisture map of Maize - Filter > 853 μm

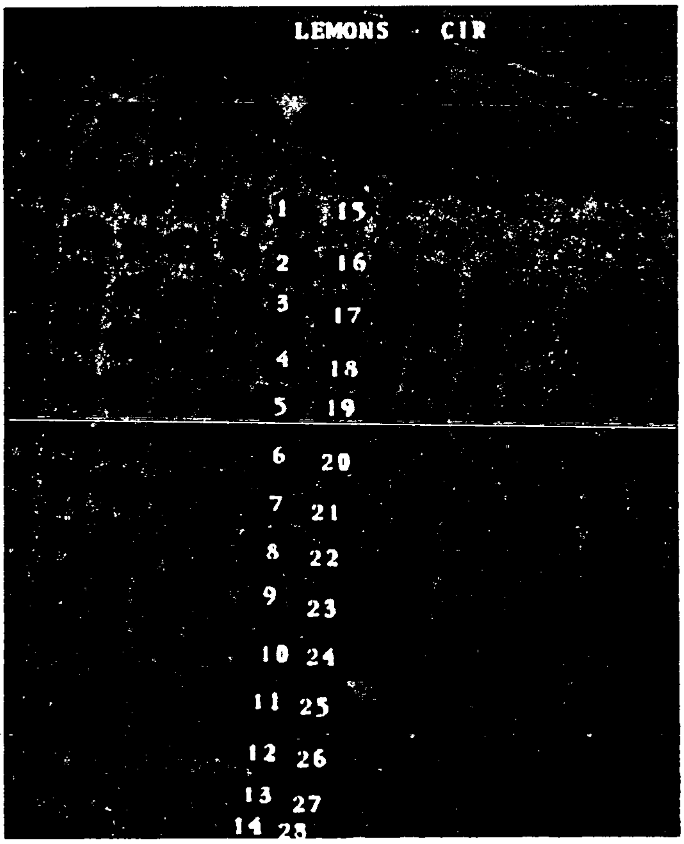

(A)

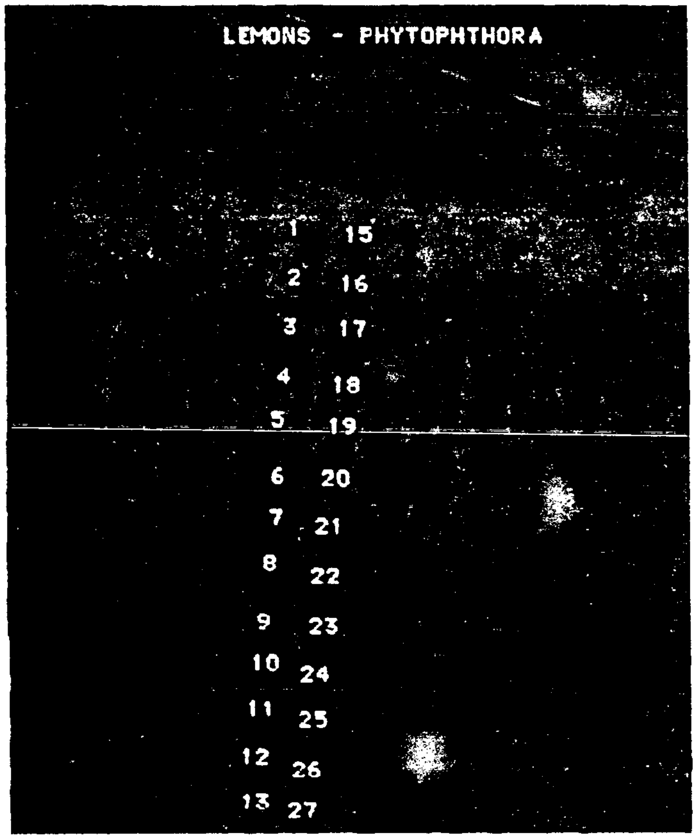

(B)

Figure 16 CIR scene and Feature Map (B) of a Lemon orchard affected by Rootrot disease.

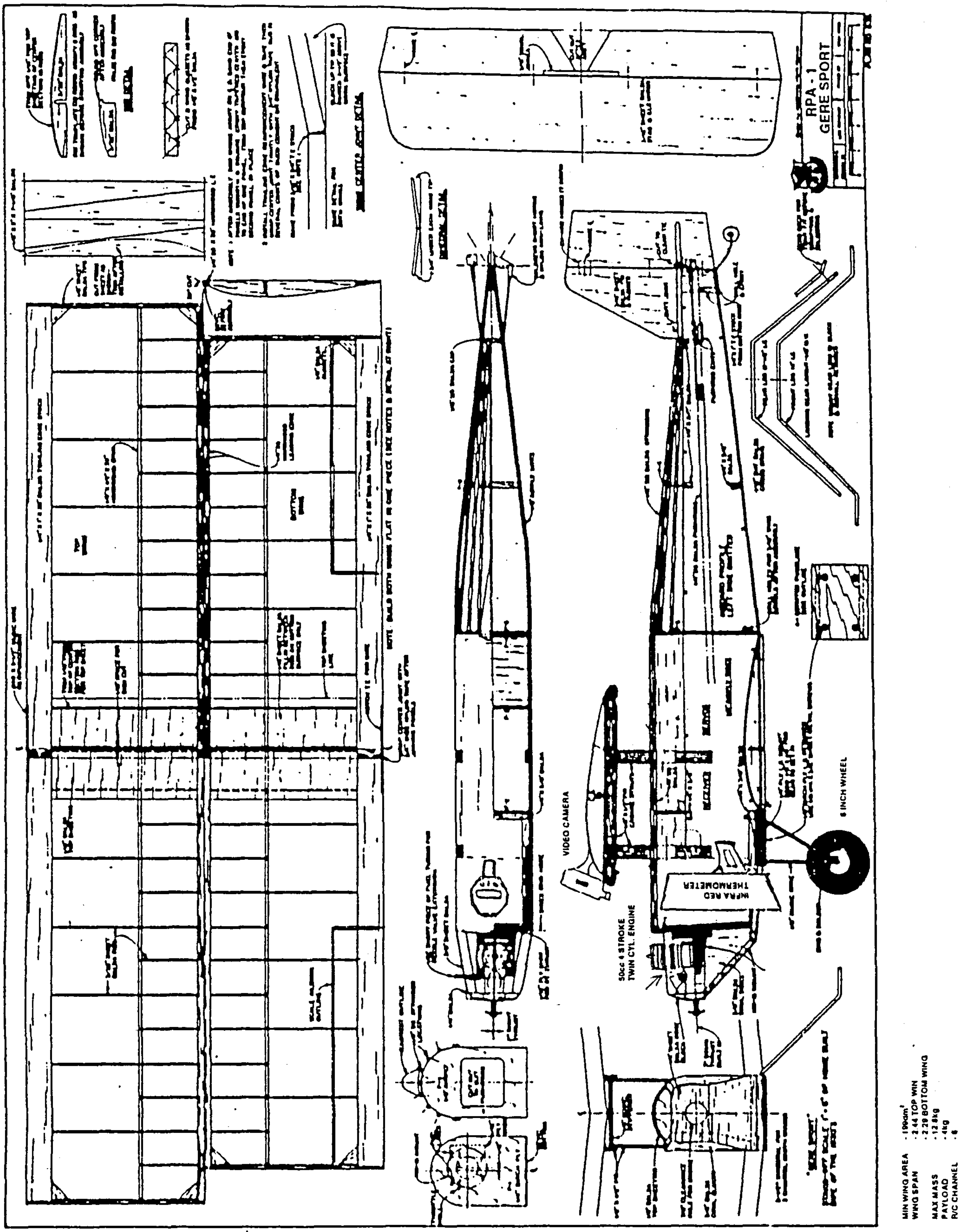

Figure 17

RPA - 1

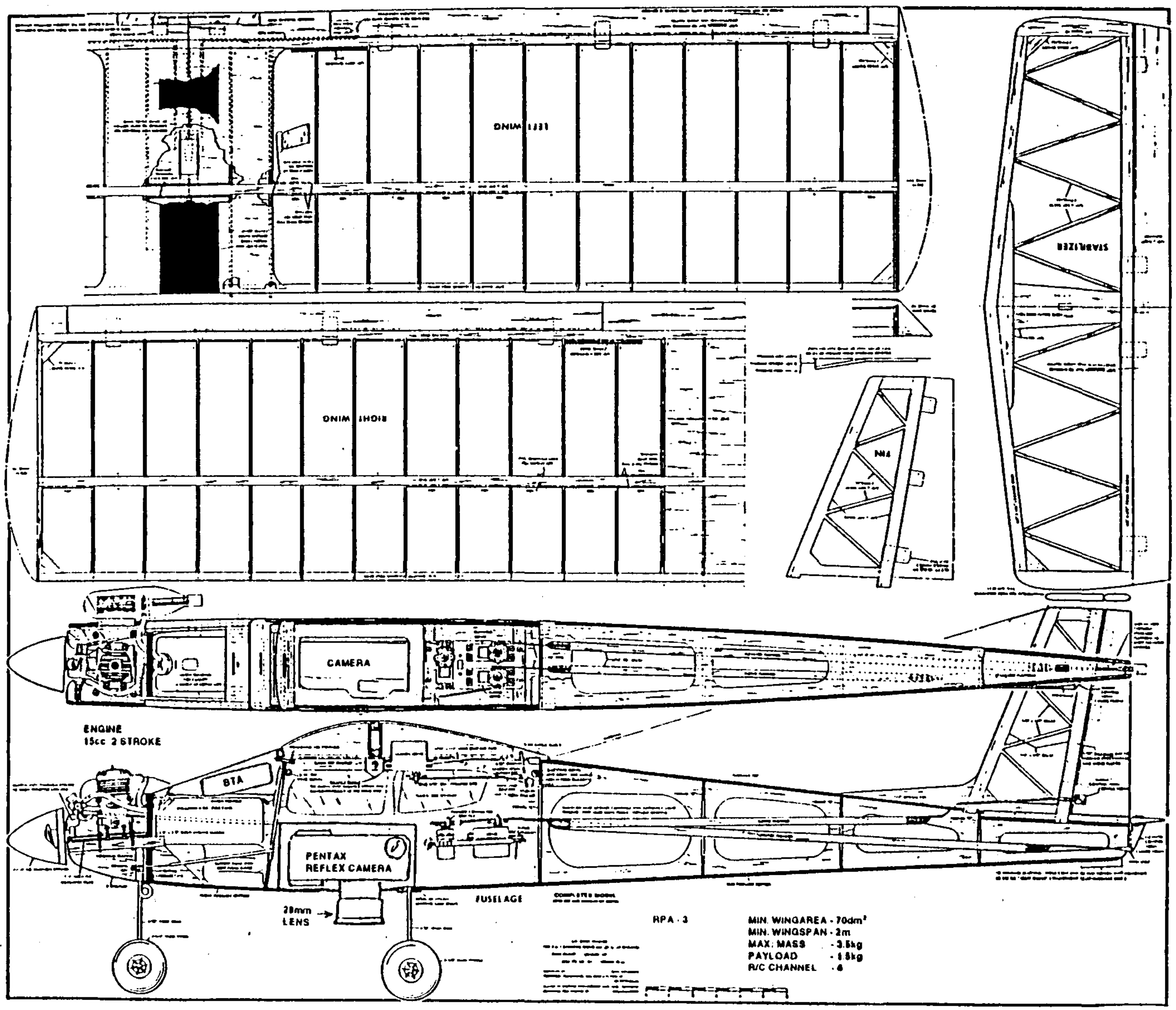

Figure 18

RPA - 3

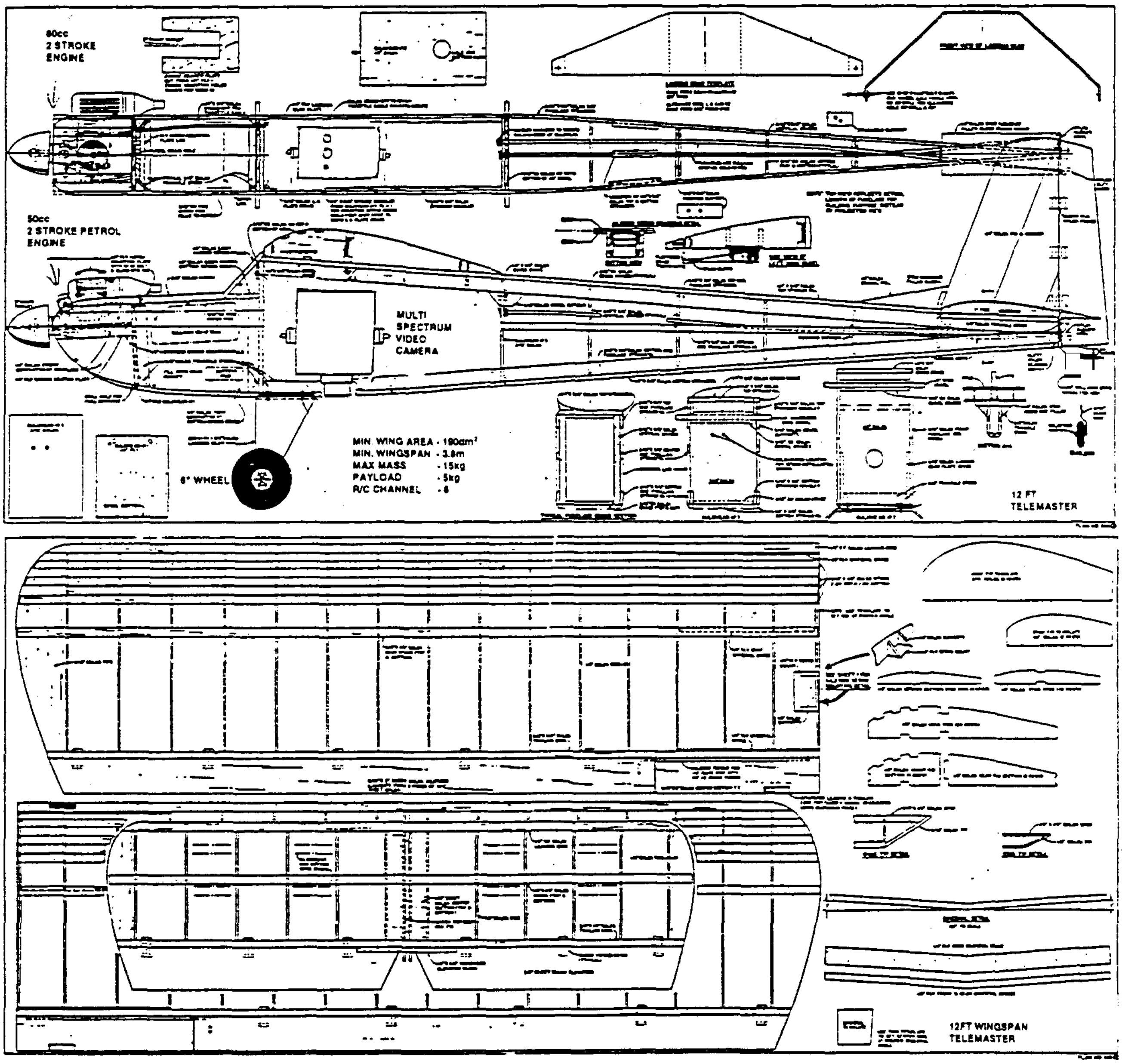

Figure 19

RPA - 5

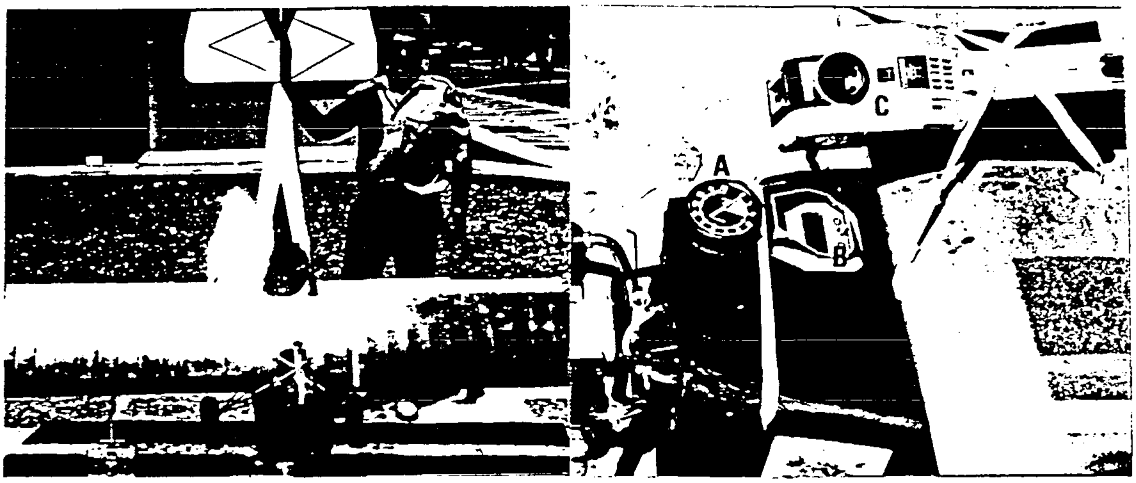

Figure 1. RPA-1 (left) and instrumentation (Right).
A - Altitude meter, B - IR Thermometer and C - Video camera

Figure 2. RPA-2 (left) and cameras (Right).
A - Omni directional antenna, B- 35 mm Reflex camera
and C - Video camera.

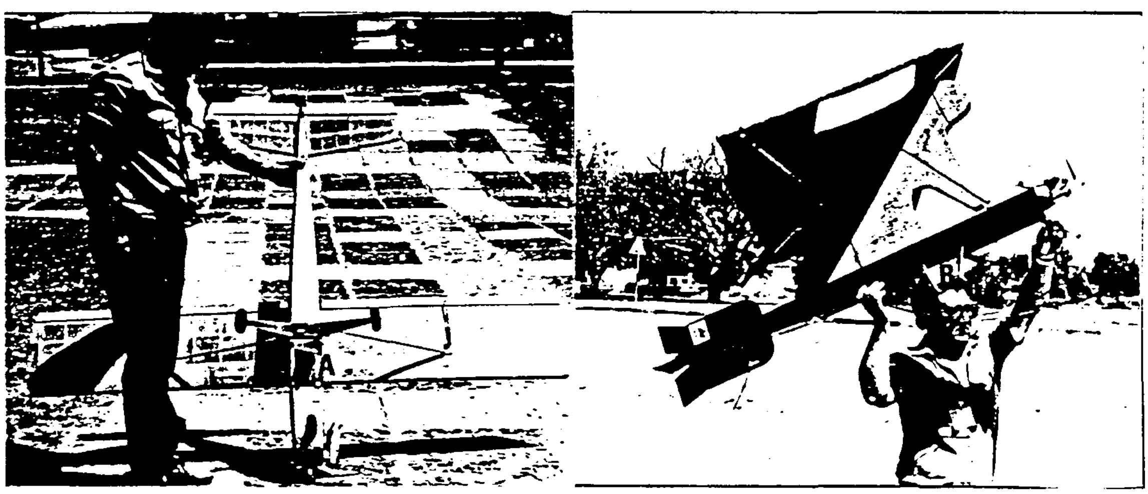

Figure 3. RPA-3 (Left) with 35 mm Reflex camera (A).
RPA-4 (Right) with camera box (B).

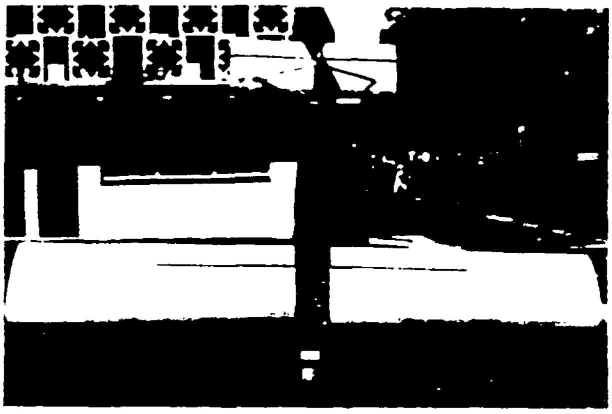

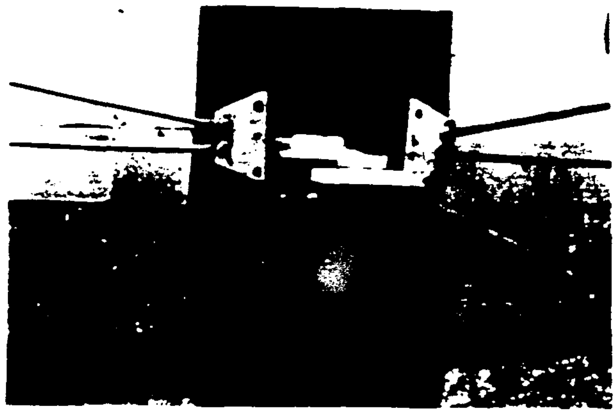

Figure 4
RPA - 5 (left) and Multi spectrum video camera (right) mounted behind the landing gear.

Figure 5. Parachute retrieving system

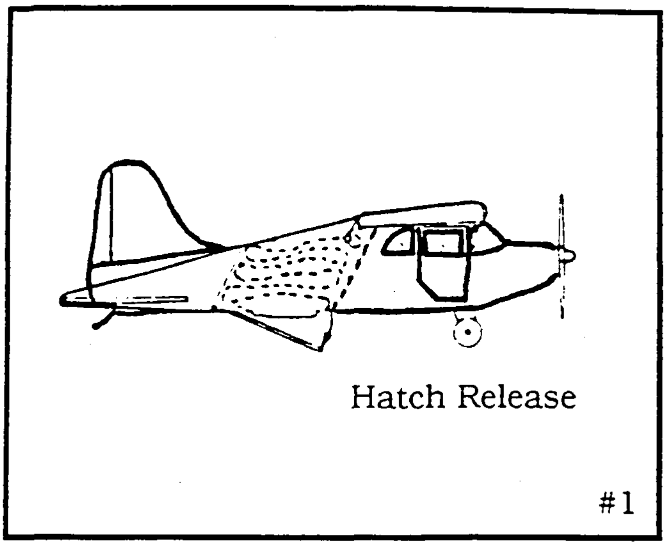

Sketch #1: Deployment of the Air Brake beginsby actuating the proper servo to release the flush mounting hatch cover. As the hatch cover opens, it is caught by the passing air and carried away from the plane. This action deploys the drogue chute.

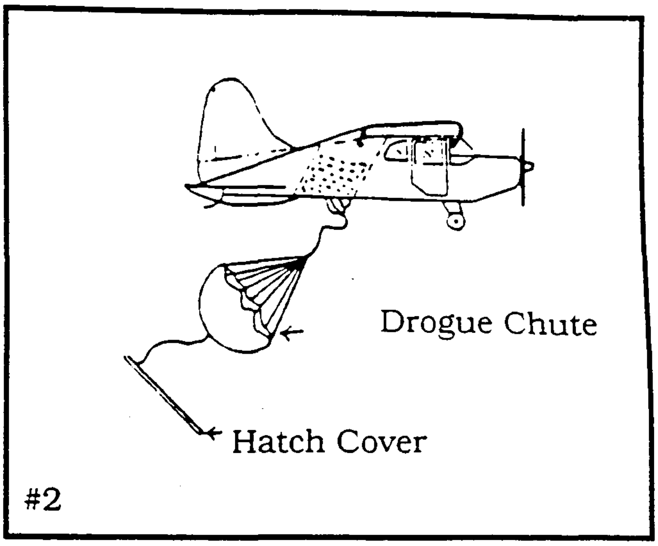

Sketch #2: The air resistance provided by both the hatchcover and the drogue chute serve to pull the main chute from the container. The main chute will be pulled clear of the plane by the drogue chute before inflating.

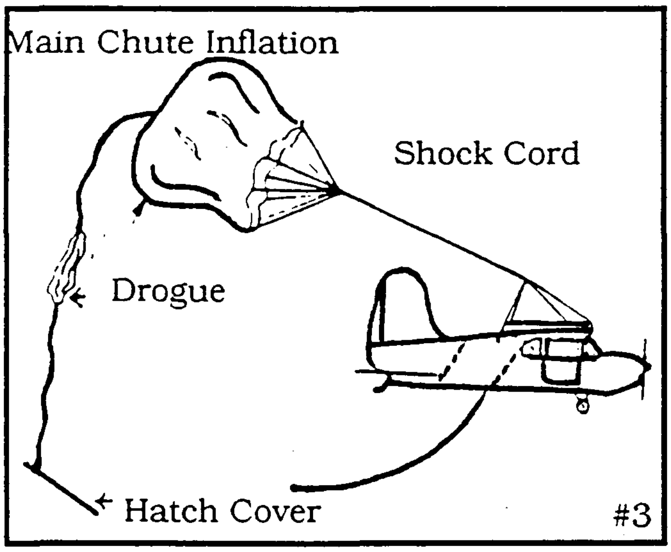

Sketch #3: This sketch shows how the riser cord and shock cord come into play to absorb the energy of the main chute inflation. Note how the Aiir Brake can be attached to the wing hold-down pegs via the harness assembly. Other methods of attachment include fuselage slings and senter of gravity anchor point with stabilizer lines.

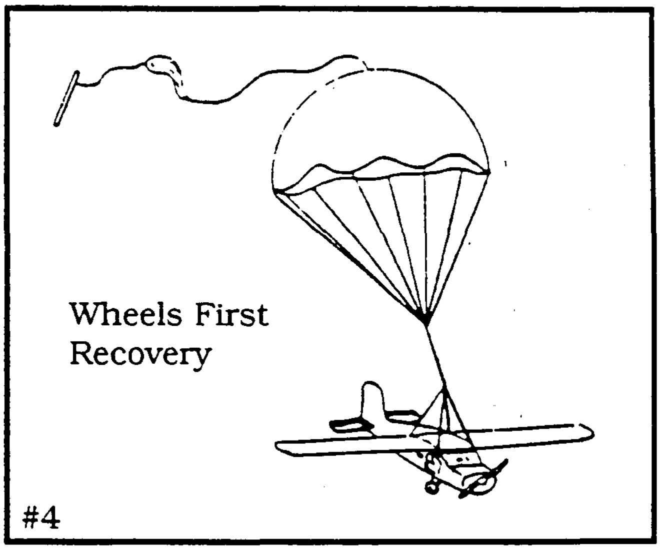

Sketch #4: The parachute deploys in less than 2 seconds, halting the forward progress of the plane. The plane is then lowered to the ground in a wheels-first attitude which allows any impact to be absorbed by the landing gear.

Fig. 6.1 $\Delta T = Tc - Ta$ for Maize Measured at 50 and 200m Altitudes

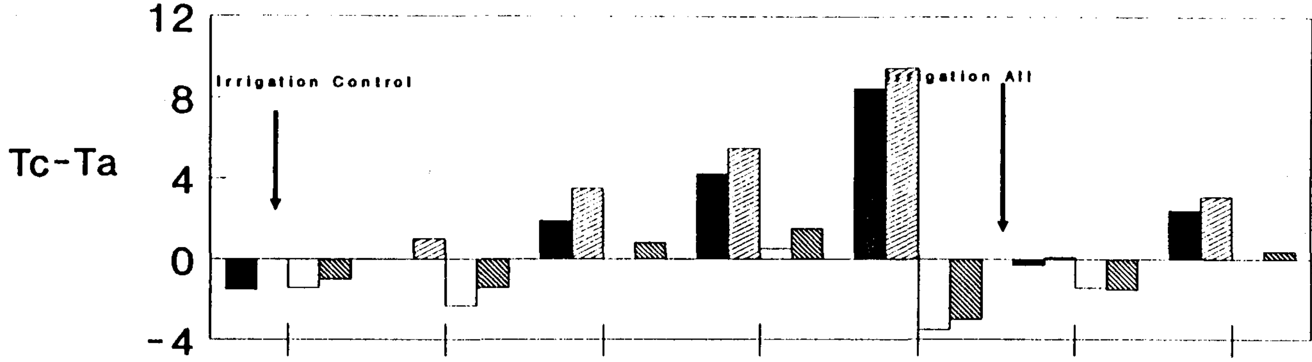

Julian Days	40	42	44	46	48	50	52
Stress-Blk 50m	-1.5	0	1.9	4.2	8.5	-0.3	2.4
Stress-Blk 200m	0	1	3.5	5.5	9.5	0.1	3.1
Control-Blk 50m	-1.4	-2.3	0	0.5	-3.5	-1.4	0
Control-Blk 200m	-1	-1.4	0.8	1.5	-3	-1.5	0.4

TREATMENTS

Stress-Blk 50m   Stress-Blk 200m
Control-Blk 50m   Control-Blk 200m

9 February - 20 February 1989

Fig. 6.2 ΔT =Tc-Ta on Wheat Measured by aerial- and handheld IR

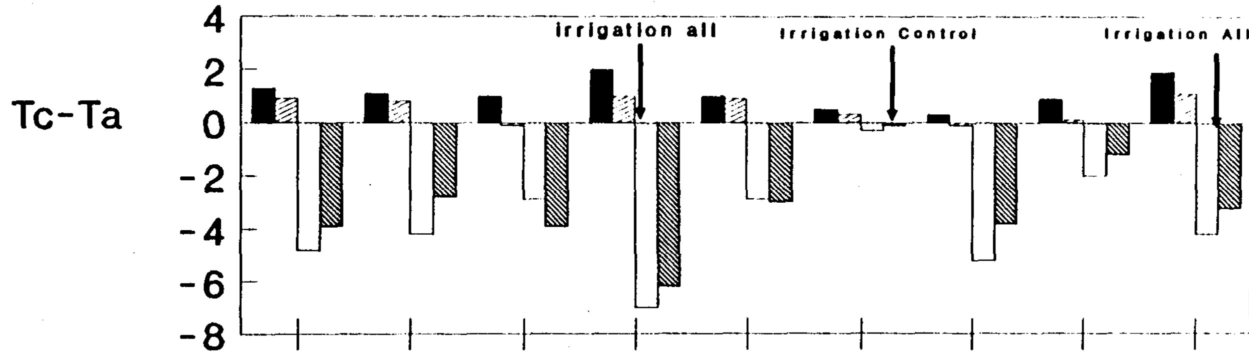

Julian Days	248	250	252	254	256	258	260	262	264
STRESS Blk Aerial IR	1.3	1.1	1	2	1	0.5	0.3	0.9	1.9
STRESS Blk Hand IR	0.9	0.8	-0.1	1	0.9	0.3	-0.1	0.1	1.1
CONTRL Blk Aerial IR	-4.8	-4.2	-2.9	-7	-2.9	-0.3	-5.2	-2	-4.2
CONTRL BLK Hand IR	-3.9	-2.8	-3.9	-6.2	-3	-0.1	-3.8	-1.2	-3.2

TREATMENTS

STRESS Blk Aerial IR   STRESS Blk Hand IR

CONTRL Blk Aerial IR   CONTRL BLK Hand IR

28 August - 14 September 1989

Fig. 7.1.1 Canopy Temperature of Soybean
8 March - 18 March 1989

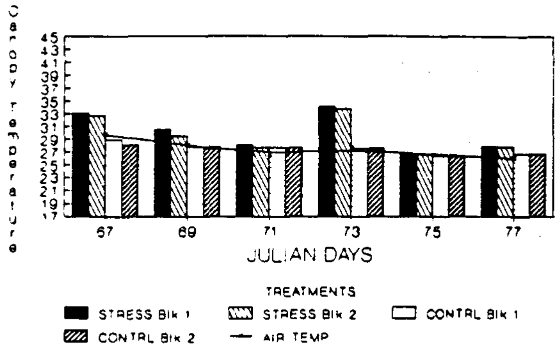

Fig. 7.1.2 Canopy Temperature of Soybean
15Feb - 17 March 1990

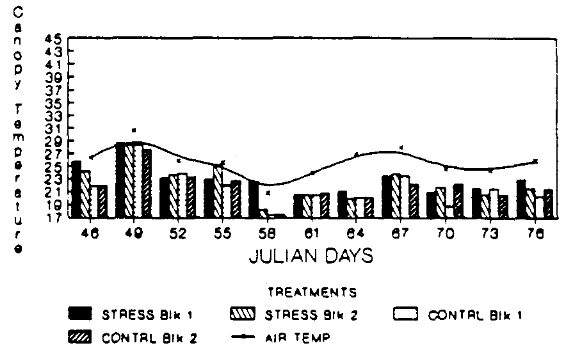

Fig. 7.1.3 Canopy Temperature of Soybean
25 Feb -13 March 1991

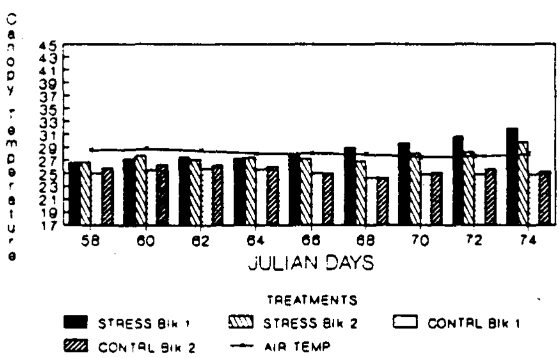

Fig. 7.1.4 Canopy Temperature of Soybean
28 Jan - 15 March 1992

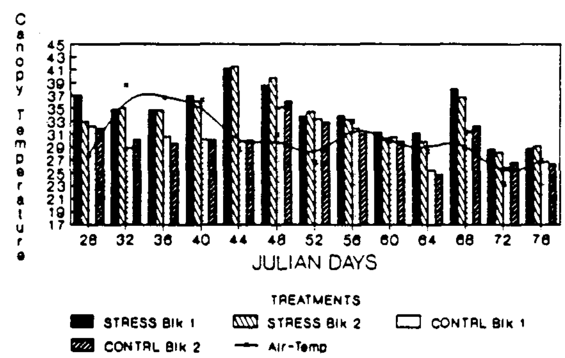

Fig. 7.1 Tc and Ta on Soybean for 1989 - 1992 seasons

Fig. 7.1.1 Canopy Temperature of Soybean
8 March - 18 March 1989

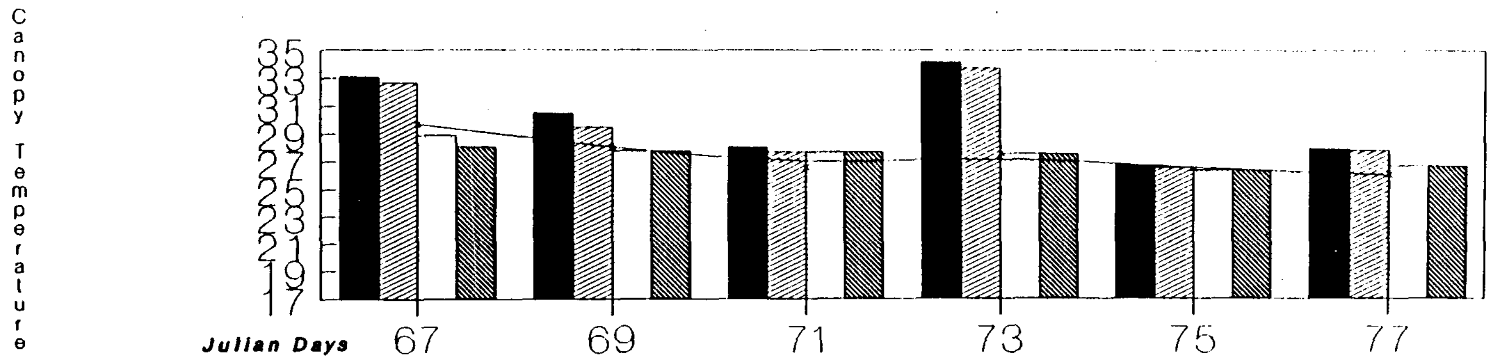

STRESS Blk 1	33.1	30.5	28.1	34.2	26.8	27.9
STRESS Blk 2	32.7	29.5	27.7	33.8	26.6	27.8
CONTRL Blk 1	28.9	27.8	27.7	27.6	26.4	26.7
CONTRL Blk 2	28.1	27.8	27.7	27.6	26.4	26.7
AIR TEMP	29.7	28	26.6	27.6	26.5	26

TREATMENTS

STRESS Blk 1 STRESS Blk 2 CONTRL Blk 1

CONTRL Blk 2 AIR TEMP

Fig. 7.1.2 Canopy Temperature of Soybean
15 Feb - 17 March 1990

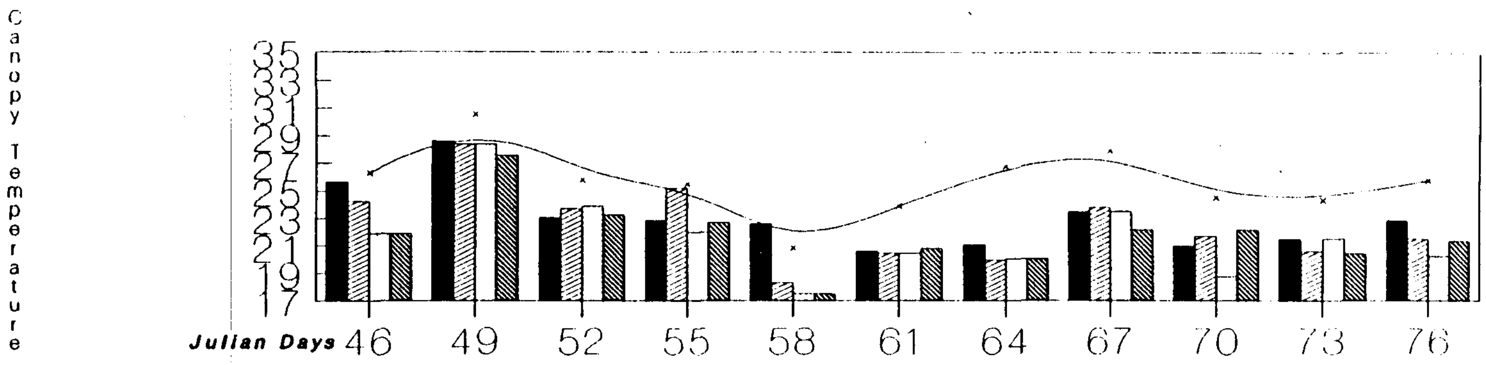

STRESS Blk 1	25.7	28.6	23.1	22.9	22.6	20.6	21.1	23.5	21	21.5	22.9
STRESS Blk 2	24.2	28.4	23.7	25.2	18.3	20.5	20	23.8	21.7	20.6	21.5
CONTRL Blk 1	21.9	28.4	23.9	22	17.5	20.5	20.1	23.5	18.8	21.5	20.3
CONTRL Blk 2	21.9	27.6	23.3	22.7	17.5	20.8	20.1	22.2	22.2	20.5	21.4
AIR TEMP	26.3	30.5	25.8	25.5	20.8	23.9	26.8	27.9	24.5	24.3	25.8

TREATMENTS

STRESS Blk 1 STRESS Blk 2 CONTRL Blk 1
CONTRL Blk 2 AIR TEMP

Fig. 7.1.3 Canopy Temperature of Soybean 25 Feb -13 March 1991

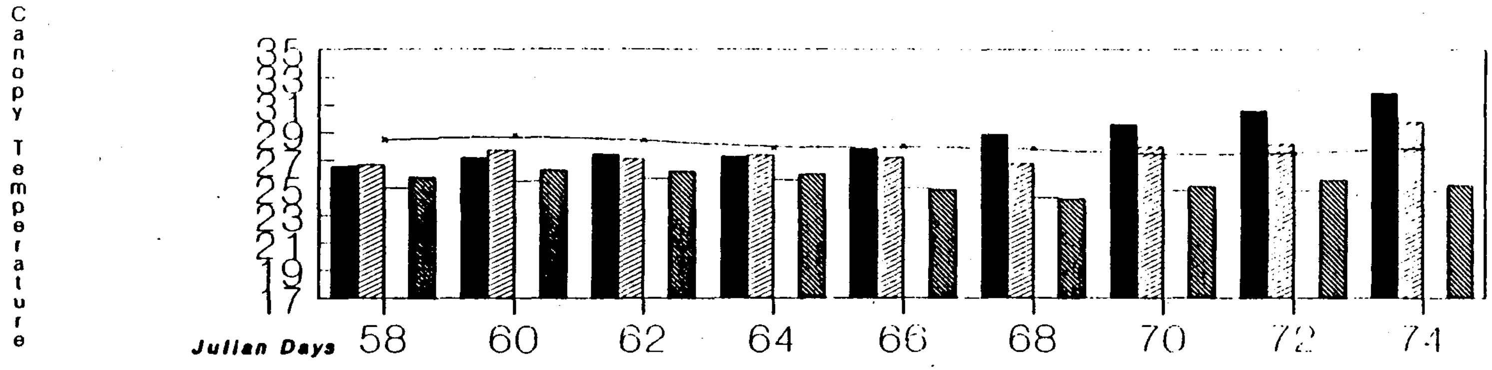

	58	60	62	64	66	68	70	72	74
STRESS Blk 1	26.6	27.2	27.5	27.3	27.8	28.9	29.6	30.6	31.9
STRESS Blk 2	26.7	27.7	27.1	27.4	27.2	26.8	28	28.2	29.8
CONTRL Blk 1	25	25.5	25.7	25.6	25	24.3	24.8	24.8	24.8
CONTRL Blk 2	25.8	26.3	26.2	26	24.9	24.2	25.1	25.6	25.2
AIR TEMP	28.5	28.8	28.5	27.9	28	27.9	27.3	27.5	27.9

TREATMENTS

STRESS Blk 1   STRESS Blk 2   CONTRL Blk 1

CONTRL Blk 2   AIR TEMP